Effect of growth factors on T-lymphocyte induced keratinocyte apoptosis

Ilse Sofia Daehn

Department of Medicine-Biotechnology

Flinders University of South Australia

A thesis submitted for the degree of

Doctor of Philosophy

January 2007

For my family and Tom

"Happy is he who gets to know the reasons for things."

Virgil (70-19 BCE)
Roman poet.

Table of Contents

Chapter 2

MATERIALS AND METHODS

Chapter 3

Sodium butyrate induced HaCaT apoptosis

Chapter 4

Jurkat induced HaCaT apoptosis

Chapter 5

Primary T-lymphocyte induced keratinocyte apoptosis

Chapter 6

TGFβ and IGF-I effects on T-lymphocyte induced keratinocyte apoptosis

Chapter 7

Effects of WGFE on T-lymphocyte induced keratinocyte apoptosis

Chapter 8

DISCUSSION

Declaration

" I certify that this thesis does not incorporate without acknowledgement any material previously submitted for a degree or diploma in any university; and that to the best of my knowledge and belief it does not contain any material previously published or written by another person except where due reference is made in the text"

Ilse S. Daehn

January 2007

Acknowledgements

I would like to take this opportunity to thank a number of people without whose help and support this thesis would have never been possible. A special acknowledgment to my supervisor Dr Tim Rayner, for the valuable guidance and support over these last few years, without whose knowledge and assistance this study would not have been successful. I will take the upside down triangle ▼ approach wherever I go! I would like to thank Dr Antiopi Varelias for the encouragement, advice and friendship. I also express my gratitude for Dr Peter Macardle and Dr Allison Cowin who have provided valuable advice and feedback to this thesis. In addition I would like to thank Dairy Australia and The Queen Elizabeth Hospital Research Foundation for providing me with financial support to conduct my studies.

Special thanks to Mrs Silvia Nobbs for her invaluable expertise and help with the flow cytometry work. I also thank WCH Haematology department for bleeding me, yes there is literally blood, sweat and tears in the making of this thesis… My appreciation also goes to the staff at CHRI and TGR-Biosciences for their allowing me to perform experiments using their equipment, for their valuable intellectual input and constructive criticism.

A special acknowledgment to Ken and Adrian from the TQEH animal house, as well as Madeline and Ashley, for making the days at TQEH so much fun. A super thanks to the

CHRI crew: Marko, Prodell, Mic, Donato, Pallave, Naoms, Rogy, Walter and LJ with whom we shared so many funny moments including those unforgettable conversations…, the Torrens runs, coffee schemes, the pub o'clocks, those crazy pubcrawls... I would like to also thank everyone involved in the making of the CHRI calendar! Thanks to the BioHazardous and the Sand-Sationals. Special thank you to those close friends who I can always count on and have contributed to my sanity in so many ways; my Vec, Dave and Olgi… I love you guys.

I cannot end without thanking my parents, whose courage and determination in life will always inspire me. To my sisters whom I love and finally to my husband Tom, who's constant support, encouragement and love, helped me finish this thesis. A part of you all is in here, in some form, somewhere… I am extremely grateful, I could not have done it with out you, so it is to you that I dedicate this work.

Publications arising from this project

(see Appendix)

Daehn I, Varelias A, Rayner T. Sodium butyrate induced keratinocyte apoptosis. *Apoptosis*. 2006 Aug;11(8):1379-90.

Ruzehaji G, Daehn I, Varelias A, Rayner T. Exploring cellular interactions relevant to wound healing. *Primary Intention*. 2006 Feb;14(1):22-30.

Abbreviatons

α6	alpha-6 integrin
ACD	allergic contact dermatitis
AE	atopic eczema
BSA	bovine serum albumin
DNA	deoxyribonucleic acid
DMSO	dimethyl sulfoxide
DMEM	dulbecco's modified eagle's medium
FACS	fluorescence activated cell sorter
FBS	fetal bovine serum
FasL	Fas ligand
FITC	fluorescein isothiocyanate
HLDA	human cell differentiation antigens
HDI	histone deacetylase inhibitor
hrs	hours
ICAM-1	intracellular adhesion molecule
IGF-I	insulin-like growth factor-I
IGFBP	IGF-binding proteins
IFNγ	interferon γ
Ig	immunoglobulin
IL	interleukin

LFA-1	lymphocyte function-associated antigen-1
LR3-IGF	LONG™R3 IGF-I
mAb	monoclonal antibody
mins	minutes
MFI	mean fluorescence intensity
NF-κβ	nuclear factor κβ
NHEK	normal human epidermal keratinocytes
PARP	poly (ADP-ribose) polymerase
PBS	phosphate buffered saline
PE	phycoerythrin
PI	propidium iodide
PMA	phorbol myristate acetate
PS	phosphotidylserine
RT	room temperature
rpm	revolutions per minute
TGFβ	transforming growth factor β
Th	T helper cell
TIMs	topical macrolide immunomodulators
TNFα	tumour necrosis factor α
TRAIL	tumour necrosis related apoptosis-inducing ligand
WGFE	whey growth factor extract
x g	relative centrifugal force (g-force)

THESIS SUMMARY

Atopic eczema is a T-lymphocyte mediated chronic inflammatory skin disorder. The interaction of CD4+ T-lymphocytes with epidermal keratinocytes results in dysregulated, chronic inflammation and altered barrier function. T-lymphocyte induced keratinocyte apoptosis has been proposed as a mechanism by which epidermal integrity is impaired in eczema. Apoptosis of keratinocytes is thought to result from T-lymphocyte associated Fas ligand (FasL) binding to the death receptor Fas on keratinocytes. The primary aim of this project was to characterize the induction of keratinocyte apoptosis by T-lymphocytes and address the hypothesis that insulin-like growth factor-I (IGF-1), transforming growth factor β_1 (TGFβ_1) and a milk derived growth factor extract containing TGFβ and IGF-I (whey growth factor extract; WGFE) protect keratinocytes from T-lymphocyte mediated apoptosis.

To address the aims of this project, an *in vitro* co-culture model was developed combining T-lymphocytes with keratinocytes. Co-cultures were initially established using human Jurkat T-lymphocytes and human HaCaT keratinocytes with more extensive characterisation undertaken using primary CD4+ T-lymphocytes together with HaCaTs or normal human epidermal keratinocytes (NHEK). Annexin V and propidium iodide staining was established as the primary method for measuring keratinocyte apoptosis with this validated using sodium butyrate a known inducer of apoptosis. Changes in nuclear fragmentation and cell morphology were also examined as a key

feature of apoptosis. The involvement of the Fas pathway was investigated by assessing T-lymphocyte FasL expression, keratinocyte Fas expression and downstream caspase activation. Inflammatory cytokines IFNγ and TNFα were also examined due to their ability to induce Fas expression.

Studies performed with T-lymphocytes demonstrated that keratinocyte apoptosis was induced, with this due primarily to direct T-lymphocytes and keratinocytes interactions, rather than soluble mediators in the co-culture milieu. Activated T-lymphocytes were found to have high levels of FasL and to upregulate keratinocyte Fas expression. The increased keratinocyte Fas was associated with increased IFNγ levels in the co-culture media and activation of the caspase cascade. A Fas blocking antibody prevented T-lymphocyte induced keratinocyte apoptosis demonstrating that this was a Fas dependent event.

As the primary function of keratinocytes is to terminally differentiate, the differentiation status of the cells induced to undergo apoptosis was examined. It was demonstrated that T-lymphocytes decrease the intensity of α6 integrin expression by the keratinocytes. This marker identifies undifferentiated basal cells as high expressors of α6, with cells in the early stages of differentiation pathway found to be low expressors of α6. Co-staining with Annexin V demonstrated that the apoptotic keratinocytes were low expressors of α6 and thus cells committed to the early stages of differentiation. This suggested that the T-lymphocytes initiated the onset of keratinocyte terminal differentiation with this linked

to the cells being more susceptible to death induced by T-lymphocyte by activation of the Fas pathway.

The ability of TGFβ_1, IGF-I and WGFE to inhibit T-lymphocyte induced keratinocyte apoptosis was examined. A combination of recombinant TGFβ (10ng) & IGF-I (100ng) was able to significantly inhibit keratinocyte apoptosis. A similar result was obtained with WGFE, and although these growth factor treatments were able to reduce the elevated IFNγ levels in the co-culture media, they did not reduce T-lymphocyte induced Fas upregulation. The TGFβ_1 and IGF-I combination as well as WGFE did however prevent the T-lymphocyte induced shift from α6 bright to dim expressing keratinocytes. As such, the growth factor combinations appeared to protect the keratinocytes from T-lymphocyte mediated apoptosis by preventing them from committing to terminal differentiation.

The studies in this thesis have characterised the Fas associated mechanisms by which T-lymphocytes induce keratinocyte apoptosis and suggest specific growth factor combinations may have the potential to ameliorate the reduced barrier function associated with inflammatory skin conditions such as atopic eczema.

CHAPTER 1

1 INTRODUCTION

Atopic eczema (AE) is the most common skin disease affecting children (Leung 2000). There has been an increase in the prevalence of AE over the last 40 years and it is now estimated to affect approximately 10–20% of children worldwide (Leung & Boguniewicz 2003, Tewari *et al.* 1995). There is presently no cure for AE and current therapies only treat the symptoms and have a number of adverse side effects. As such, there is a need to identify of agents that can target key aspects of AE pathology to minimise the reliance on current treatments and decrease side effects. The main objective of this thesis is to examine whether growth factors such as IGF-I and TGFβ_1 can target these key aspects of AE and be used as a novel approach for improving clinical outcomes, particularly in children. In this chapter an overview of the pathology of AE will be presented, followed by a more detailed discussion of key skin-cell specific effects associated with this condition and an examination of the treatment regimens in current use. This chapter will also introduce evidence supporting the use of growth factors as agents with the potential to ameliorate AE.

1.1 The skin's barrier function

The skin is a self-renewing organ and functions to provide a protective physical barrier against environmental impacts such as UV irradiation and is the first line of defense

against the invasion of microbiological agents. The skin also plays a crucial role in maintaining body temperature, electrolyte and fluid balance and providing a sensory function (Chuong *et al.* 2002).

A histological section in Figure 1.1 demonstrates the two main layers in human skin, the dermis and the epidermis. The dermis is composed of fibroblasts and contains bundles of collagen which give the skin its characteristic elasticity, firmness and strength. It also plays an important role in thermoregulation and supports the vascular network of the skin. The focus of this thesis however, is on the most superficial layer of the skin, the epidermis. The epidermis is made up of several layers of epidermal keratinocytes that are responsible for maintaining the barrier function.

The skin's barrier function is attributed to the unique capacity of keratinocytes to undergo terminal differentiation, discussed in detail in the next section, in order to form a thin but highly effective layer of dead keratinocytes known as the stratum corneum. The stratum corneum is the outermost layer of the skin and represents a major component of the innate immunity and provides the first line of defense (Harder & Schroder 2005). Maintenance of barrier function is crucial, because if it is disrupted, the individual becomes susceptible to infection. To contend with bacteria, fungi or viruses breaking through this barrier, the immune system in the skin has evolved to respond quickly. Keratinocytes possess various pathogen recognition alert signalling systems and produce a wide assortment of anti-infectious agents including complement,

defensins, cathelicidins, cytokines, chemokines and reactive oxygen species (Nicholson *et al.* 1995, Park & Barbul 2004).

1.2 Keratinocyte differentiation

Keratinocyte differentiation is a dynamic self-renewing process that ensures homeostasis of the epidermis and maintenance of barrier function. Basal keratinocytes are mitotic cells located in the basal layer on the basement membrane (Figure 1.1). The basal layer consists of a population of long-lived stem cells that cycle slowly and produce a large pool of actively dividing, but short-lived transient amplifying cells (Webb *et al.* 2004). These transient amplifying cells proliferate and then migrate from the basal layer to form post mitotic suprabasal cells in the spinous layer. Associated with their differentiation, suprabasal cells undergo a series of morphological and biochemical changes and produce different patterns of intermediate filament proteins called keratins. These cells then form the granular layer (Polakowska *et al.* 1994). Due to decreased blood supply from the dermis, live cells in the granular layer begin to lose their nucleus. Finally, the keratinocytes terminally differentiate resulting in the complete disintegration of the nucleus, mitochondria and ribosomes. These non-metabolic, differentiated cells (corneocytes), accumulate and form a rigid cornified envelope called the stratum corneum (Mammone *et al.* 2000a, Norris 1995, Schoop *et al.* 1999). The final stage of differentiation involves cleavage of profilaggrin into 10–12 copies of the 37-kDa filaggrin protein (Gan *et al* 1990). These polypeptides aggregate the keratin cytoskeleton system to form a dense protein lipid matrix that is cross-linked by transglutaminases results in the formation of the cornified cell envelope (Palmer *et al* 2006) together with

Figure 1.1

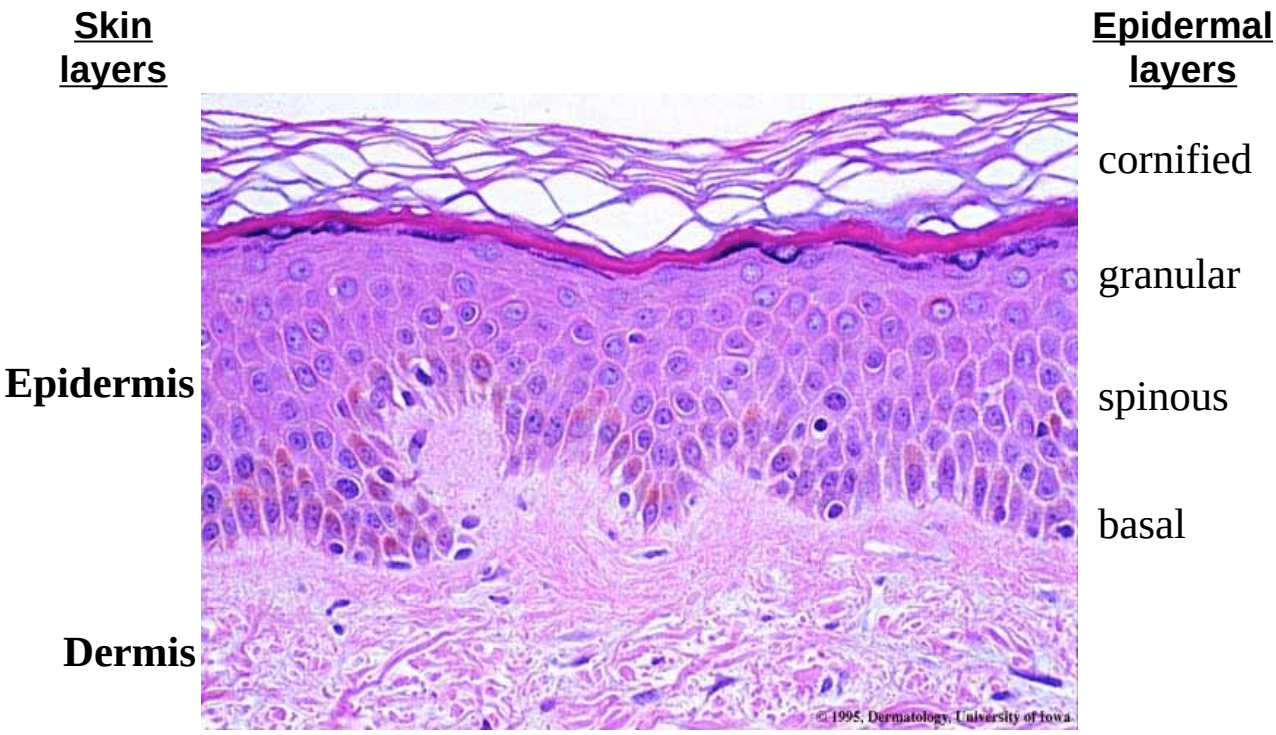

Figure 1.1- Representative histological section of human skin. The skin is composed of two layers, the outer epidermis and the underlying dermis. The epidermis is made up of principally keratinocyte cells which are anchored to a basement membrane. The epidermis has four main layers: the cornified layer or stratum corneum, the granular layer or stratum granulosum, the spinous layer or stratum spinosum, and the basal layer or stratum basale. The keratinocytes in the granular, spinous and basal layers are the living and growing cells of the epidermis which mature, and gradually move up towards the surface of the skin where they die and become part of the stratum corneum.The stratum corneum is the layer of dead keratinocytes that forms a protective barrier over the underlying living cells.

the production of structural proteins such as involucrin and loricrin (Polakowska *et al.* 1994). This structure prevents epidermal water loss and also impedes the entry of allergens, toxic chemicals and infectious organisms.

1.2.1 Keratinocyte cell death

The process of keratinocyte terminal differentiation is a specialised, developmentally associated form of programmed cell death (Henseleit *et al.* 1996, Polakowska *et al.* 1994). Due to keratinocytes being constantly exposed to adverse environmental stimuli, they are challenged to avoid premature cell death, as this would compromise barrier function. Consequently, keratinocytes have developed resistance against environmental or chemical stressors by tightly regulated keratinocyte proliferation, differentiation and death pathways. However, under particular stimuli, keratinocytes are forced to self-destruct by one of two mechanisms, these being necrosis or apoptosis.

1.2.1.1 Necrosis

Keratinocyte necrosis may be caused by toxic chemical or physical trauma and results in damage to cell organelles and the cell membrane (Henseleit *et al.* 1996). Necrosis is morphologically characterised by disruption of membranes and rapid induction of inflammation (Henseleit *et al.* 1996, Kerr *et al.* 1979). Exposure to high doses of UV radiation is often responsible for keratinocyte necrosis, inducing immediate membrane and organelle damage (Mammone *et al.* 2000a).

1.2.1.2 Apoptosis

Unlike necrosis, apoptosis is an active, energy dependent and genetically controlled process of self-destruction, which is induced in skin by physical, pharmacological or environmental stimuli (Henseleit *et al.* 1996, Mammone *et al.* 2000a, Norris 1995). Although resulting in the same end-point as necrosis, apoptosis is a morphologically distinct form of cell death. Apoptosis is characterised by cell shrinkage, membrane blebbing, condensation of the cytoplasm and nucleus, chromatin fragmentation and dispersion of cells into apoptotic bodies. These are often phagocytosed by neighbouring cells (Haake & Polakowska 1993, Kerr *et al.* 1972).

Differing from keratinocyte terminal differentiation, which also leads to de-nucleation (Schoop *et al.* 1999), apoptosis results in DNA fragmentation by activation of DNA fragmentation factor (DDF) resulting in DNA cleavage and ultimately the disassembly of the cell (Gandarillas *et al.* 1999, Liu *et al.* 1997, Polakowska *et al.* 1994). Terminally differentiating keratinocytes also synthesise keratin proteins, which are important for the maintenance of skin barrier function and are not a feature of cells undergoing apoptosis (Marks 2004). Apoptosis and terminal differentiation are also temporally disassociated, such that terminal differentiation occurs progressively over a period of two-four weeks, whereas once induced, apoptosis can result in elimination of cells within hours (Gandarillas *et al.* 1999, Kerr *et al.* 1972).

Apoptosis plays an important role in the development and maintenance of tissue homeostasis, for example in promoting resolution of inflammation by inducing T-

lymphocyte death, which prevents excessive immune reactivity (Kobayashi *et al.* 2003). It is generally considered that keratinocyte apoptosis has evolved to ensure the removal of damaged cells, particularly those with unrepairable DNA damage generally caused by UV radiation, which could ultimately result in skin carcinoma (Soehnge *et al.* 1997).

1.3 Death receptor pathways

Keratinocyte apoptosis may be induced by activation of death receptor pathways from the tumor necrosis factor (TNF) family including tumour necrosis related apoptosis-inducing ligand receptors (TRAIL-R) and Fas. TRAIL is a recently identified molecule characterized by its ability to induce apoptosis in many cancer and transformed cell lines including HaCaT keratinocytes (Leverkus *et al.* 2003). The sensitivity to TRAIL induced apoptosis of keratinocytes differs between differentiated and undifferentiated cells, since undifferentiated cells are more susceptible to apoptosis (Jansen *et al.* 2003).

1.3.1 Fas induced apoptosis

Apoptosis can be induced upon interaction of the death receptor Fas (CD95) with Fas ligand (FasL/CD178) (Quirk *et al.* 1998). Both Fas and FasL are expressed in the epidermis (Viard-Leveugle *et al.* 2003) with increased Fas expression by keratinocytes in UV irradiated skin suggesting that death via Fas activation plays an important role in UV-induced keratinocyte apoptosis (Mammone *et al.* 2000a). Fas may also be important in the pathogenesis of inflammatory skin disorders such as AE and psoriasis as high levels of Fas are expressed by keratinocytes in lesional skin (Norris 1995). The events

downstream of the Fas/FasL interaction involve the binding of cytoplasmic Fas antigen death domain (FADD) to the receptor complex and recruitment of the protease caspase 8 or FLICE/MACH (Kuwana *et al.* 1998) to initiate a cascade of proteolytic events.

1.3.2 The Caspase Cascade

Death receptor-triggered apoptosis initiates an intracellular cascade in which a series of cystein proteases known as caspases become activated resulting in cleavage of cellular substrates, activation of endonucleases, nuclear fragmentation and cell death (Quirk *et al.* 1998). Apoptosis can proceed by either the extrinsic (type I) or intrinsic (type II) pathways shown in Figure 1.2 a and b respectively. The extrinsic apoptosis pathway is activated in type I cells by the formation of the death inducing signalling complex (DISC). This occurs upon Fas activation, recruitment of the cytoplasmic FADD and the protease caspase 8 (Barnhart *et al.* 2003, Kuwana *et al.* 1998). Caspase 8 cleaves plectin, a major cross-linking protein involved in apoptosis-induced reorganization of the actin cytoskeleton, which results in membrane alteration and phosphotidylserine (PS) translocation (Barnhart *et al.* 2003, Stegh *et al.* 2000a). Caspase-8 activation also induces the cleavage of downstream effector caspases such as caspase 3, 6 and 7 which are responsible for the characteristic changes associated with apoptosis such as nuclear condensation and fragmentation (Figure 1.2 a; (Ortiz *et al.* 2001)). In contrast, type II cells rely on mitochondrial amplification of the death signal and activation of the intrinsic pathway. This involves caspase 8 cleavage and activation of pro-apoptotic Bcl-2 family members resulting in a change in mitochondrial outer membrane permeability and integrity leading to the release of cytochrome *c* (Kuwana *et al.* 1998, Moreau *et al.*

2003). Cytochrome *c*, adaptor protein Apf-1 and pro-caspase 9 form an apoptosome that activates caspase-9, which in turn activates effector caspase 3 (Figure 1.2 b; (Barnhart *et al.* 2003)).

Caspase 3 is considered the major executioner enzyme. It cleaves Poly (ADP-ribose) polymerase (PARP), a DNA-binding enzyme involved in genome surveillance and DNA repair, generating two inactive fragments (Decker & Muller 2002). PARP cleavage induces the subsequent release of apoptosis-inducing factor (AIF) that is involved in causing chromatin condensation (Hong *et al.* 2004). Caspase 3 also activates the DNA fragmentation factor (DDF) resulting in DNA cleavage and fragmentation and ultimately the disassembly of the cell (Hirata *et al.* 1998, Liu *et al.* 1997, Maher *et al.* 2002, Quirk *et al.* 1998)

1.4 Atopic eczema

Atopy is defined as hypersensitivity of skin and mucus membranes to environmental substances and is associated with an increase in IgE production (Hanifin & Chan 1995, Jeong *et al.* 2003, Moore *et al.* 1993). It has been demonstrated that the majority of children with AE exhibit high serum levels of allergen specific IgE (Novak *et al.* 2003). The onset of AE can occur in the first weeks or months of life, although it may disappear as the child matures, it can also persist into adult life (Charman & Williams 2002, Kemp 1999). Most children with AE also develop other atopic disorders including perennial allergic rhinitis or asthma later in life (Kluken *et al.* 2003, Leung 2000). The IgE-

Figure 1.2

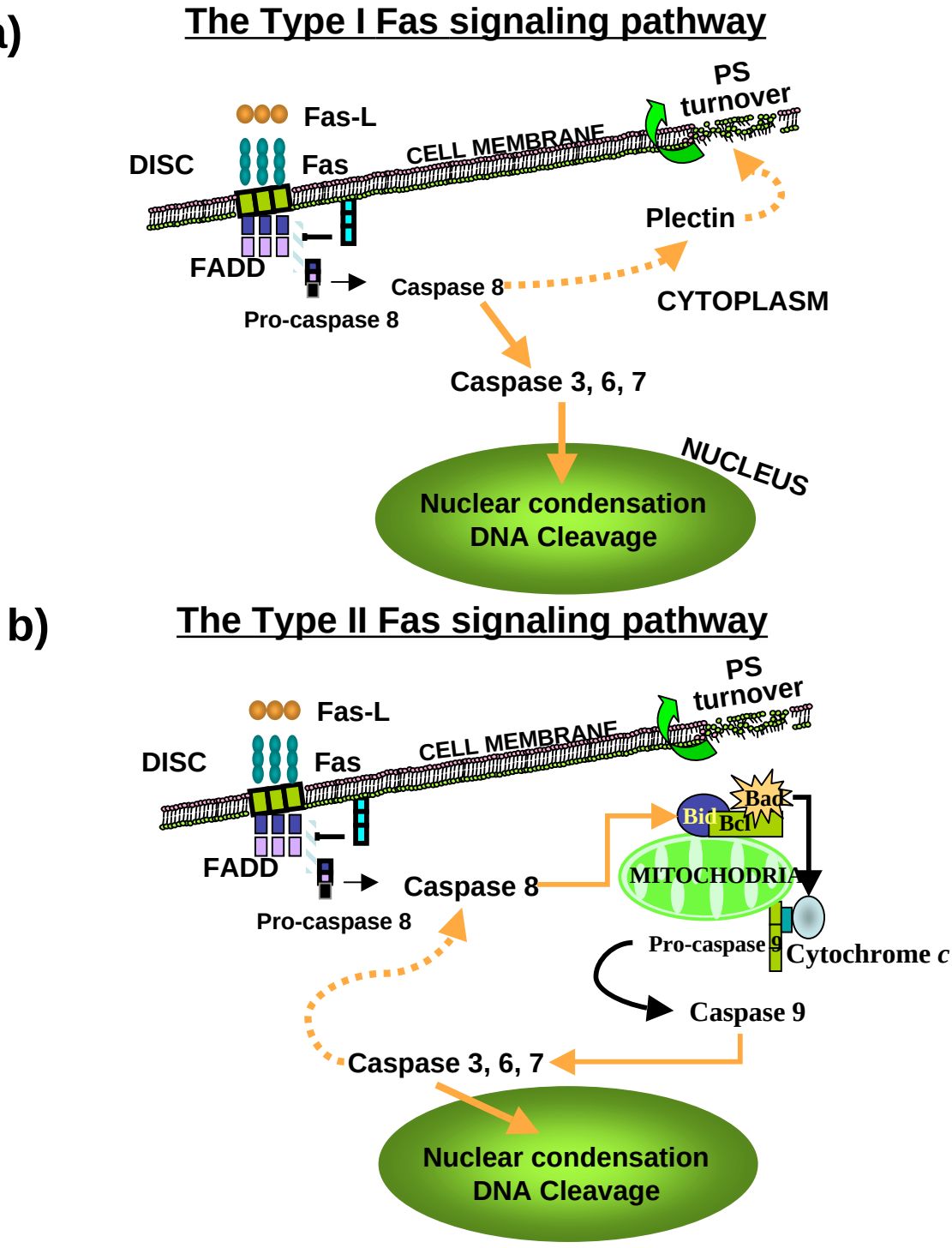

Figure 1.2- The Fas signalling pathways. a) The Type I Fas signalling pathway or extrinsic pathway is activated upon the binding of Fas to FasL and subsequent activation of the apoptotic signaling through a cytoplasmic domain (death domain) that interacts with signaling adaptors including FADD to activate the caspase cascade. Caspase-8 is the first activated, to then cleave and activate downstream caspases. b) the Type II Fas signalling pathway or intrinsic mitochondrial pathway involves Fas to FasL interaction, activation of caspase 8 and subsequent release of cytochrome c from mitochondria, self-cleavage and activation of caspase-9. Caspase-3, -6 and-7 are downstream caspases that are activated by the upstream proteases and cleave a variety of cellular substrates that lead to cell death.

mediated allergic response in AE is often triggered and maintained by common environmental factors such as aeroallergens, food allergens or autoallergens, irritants and microbial factors (e.g. *Staphylococcus aureus*) (Charman & Williams 2002, Kluken *et al.* 2003, Wuthrich & Schmid-Grendelmeier 2002).

1.4.1 Impact of atopic eczema

AE is a disorder that can have considerable effects on the individual, due to a large proportion (~60%) of children reported to suffer sleep deprivation from pruritus-induced scratching. One study reported that the morbidity scores of AE rate highly when compared to other skin diseases due to the physical impact of the condition on children, which often results in significant psychosocial problems (Charman & Williams 2002). Moreover, AE can also be a considerable financial burden on a family with direct costs of treatment and indirect loss of employment by carers estimated to be between AUD$1142 per year for a child with mild eczema to AUD$6099 per year for a child with severe eczema (Jenner *et al.* 2004, Kemp 1999).

1.4.2 Prevalence and diagnosis of atopic eczema

Eczematous disorders account for a large proportion of all skin diseases and constitute a major health problem worldwide. In the past three decades an increase in the prevalence of AE has been observed, especially in westernised countries (Ring *et al.* 2001). In particular, the International Study of Asthma and Allergies in Childhood in 2002 identified Australia to be among the countries having a very high incidence of AE

(Kemp 1999). One theory for explaining the increasing prevalence of this disease is the "hygiene hypothesis". This theory contends that children in Western countries are leading a cleaner life resulting in less exposure to dirt, due to improved household amenities and higher standards of personal cleanliness. This in turn results in immune systems having less exposure to parasites and other pathogens and a more widespread incidence of atopic disease (Strachan 1989, Strachan 2000).

AE has been identified as a complex multifactorial disease. Wide variations in prevalence identified both within and between countries inhabited by similar ethnic groups suggest that environmental factors are critical in determining the incidence of this disease (Leung 2000). However, genetic factors are thought to also play a dominant role in predisposing for this condition, since the incidence rate doubles if one parent has AE and is tripled if both parents are affected (Kluken *et al.* 2003). As such, positive parental history of allergy is the strongest risk factor associated with the occurrence of AE. The development of AE also appears to be influenced by the major histocompatibility complex class II genes on chromosome 6 and the “interleukin cluster” on 5q23-31 (Elliott & Forrest 2002, Girolomoni *et al.* 2001, Wuthrich & Schmid-Grendelmeier 2002). Genome-wide analysis has shown several linkage peaks for AE, including the region of 1q21 encompassing the Filaggrin locus (encoded by FLG) (Cookson *et al.* 2001). Furthermore, two common independent loss-of-function genetic variants (R510X and 2282del4) of FLG were associated with a poorly formed stratum corneum and demonstrated to be very strong predisposing factors for atopic dermatitis.

Figure 1.3

a)

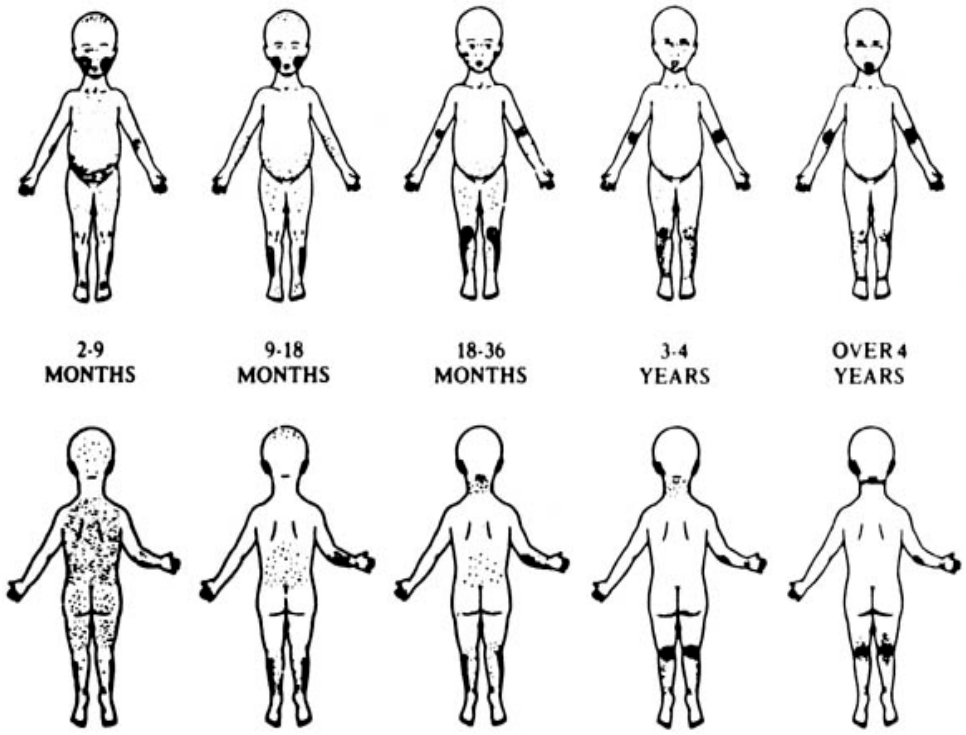

b)

c)

Figure 1.3- The clinical symptoms of atopic eczema. a) typical distribution of atopic eczema lesions: Facial and extensor surfaces in infants and young children and flexure lichenification in older children and adults. b) and c) demonstrate the typical morphology and distribution of atopic eczema lesions such as facial rash in an infant and rash in flexural regions in older children and adults.

This would indicate that heritable skin barrier defects involving 1q21-encoded epithelial barrier proteins may be highly prevalent or even a prerequisite for atopic dermatitis (Palmer *et al*. 2006). Together these provide further evidence of genetic involvement in this disorder.

The current diagnosis of AE is based on the personal or family history of atopic disease and a typical distribution of lesions found predominantly on the facial and extensor surfaces of infants (Figure 1.3 a and b), and flexural regions of older children and adults (Figure 1.3 a-c) (Parnia & Frew 2000). Other clinical symptoms include the presence of cutaneous hyper-reactivity, dry skin and intense pruritus which leads to scratching and subsequent trauma-induced inflammation and impaired barrier function (Leung 2000).

1.4.3 T-lymphocyte response

AE is thought to be mediated primarily by T-lymphocytes. This section will discuss in general the different T-lymphocytes and their subtypes, followed by their involvement in skin inflammation.

T-lymphocytes express an array of T-lymphocyte surface molecules during maturation in the thymus. T-lymphocytes begin as Th0 type cells (Biedermann *et al.* 2004) and then become either cytotoxic, characterised by the surface expression of CD8, or helper T-lymphocytes, which are characterised by CD4 expression. It has been demonstrated that the dermal cellular infiltrate in AE and allergic contact dermatitis contains both CD8+ and CD4+ T-lymphocytes (Akdis *et al.* 2000, Girolomoni *et al.* 2001, Traidl *et al.* 2000).

CD8+ T-lymphocytes can respond to superantigen stimuli and these T-lymphocytes contribute to the production of IgE and increase the IgE receptor FceRI expression (Leung & Boguniewicz 2003). CD8+ T-lymphocytes have also been associated with stimulating eosinophil survival in eczema lesions (Akdis *et al.* 2001). Allergen specific T-lymphocyte responses to food and aeroallergens are confined however to CD4+ T-lymphocytes. CD4+ T-lymphocytes are further subdivided into either Th1 (Type 1) or Th2 (Type 2) as defined by their distinct cytokine profiles (Zhang *et al.* 1998).

1.4.3.1 Th1 T-lymphocyte response

Th1 cells drive cell-mediated immunity against viral, fungal, and myobacterial infections in the skin. They express chemokine receptors CCR5 and CXCR3 and are attracted by ligands such as CCL5 (RANTES) and CXCL9-10 (Mig, IP-10) (Girolomoni *et al.* 2001, Sebastiani *et al.* 2002). Th1 cells produce potent pro-inflammatory cytokines such as IFNγ, TNFα, interleukin-2 (IL-2) and IL-17, and in conjunction with antigen presenting cells (APC) they produce IL-12 (Akdis *et al.* 2000).

1.4.3.2 Th2 T-lymphocyte response

Th2 cells are directly associated with allergic inflammation, promotion of humoral immunity and enable production of antibodies by B-cells (Nomura *et al.* 2003). They express chemokine receptors CCR3, CCR4 and CCR8 and are attracted by chemokines CCL17/thymus and activation regulated chemokine (TARC) (Leung & Boguniewicz 2003, Sebastiani *et al.* 2002, Vestergaard *et al.* 2000). Th2 cells produce cytokines

including IL-4, IL-13, and IL-5 (Nomura *et al.* 2003). Th2 inflammation in the skin is promoted by IL-10 and Prostaglandin E_2 (PGE_2) from activated monocytes (Werfel T 2002).

1.4.4 The T-lymphocyte response in atopic eczema

Figure 1.4 overviews of the cellular events that occur in the development of AE. In AE, presentation of an allergen by APC triggers T-lymphocyte activation and clonal expansion in the lymph nodes. T-lymphocytes then migrate and infiltrate into the skin causing erythema (Werfel T 2002). Almost all of the T-lymphocytes homing to the skin are Th2 and express the cutaneous lymphocyte-associated antigen (CLA) molecule on their surface (Akdis *et al.* 2000, Akdis *et al.* 2003).

In this early acute phase of the disease, Th2 also expressing CCR4+ cells are attracted to the skin by CCR4 agonist CCL17/TARC released by allergen activated keratinocytes (Nakatani *et al.* 2001, Sumiyoshi *et al.* 2003, Zheng *et al.* 2002) (Figure 1.4). Evidence of increased IL-4 mRNA levels on skin patch tests from atopic patients, demonstrated that this T-lymphocyte response occurs within 24 hrs of allergen exposure (Thepen *et al.* 1996). The Th2 cytokines then promote eosinophil infiltration, which is associated with the maintenance of chronic inflammation (Spergel *et al.* 1999), and help B cells produce IgE and IL-13 (Trautmann *et al.* 2000a). Although acute AE is characterized by a Th2 response resulting in increased IL-4, IL-5 and IL-13 levels, as the disease progresses over time, there is a shift from a Th2 towards a chronic Th1 response (Figure 1.4). The Th1 response in AE is characterised by increased levels of IFNγ and reduced levels of

Figure 1.4

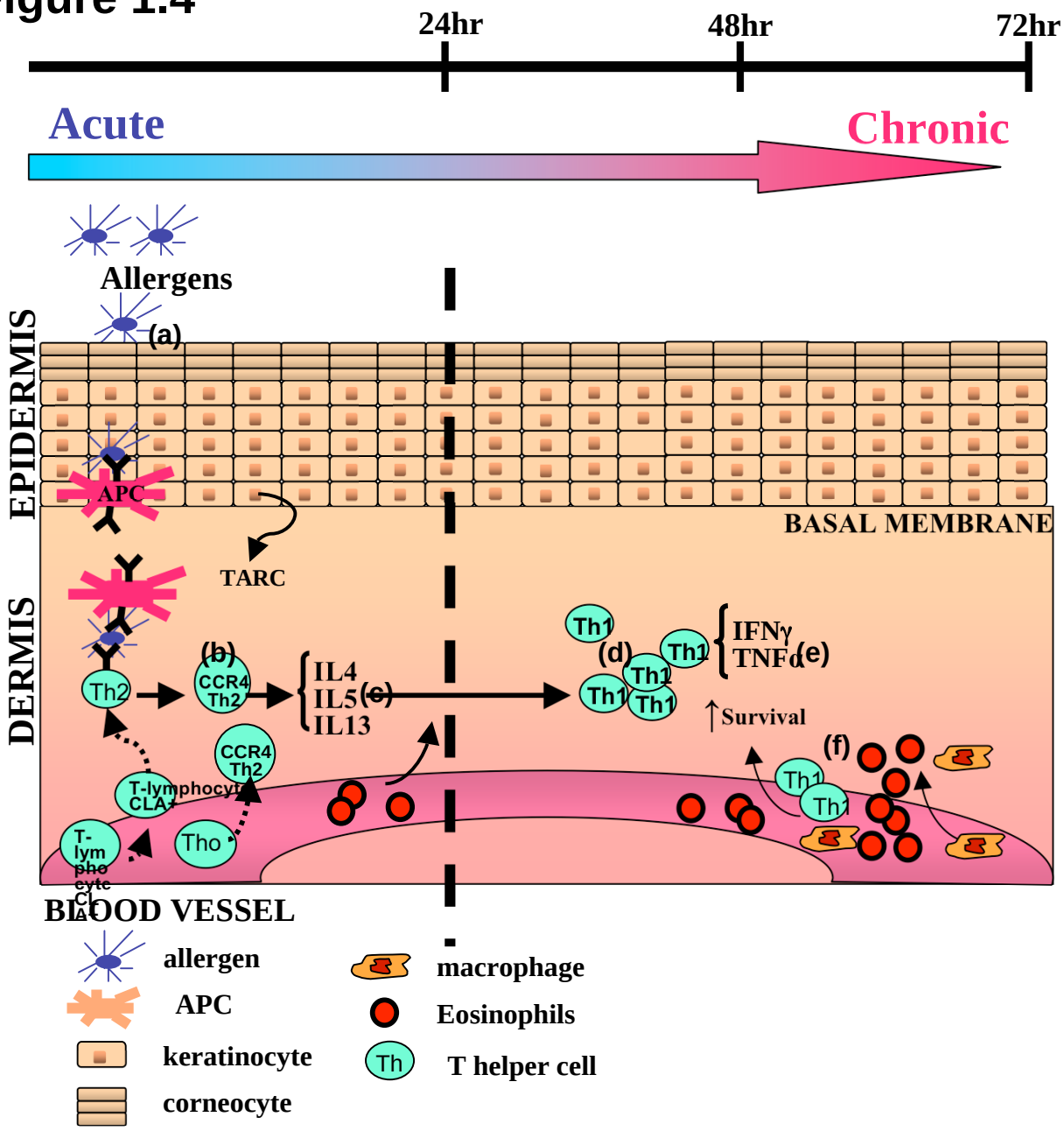

Figure 1.4- The cellular events in atopic eczema. Allergen-specific T-lymphocytes (T-lymphocytes) from peripheral blood of AE patients show a dysregulation of Th1 and Th2 T-lymphocyte cytokines. (a) Antigen presenting cells trigger T-lymphocyte activation and clonal expansion upon presentation of an allergen at the surface of skin. (b) In the early acute phase of the disease, Th2 T-lymphocytes expressing CCR4+CLA+ are attracted to AE skin by TARC which is released by allergen activated keratinocytes. These CCR4+CLA+ T-lymphocytes migrate and infiltrate into the skin causing erythema. (c) There is an increase in IL4, IL5 and IL13 involved in promoting eosinophil infiltration and survival. (d) The disease progresses towards chronic inflammation associated with a Th1 response. (e) The Th1 cytokines (IL-2 IFNγ, TNFα) play an important role in cell-mediated immunity, skin hypertrophy and T-lymphocyte growth and activation. (f) An increase in survival of Th1 T-lymphocytes in AE lesions, result in persistent inflammation and further infiltration of eosinophils and microphages into the skin which contribute to the elicitation and progress of AE. The figure is a modification from **Leung et al, 2000.**

IL-4 and IL-13 in AE skin (Spergel *et al.* 1999). Consistent with this report, Thepen et al, have demonstrated an increase in IFNγ mRNA expression levels in T-lymphocytes from AE patients 48 to 96 hrs after challenge skin patch tests (Thepen *et al.* 1996). Increased Th1 cell survival in the skin and persistence of the chronic response is characteristic of the dysregulated immune response to allergens that occus in AE.

1.4.5 Dysregulated immune response in atopic eczema

The skin in AE patients is characterised by increased immigration and retention of inflammatory T-lymphocytes resulting in an earlier and more pronounced inflammatory response. During inflammation, excess and damaged T-lymphocytes are removed by a process called activation induced cell death (AICD) (Schmitz *et al.* 2003). AICD is a form of apoptosis that plays an important role in maintaining homeostasis of the immune response by promoting its resolution (Buckley *et al.* 2001, Kobayashi *et al.* 2003). In conditions such as AE, it has been suggested that the resolution phase becomes disordered in the skin of patients with AE, resulting in increased T-lymphocyte survival in the skin as well as increased allergen specific IgE (Akdis *et al.* 2000, Strauss *et al.* 2003, Trautmann *et al.* 2000a). This leads to a further increase in T-lymphocyte activation and subsequent secretion of inflammatory cytokines (Lomo *et al.* 1995, Sebastiani *et al.* 2002, Trautmann *et al.* 2000b). Consequently these cytokines enhance the allergic response by supporting the hyper induction of IgE and promote eosinophil survival ultimately resulting in a chronic persistent inflammation (Akdis *et al.* 2002) (Figure 1.5). The dysregulated response of T-lymphocytes to allergens and increased T-lymphocyte survival has been suggested to be largely influenced by the

microenvironment within the epidermis and the dermis, which further contributes to the pathogenesis of AE and allergic contact dermatitis (ACD) (Buckley *et al.* 2001, Trautmann *et al.* 2001a).

1.4.6 Keratinocyte apoptosis in atopic eczema

T-lymphocyte induced keratinocyte apoptosis is one of the key pathological events responsible for the development of skin lesions. The cellular events that occur from the dysregulated immune response which result in keratinocyte apoptosis in AE are illustrated in Figure 1.5.

Activated T-lymphocytes in skin lesions have been shown to express and secrete high levels of FasL (Trautmann *et al.* 2000a). Some of these FasL expressing T-lymphocytes penetrate the basement membrane and reach the intracellular space between epidermal keratinocytes. As described in Section 1.4.4, in the chronic phase of AE there is an increase in IFNγ. IFNγ contributes to the disease by inducing keratinocyte Fas expression (Trautmann *et al.* 2000a). The binding of T-lymphocyte associated FasL or soluble FasL to increased keratinocyte Fas in the epidermis is thought to ultimately result in keratinocyte apoptosis (Henseleit *et al.* 1996, Traidl *et al.* 2000, Trautmann *et al.* 2000a) (Figure 1.5 a).

Once keratinocytes have been induced to undergo apoptosis, intercellular cohesion is disrupted and they form apoptotic bodies. This in turn results in increased vesiculation known as epidermal spongiosis; the visible histological hallmark of the epidermis in AE,

Figure 1.5

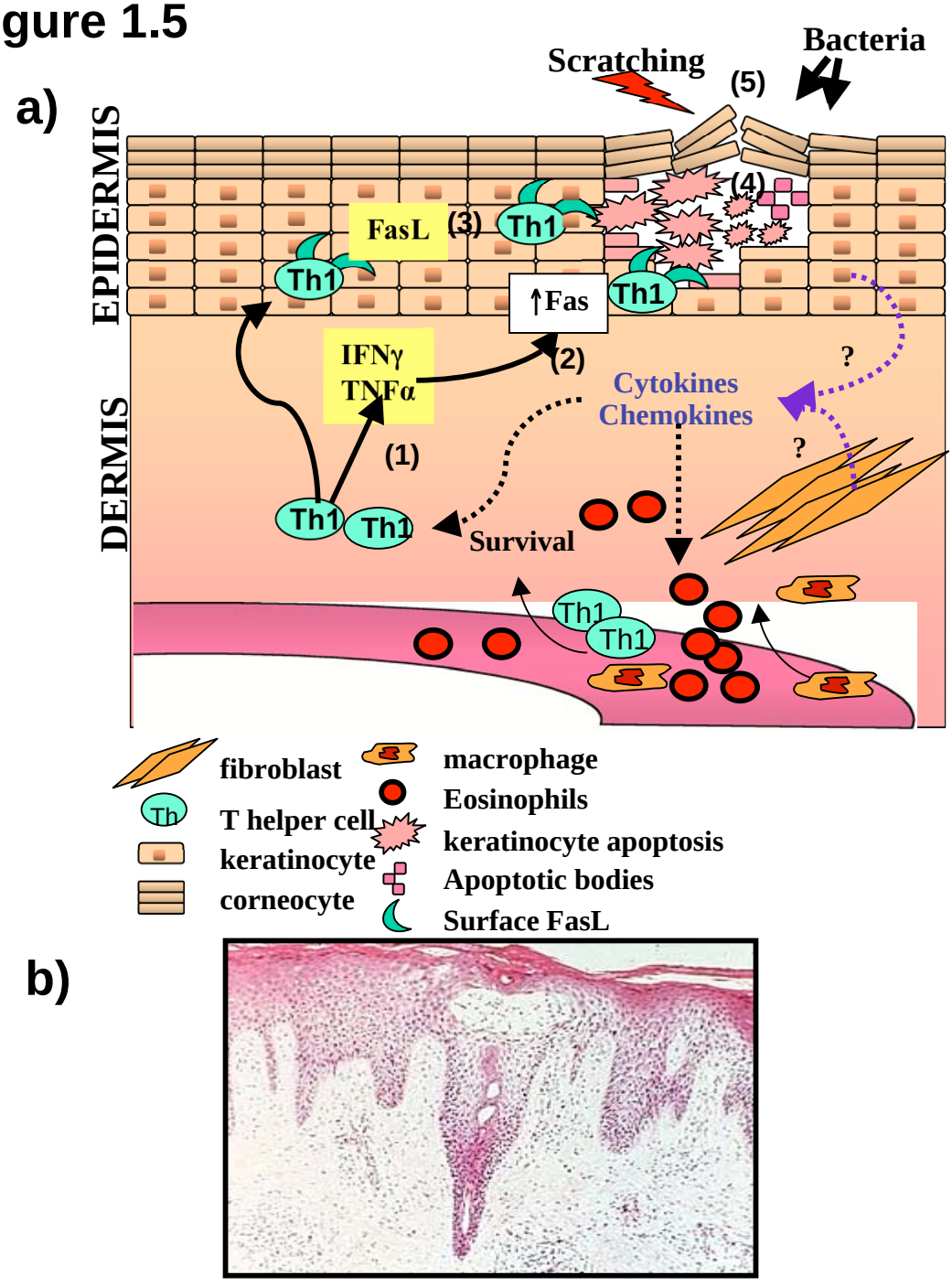

Figure 1.5- Keratinocyte apoptosis in atopic eczema. a) T-lymphocytes induce keratinocytes apoptosis in atopic eczema. The key pathogenic steps involve (1) IFNγ secreted by activated CD4+ T-lymphocyte (T helper)) in the skin enhance the expression of (2) Fas on keratinocytes. (3) The infiltration of activated T-lymphocyte into the epidermis results in the interaction of T-lymphocyte-bound and soluble Fas ligand produced by activated T-lymphocyte with Fas on the keratinocytes subsequent activation of the apoptotic pathways (4). The apoptosis of keratinocytes results in impairment of the cohesion between keratinocytes (spongiosis), DNA fragmentation and apoptotic body formation. (5) Finally, keratinocyte apoptosis together with scratching results in disrupted barrier function, allowing more allergens and bacteria into the skin lesion. The figure is a modification from **Trautmann et al, 2000.** b) Spongiosis, a histologic hallmark of atopic skin characterized by keratinocyte apoptosis, intercellular edema and intra-epidermal vesicles.

and impairment of barrier function (Trautmann *et al.* 2001b, Trautmann *et al.* 2001a) (Figure 1.5 b). Trauma from scratching due to increased pruritus also contributes to barrier disruption (Nomura *et al.* 2003). Loss of barrier function makes the skin more susceptible to infectious agents and more accessible to allergens, thus promoting amplification of the inflammatory process (Akdis *et al.* 2000, Buckley *et al.* 2001) (Figure 1.5 a).

1.4.7 The role of keratinocytes in atopic eczema

In AE patients, allergen activated keratinocytes contribute to the abnormal levels of cytokine and chemokine production in the skin (Giustizieri *et al.* 2001, Goebeler *et al.* 2001). This abnormal microenvironment favours the persistence of inflammation and contributes to increased keratinocyte apoptosis.

Keratinocytes from AE patients release increased amounts of the cytokines IL-1a, IL-1 receptor antagonist and TNFα which magnify the inflammatory response, as well as increase levels of granulocyte macrophage colony stimulating factor (GM-CSF), that is known to promote the proliferation of eosinophils (Pastore *et al.* 1997, Pastore *et al.* 1998). Keratinocytes from AE patients also respond differently to inflammatory stimuli compared to normal keratinocytes. When exposed to T-lymphocyte cytokines such as IFNγ, TNFα and IL-4, they release the pro-inflammatory chemokines CXCL10 and CCL17 which help recruit T-lymphocytes into the skin. It has also been demonstrated that keratinocytes from atopic patients express high affinity receptors for IFNγ (Pastore *et al.* 1998, Sayama *et al.* 1994). The retention of T-lymphocytes and eosinophils by

keratinocytes in AE skin is attributed to the increase in adhesion molecule expression such as adhesion molecule-1 (ICAM-1), vascular cell adhesion molecule-1 (VCAM-1), E-selectin, and P-selectin (de Vries *et al.* 1998). Supporting this view, it has been shown that inflammatory cytokines released during inflammation, including IFNγ, TNFα or IL-4, assist the retention of T-lymphocytes in the skin by increasing adhesion molecule expression (Akdis *et al.* 2001, de Vries *et al.* 1998, Sayama *et al.* 1994, Sumiyoshi *et al.* 2003).

1.5 Current therapies for atopic eczema

Current therapies can suppress the symptoms of AE, however they cannot cure the disease. The current regimes include identifying and eliminating initiating factors such as allergens, the use of antihistamines, conventional anti-inflammatory agents or alternative therapies. In some patients first generation oral H1 antihistamines may offer some symptomatic relief of the pruritus (Leung & Boguniewicz 2003). However, these agents have sedative effects and should not be used in children. UV light therapy may be considered for patients who are resistant to conventional therapy with chronic recalcitrant AE, as it appears to have anti-inflammatory and antibacterial effects (Aragane *et al.* 1998). Furthermore, the use of alternative therapies such as intravenous immunoglobulins (IVIg), a blood product prepared from the pooled plasma of healthy donors, also has been investigated and shown to benefit patients with severe AE, potentially by modulation of the mediators of the disease (Jolles *et al.* 2000, Trautmann *et al.* 2001c, Viard *et al.* 1998).

1.5.1 Anti-inflammatory therapies targeting T-lymphocyte activation

Topical corticosteroids are potent anti-inflammatory drugs commonly used for treating mild to moderate AE. These anti-inflammatory agents suppress the immune response primarily by decreasing T-lymphocyte activation. T-lymphocyte activation is inhibited by decreasing the expression of transcription factors such as AP-1 and NF-κβ (Trautmann *et al.* 2001c). Corticosteroids have also been reported to potentially control skin inflammation by regulating the gene expression of chemokines involved in the recruitment of T-lymphocytes (Langeveld-Wildschut *et al.* 2000). Furthermore, high-dose dexamethasone also directly inhibits Fas-mediated keratinocyte apoptosis (Trautmann *et al.* 2001c). However, the long-term use of corticosteroids is associated with a number of adverse side-effects such as skin atrophy (Leung & Boguniewicz 2003).

Therapeutic trials using corticosteroid in combination with immunosuppressive agents such as cyclosporin A, have shown to be beneficial for patients with severe AE (Leung 2000). However, side effects associated with cyclosporin A include nausea, abdominal discomfort, paresthesis, hypertension, hyperbilirubinemia and renal impairment. Discontinuation of this treatment often results in rapid relapse of the disease (Sidbury & Hanifin 2000).

More recently, the use of topical macrolide immunomodulators (TIMs) such as tacrolimus (FK506) and pimecrolimus (SDZ ASM 981) have been reported to reduce the clinical symptoms. They have also been shown to be effective at treating moderate to

severe AE in 70-80% of patients by inhibiting T-lymphocyte activation (Sidbury & Hanifin 2000). TIMs act by binding to immunophilins and form complexes that interfere with calcineurin and nuclear factor of activated T-lymphocytes, which in turn affects activation by IL-2 important for clonal expansion (Boguniewicz 2003). TIMs have been demonstrated to reduce pruritus within 3 days with no apparent side effects in adults or children, however, 20-30% of patients have shown to be unresponsive to treatment (Leung & Boguniewicz 2003, Reitamo 2002). Concerns about the risk of cancer by the use of TIMS have been proposed in a publication released in January 2006 by the US Food and Drug Administration (FDA) website (New warnings for two eczema drugs 2006). The FDA issued a black box warning on these compounds because of possible concerns of increased long-term malignancy risk due to systemic immunosuppression. To date, studies from clinical trials, systemic absorption, and post-marketing surveillance show no evidence for this systemic immunosuppression or increased risk for any malignancy (Ormerod *et al.* 2005, Arellano *at al.* 2007).

1.5.2 Can keratinocyte apoptosis be a therapeutic target?

There are no medications at present that specifically prevent keratinocyte apoptosis and the breakdown of the epidermal barrier, a key pathogenic mechanism in AE. Understanding the molecular mechanisms responsible for T-lymphocyte induced keratinocyte apoptosis may enable the development of therapeutic agents suitable for the treatment of AE. The identification of treatments that can target multiple aspects of AE, such as inflammation and keratinocyte apoptosis may provide a more effective option for patients that do not respond to current medications.

1.6 Growth Factors in skin homeostasis

Growth factors play an important role in normal human skin function as they regulate cell proliferation, migration and differentiation (Brown *et al.* 1997, Dahler *et al.* 2001, Hashimoto *et al.* 2000, Hyde *et al.* 2004). They help maintain skin homeostasis by providing a cell to cell communications system in a paracrine and autocrine manner. For instance, fibroblast growth factor (FGF) and keratinocyte growth factors (KGF or also known as FGF7) regulate keratinocyte proliferation and differentiation via a double paracrine loop between keratinocytes and fibroblasts (Sabine *et al.* 2001). Keratinocytes produce several members of the epidermal growth factor (EGF) family, such as transforming growth factor-alpha (TGFα), amphiregulin, and heparin-binding EGF-like growth factor (HB-EGF). These factors can regulate growth and differentiation of normal keratinocytes by serving as autocrine ligands for the EGF receptor (EGFR) (Barnard *et al.* 1994, Stoll *et al.* 1998, Feliciani *et al.* 1996) and have been shown to play an active role in cutaneous immunoregulation (Cook *et al.* 1991, Cook *et al,* 1990). Other growth factors such as PDGF, play the important role of stimulating growth of connective tissue during chronic inflammation and wound healing (Heldin *et al.* 1989, Paulsson *et al.* 1987) and to induce collagenase production and collagen synthesis (Tan *et al.* 1995).

Insulin-like growth factor-I (IGF-I) has been shown to play a critical role in normal epidermal development, as transgenic mice lacking the IGF-I receptor develop an abnormally thin epidermis with no spinous layer (Liu *et al.* 1993). Addition of IGF-I

enhances wound healing and skin regeneration by its ability to increase keratinocyte proliferation and migration (Hyde *et al.* 2004, Lynch *et al.* 1989) as well as playing a role in and melanocyte growth and function (Edmondson *et al.* 1999). Reports also demonstrate that IGF-I is involved in preventing apoptosis in response to UV and Fas mediated cell death (Decraene *et al.* 2002, Walsh *et al.* 2002, Wu *et al.* 1996). The transforming growth factor β (TGFβ) signalling pathway exerts a wide range of biological effects including suppressing growth and differentiation, regulating adhesion and induction of extracellular matrix proteins (Dahler *et al.* 2001, Hashimoto 2000, Hodge *et al.* 2002, Wang 2001). Similar to IGF-I, TGFβ isoforms also have profound effects in wound healing in the absence of increased inflammation (Amendt *et al.* 1998, Ferguson 1994, Lynch *et al.* 1989) and loss of TGFβ has been demonstrated to be implicated in malignant skin cancer progression (Cummings *et al.* 2004, Glick *et al.* 1993).

Despite the extensive literature on the role of there growth factors in skin, to date no studies have addressed their effect on keratinocyte apoptosis induced by T- lymphocytes in AE. The primary aim of this thesis is to determine if insulin-like growth factor-I (IGF-I) and transforming growth factor β_1 (TGFβ_1) can ameliorate T-lymphocyte induced keratinocyte apoptosis. To address this aim recombinant growth factors will be examined along with a milk derived growth factor extract containing TGFβ and IGF-I.

This section presents an overview of the role of IGF-I and TGFβ_1 in skin and introduces whey growth factor extract (WGFE), a natural source of IGF-I and TGFβ. This section

provides the rationale to supports the use of IGF-I, TGFβ_1 and WGFE as potential therapeutic approaches for treating AE.

1.6.1 IGF-I

IGF-I is a 70 amino acid, 7.6kDa, single chain non glycosylated polypeptide with a similar structure to insulin. IGF-I is produced by keratinocytes in the stratum granulosum or by dermal fibroblasts and acts through the IGF-I receptor (IGF-IR), which is highly expressed by basal keratinocytes in a paracrine manner (Rudman *et al*. 1997, Tavakkol *et al.* 1999, Barreca *et al.* 1992). The binding of IGF-I to IGF-1R results in the activation of signalling molecules including phosphoinositol 3-kinase and serine/threonin kinase Akt (protein kinase B; Figure 1.6 a) (Wu *et al.* 2004). Activation of these pathways elicits a variety of biological responses including cell survival (Decraene *et al.* 2002, Heron-Milhavet *et al.* 2001). IGF-I function is also modulated by a family of high affinity binding proteins (IGFBPs) that sequester free IGFs (Butt et al. 1999). IGFBP3 has been shown to be the major binding protein secreted by keratinocytes expressed exclusively by selected basal keratinocytes (Edmondson *et al.* 1999a, Edmondson *et al.* 2001). IGFBP3 has been suggested to also have IGF independent activity in the skin such as keratinocyte differentiation (Edmondson *et al.* 2001). When defining IGF-IR activation, the synthetic IGF-I analogue, LR3-IGF-I, which has a lower binding affinity to IGFBPs, is often used, as it has greater affinity for IGF-IR and has been shown to be more active in a physiological system than native IGF-I (Francis *et al.* 1992, Tomas *et al.* 1993).

1.6.2 TGFβ

Transforming growth factor-β (TGFβ) is a 25-kDa polypeptide involved in the regulation of many cell, tissue and organ functions. There are three distinct isoforms of TGFβ in mammals: TGFβ1, TGFβ2 and TGFβ3 and in skin these exert a wide range of biological effects. The effects of TGFβ are mediated by specific cell surface receptors: type I (TGFβR1), type II (TGFβR2) and type III (TGFβR3). TGFβ stimulates cells by binding to TGFβR2 receptor which phosphorylates TGFβR1 and results in subsequent activation of serine/threonine kinases (Wang 2001) (Figure 1.6 b). TGFβR1 has been shown to be restricted to the basal layer of normal skin with very little expression by the suprabasal layers, whereas TGFβR2 has been observed throughout the epidermis and by fibroblasts within the dermis (Cowin *et al.* 2001). The type III receptor has been proposed to present TGFβ to TGFβR2 by forming a non-covalent heteromeric complex (Lopez Casillas *et al.* 1994). The signal is then transmitted to the nucleus via activated Smad proteins and this signalling pathway is evident in keratinocytes (Gorelik *et al.* 2000, Shin *et al.* 2001, Sumiyoshi *et al.* 2003, Tam *et al.* 1998) (Figure 1.6 b). As the major signalling mediators of TGF superfamily, Smads are actively involved in maintaining skin homeostasis as well as tumor suppression during skin carcinogenesis (He W *et al.* 2001).

Several transgenic mouse models have been generated in which TGFβ family members have been targeted to the skin with different keratin or structural gene promoters. These models have produced distinct phenotypes ranging from inhibition of tumor promoter-

induced proliferative stimulation (Cui *et al.* 1995, Blessing *et al.* 1995), neonatal lethality, epidermal and follicular hypoproliferation (Sellheyer *et al.* 1993, Blessing *et al.* 1996), epidermal hyperproliferation, inflammation, and hair loss (Blessing *et al.* 1996). These studies would imply that in addition to its role in maintenance of skin homeostasis, alterations in TGFβ signalling pathway or differences in expression of TGFβ can contribute to skin carcinogenesis as well as produce significantly different phenotypes in the epidermis.

1.6.3 Growth factor effects in keratinocyte apoptosis

Deficiencies in growth factors have been demonstrated to lead to the activation of apoptosis pathways which subsequently result in nuclear condensation and DNA fragmentation (Brown & Phipps 1996, Quirk *et al.* 2000). The effects of IGF-I or TGFβ on T-lymphocyte induced keratinocyte apoptosis in the context of inflammatory skin diseases such as AE has not been previously examined. Studies using granulosa cells have demonstrated that combinations of IGF-1, epidermal growth factor (EGF) and basic fibroblast growth factor (FGF) have the capacity to inhibit inflammatory cytokine induced apoptosis by downregulating Fas expression (Quirk *et al.* 2000). Additionally, IGF-I has been shown to postpone the onset of UV-induced apoptosis in keratinocytes by its ability to activate the insulin-like growth factor-I (IGF-I) receptor and subsequent activation of phosphatidylinositol-3 kinase and MAP kinase. (Kuhn *et al.* 1999). There have also been reports that IGF-I promotes keratinocyte survival from UV-induced apoptosis through activation of IGF-1R mediated Akt (protein kinase B) and subsequent inhibition of the intrinsic caspase pathway by inhibiting BAD and caspase 9 activation

(Decraene *et al.* 2002). More recently, it has been shown that activation of the IGF-1R is capable of rescuing cells from UVB damage by increasing β-galactosidase activity, an enzyme that induces DNA repair (Heron-Milhavet *et al.* 2001).

TGFβ is also important for epithelial cell survival (Shin *et al.* 2001). It has been demonstrated that $TGF\beta_1$ can protect human keratinocytes (HaCaT) from serum-starvation induced apoptosis by activation of Akt (Shin *et al.* 2001), although its effect on T-lymphocyte induced keratinocyte apoptosis has not been previously investigated.

Even though the participation of the TGFβ system in inflammatory skin diseases such as AE has not been examined, Arkwright et al, demonstrated that children who were low producers of $TGF\beta_1$ are at higher risk of developing AE (Arkwright *et al.* 2001). Studies in $TGF\beta_1$ null mutated mice ($TGF\text{-}\beta_1$ (-/-)) have shown they spontaneously develop AE (Kulkarni & Karlsson 1993). These mice die within the first 3 weeks of (ex-utero) life as a result of multifocal inflammatory lesions and tissue necrosis leading to organ failure and development of progressive "waste syndrome" (Kulkarni & Karlsson 1993). Subcutaneous administration of $TGF\beta_1$ was demonstrated to suppress the skin lesions in these mice by decreasing infiltration of leukocytes and mast cells into the dermis, decreasing IgE levels and down regulating IFNγ production (Christ *et al.* 1994). These studies suggest that TGFβ may play an important role in the development of AE.

Figure 1.6

a)

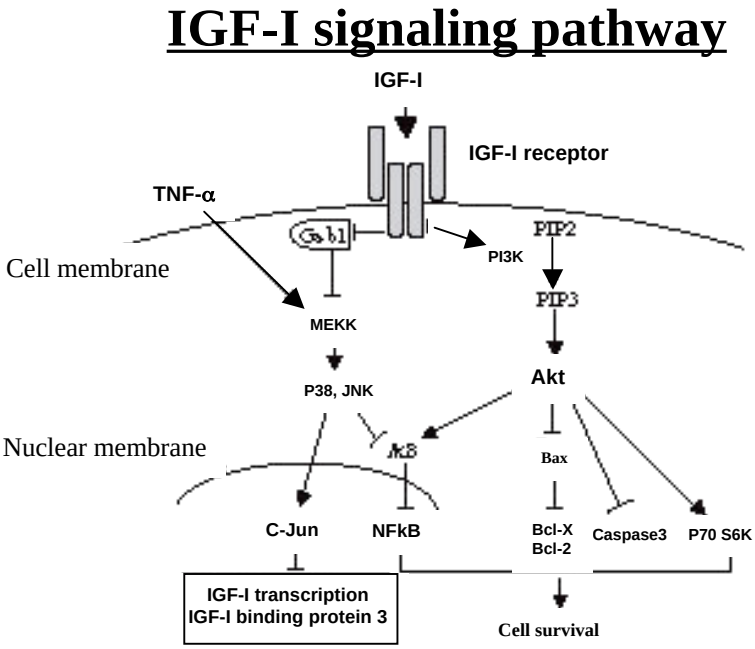

b)

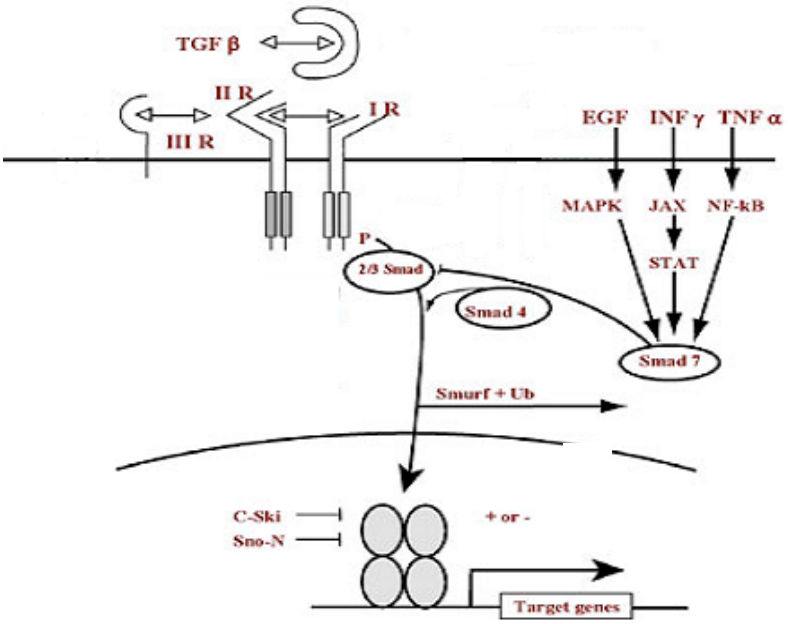

Figure 1.6- Growth Factor signalling pathways. a) The IGF-I signalling pathway is mediated by IGF-1R (figure modified from Wang M *et al.* 2003). IGF-1R stimulates PI3-kinase and the AKT to phosphorylate BAD and block apoptosis. A second pathway activated by IGF-1R involves ras mediated activation of the MAP kinase pathway to block apoptosis. b) The TGFβ signalling pathway (figure modified from Warburton D *et al.* 2003). TGFβ binding results in the formation of a ligand-receptor complex and activation of the type I receptor and subsequent phosphorylation of Smad2 and Smad3. Smad4 forms complexes with phosphorylated Smad2 and Smad3, and together they accumulate in the nucleus and bind to DNA. Smads can recruit coactivators to stimulate transcription or recruit corepressors to inhibit transcription.

1.6.4 Whey growth factor extract (WGFE) as a source of IGF-I and TGFβ

Milk is a rich source of biologically active compounds and many studies have demonstrated the immune-modulating effects of bovine milk derived products such as whey (Drenou *et al.* 1999, Stegh *et al.* 2000b). Milk and colostral whey consist of a complex mixture of proteins including: γ-globulin, β-lactobulin, α-lactalbumin, serum albumin, lactoferrin, lactoproxidase, hormones, prostaglandins and growth factors (Drenou *et al.* 1999).

Whey growth factor extract (WGFE) is a growth factor mixture refined from cheese whey that contains high levels of several growth factors including IGF-I, IGF-II, TGFβ, platelet-derived growth factor and member of EGF family; betacellulin (Belford *et al.* 1997, Francis *et al.* 1995, Rogers *et al.* 1996). This growth factor mixture has been shown to stimulate the growth of several mammalian cells *in vitro* including epithelial and fibroblastic cell lines (Belford *et al.* 1995, Francis *et al.* 1995) .

Pentilla et al. have demonstrated that WGFE can regulate immune function, as enteral administration of WGFE down regulated the peripheral immune response to oral antigen in sucking rats (Penttila *et al.* 2001). In addition to its immunomodulating effects, WGFE has been shown to stimulate wound repair activity *in vitro* and *in vivo* (Rayner *et al.* 2000), which is attributable to its ability to stimulate epithelial cell growth (Belford *et al.* 1995, Francis *et al.* 1995, Francis *et al.* 1997). WGFE also modulates the expression of the matrix metalloproteinases including MMP-2, -9 and TIMP-2 which are reported

to be elevated in chronic leg ulcers (Varelias *et al.* 2006). The anti-inflammatory and repair properties of WGFE in skin cells appear to be largely attributed to the IGF I & II and TGFβ content of the extract (Ishizaka *et al.* 1994).

The capacity of $TGF\beta_1$, IGF-I or purified whey extracts from bovine milk to protect or rescue keratinocytes from T-lymphocyte induced apoptosis is unknown. However, the ability of TGFβ and IGF-I to protect keratinocytes from apoptosis suggests these molecules may be suitable candidates for investigating their effect in protecting keratinocytes from T-lymphocyte mediated apoptosis.

1.7 Thesis Hypothesis

This project addresses the hypothesis that *"IGF-1, TGFβ and a milk derived growth factor extract containing TGFβ and IGF-I (WGFE) protects keratinocytes from T-lymphocyte mediated apoptosis"*.

1.7.1 Thesis aims

To address this hypothesis the studies in this thesis were divided into three main aims:

- Establish methods for measuring keratinocyte apoptosis

- Characterise the effect of T-lymphocytes on keratinocyte apoptosis

- Assess the capacity of TGFβ, IGF-I and WGFE to protect keratinocytes from T-lymphocyte induced keratinocyte apoptosis

CHAPTER 2

2 MATERIALS AND METHODS

2.1 Buffers and solutions

All chemicals used were of analytical grade.

2.1.1 Phosphate buffered saline (PBS)

A 20X PBS stock solution (pH 7.4) was prepared as 160 g NaCl, 4 g KCl, 23 g Na2HPO4, 4 g KH2PO4 (all from BDH Alamar, Kilsyth, AU) and dissolved in 1 litre of MilliQ water. 50ml of PBS stock solution was diluted into 950ml of MilliQ water to make up a 1x PBS solution (pH was re-adjusted pH 7.4).

Sterile PBS solution (JRH biosciences, Kansas, USA) was used in cell culture experiments. For flow cytometry phenotyping experiments, the PBS wash solution contained 0.09% sodium azide (Sigma Chemical Co.), 2% fetal bovine serum (FBS-Thermotrace, Melbourne, AU) and was stored at 4°C. The PBS wash buffer used for Western blot analysis contained 0.05% Tween 20 (Sigma Chemical) (PBST).

2.1.1.1 NP40 lysing buffer

NP40 lysis buffer (pH 7.4) was prepared with 5mM Tris-HCl (Amresco, Solon, Ohio) and 5mM EDTA (BDH Kilsyth, AU), 0.5% NP40 (Sigma Chemical Co.) in MilliQ water. The buffer was stored at room temperature.

2.1.1.2 SDS lysis buffer

Western Blot

SDS lysis buffer was prepared using 10% sodium dodecyl sulfate (SDS- Sigma Chemical Co.), 170 mM Tris-HCl, 22% glycerol (BDH Kilsyth, AU). Protease inhibitor at10ml/ml of cocktail set 1 (CalBiochem, La Jolla, CA) was added before use and the buffer was stored at -20°C.

DNA Ladder

Cell lysis buffer was prepared using 0.5% SDS, 50mM Tris-HCL (pH 8) and 20mM EDTA in MilliQ water.

2.1.1.3 Loading buffer

Loading buffer for DNA ladder gels was prepared using 1.5% agarose (Gibco BRL, Auckland, NZ) and 0.25% bromophenol blue (Sigma Chemical Co.) in MilliQ water and stored at 4°C.

2.1.1.4 Binding buffer

The binding buffer for AnnexinV and PI staining was prepared using 10mM HEPES (Sigma Chemical Co.), 140mM NaCl, 2.5mM CaCl2 (both from BDH Kilsyth, AU), in MilliQ water and the pH adjusted to 7.4.

2.1.1.5 Protease buffer

Protease buffer was used for caspase activity assays and was prepared using 50mM HEPES, 10% sucrose (Merck, Victoria. AU), 0.1% CHAPS (CalBiochem, La Jolla, CA) and supplemented with 10mM DTT (Promega, Madison, US) in MilliQ with the pH adjusted to 7.4.

2.1.1.6 Running buffer

Running buffer used in SDS-polyacrylamide gel electrophoresis for western blot analysis was prepared using 3.02 g Tris base, 14.4 g glycine (Amresco, Solon, Ohio) and 1% SDS and volume made to 1L MilliQ water.

2.1.1.7 Towbin transfer buffer

Transfer buffer used for western blot analysis was prepared using 3.03 g Tris base, 14.4 g Glycine, 1% SDS and 200ml (20%) methanol (BDH Kilsyth, AU) in 800ml MilliQ water.

2.1.1.8 TAE buffer

Tris acetate EDTA (TAE) buffer used for running DNA gels was prepared using 4.84 g Tris Base, 1.14 ml Glacial Acetic Acid (Amresco, Solon, Ohio) and 2 ml 0.5M EDTA (pH 8.0) and the volume was made to 1L with MilliQ water.

2.1.1.9 Phosphate buffer

Phosphate buffer (pH 6) used for ELISA's was prepared with 0.1M Na2HPO4 (Sigma Chemical Co.) made to 1L with MilliQ water.

2.1.1.10 Carbonate buffer

Sodium Carbonate buffer (pH 9.5) used for ELISA's was prepared using 35mM NaHCO3 and 15mM Na2CO3 (both from Sigma Chemical Co.) made up in MilliQ water.

2.2 Antibodies and staining reagents

All antibodies and secondary reagents were titrated to determine the optimal concentration for staining. Antibodies obtained from commercial sources are shown in Table 2.1. Antibodies from the HLDA workshops are shown in Table 2.2. Other reagents used for immunofluorescence staining are shown in Table 2.3.

Table 2.1 Commercial primary antibodies

Antibody	**Company**	**Clone/Isotype**	**Dilution**
Negative controls			
IgG1 negative control	BD Pharmingen, San Diego, CA	MOPC-31C	1/100
Apoptosis markers			
Mouse anti-Caspase 3	R&D Systems, Minneapolis, US	84803.111	1/100
Rabbit anti-PARP	Santa Cruz, California, US	H-250	1/200
Mouse anti-Fas	R&D Systems, Minneapolis, US	DX2	1/100
Differentiation markers			
Mouse anti-Keratin 14	Neomarkers, Fremont, CA	LL002	1/100
Mouse anti-Keratin 10	Neomarkers, Fremont, CA	DE-K10	1/100
Polyclonal goat anti-Involucrin	Santa Cruz Biotechnology, Santa Cruz, CA	N-17	1/50

Mouse Alphα6/CD49f-PE	BD Pharmingen, San Diego, CA	GoH3	1/50
T-lymphocyte markers			
Mouse anti-CD4 – PE	BD Pharmingen, San Diego, CA	RPA-T4	1/50
Mouse anti-CD11a/LFA-1-FITC	SEROTEC	38	1/50
Mouse anti-CCR4 –PE	BD Pharmingen, San Diego, CA	Ms IgG_1, κ	1/50
Mouse anti-CLA	BD Pharmingen, San Diego, CA	HECA-452	1/50
Mouse anti-TARC	BD Pharmingen, San Diego, CA	2D8.1	1/50

Table 2.2 HLDA workshop primary antibodies

Antibody	**Clone name**	**Form used**
Negative controls		
IgG1 negative control	X63	Supernatant
IgG2a negative control	Sal-5	Supernatant
IgG2b negative control	Sal-4	Supernatant
IgG3 negative control	FMC19	Supernatant
T-lymphocyte markers		
Mouse anti-CD4	OKT 4	Supernatant
Mouse anti-CD3	OKT 3	Supernatant
Mouse anti-CD8	OKT 8	Supernatant
Mouse anti-CD178/FasL	BP-13	Supernatant
Mouse anti-CD25/IL2R	7G7B6	Supernatant
Keratinocyte surface marker		
Mouse anti-CD54/ICAM-1	RR1/1	Supernatant 1/100

Table 2.3 Other reagents used

Antibody	**Company**	**Dilution**
Secondary antibodies		
Biotinylated anti- mouse	Vector Laboratories, Burlingame, Ca	1/100
Biotinylated anti- rabbit	Vector Laboratories, Burlingame, Ca	1/100
Biotinylated anti- goat	Vector Laboratories, Burlingame, Ca	1/100
Anti- mouse immunoglobulin –FITC	Sigma Chemical Co.	1/100
Anti- mouse immunoglobulin -PE	BD Pharmingen, San Diego, CA	1/100
anti-mouse-HRP IgG	Vector Laboratories, Burlingame, Ca	1/2000
anti-rabbit-HRP IgG	Vector Laboratories, Burlingame, Ca	1/1000
Streptavidin-PE	Sigma Chemical Co.	1/50

2.3 Cell culture

Cell culture experiments were performed under sterile conditions in a laminar flow cabinet. Cultures were maintained in a 5% CO2 in a 37°C incubator.

2.3.1 HaCaT Keratinocytes

The transformed human keratinocyte cell line, HaCaT, was derived from adult skin and obtained from Boukamp JCB 88 and cultured in Dulbecco's Modified Eagle's medium (DMEM- JRH biosciences, Kansas, USA) containing 0.1mg/ml Streptomycin, 100U/ml Penicillin (both from GIBCO, Auckland, NZ) and supplemented with 10% fetal bovine serum (FBS; Thermotrace, Melbourne, AU). HaCaTs were grown to 80-90% confluency in 75 cm2 flasks (Nunc, Roskilde, Denmark) before subculturing by incubating with trypsin (0.25%)-EDTA (GIBCO, Auckland, NZ) at 37°C for 10-12 min. Once the cells had detached, FBS was added to neutralise the trypsin and the harvested cells were centrifuged at 220 x g for 5 min to pellet the cells. The cells collected were resuspended with fresh DMEM and viable cells were counted using Trypan Blue (Sigma Chemical Co.). Cells were seeded at 5 x 10^5 cells/ml. The growth medium was changed the day after seeding and every second day thereafter.

2.3.2 Normal human epidermal keratinocytes

The normal human epidermal keratinocytes (NHEK) were purchased from Cambrex Bio Science Walkersville, Inc. The cells were grown in Keratinocyte Basal Medium®-2 (KBM®-2 Cambrex Bio Science) supplemented with Bulletkit® containing bovine

pituitary extract BPE (7.5 mg/ml), human recombinant epidermal growth factor hEGF (0.1 ng/ml), bovine insulin (5 μg/ml), hydrocortisone (0.5 μg/ml), and gentamicin sulphate/ amphotericin-B (50 μg/ml) (all from Cambrex Bio Science). NHEK were grown to 70-80% confluency before subculture. Subculture was performed by incubating with trypsin (0.25%)-EDTA (GIBCO, Auckland, NZ) at 37°C for 5 min. Once the cells had detached, an equal volume of soybean trypsin inhibitor (Invitrogen, Mount Waverley, Australia) was added to neutralise the trypsin. The harvested cells were centrifuged at 220 x g for 5 min. The NHEKs collected were resuspended with fresh KBM and viable cells were counted using Trypan Blue. Cells were seeded at 2 x 10^5 or 5 x 10^5 cells/ml. The growth medium was changed the day after seeding and every second day thereafter. Only second or third passage NHEKs, grown to sub-confluence in KBM were used in the experiments.

2.3.3 Jurkat T-lymphocytes

The Jurkat T-lymphocyte/lymphocyte line was cultured in RPMI 1640 (JRH biosciences, Kansas, USA) containing 2mM L-glutamine (GIBCO, Auckland, NZ), 0.1mg/ml streptomycin, 100U/ml penicillin and supplemented with 10% FBS. Jurkat T-lymphocytes were grown to confluence in 75 cm2 flasks (Nunc, Roskilde, Denmark) before subculturing (every second or third day). Cells were centrifuged at 220 x g for 5 min to pellet the cells and then resuspended with fresh RPMI 1640. Viable cells were counted using Trypan Blue. The growth medium was changed the day after seeding and every second day thereafter.

2.3.4 Primary T-lymphocytes

Primary T-lymphocytes were prepared from 20-30 ml of human venous blood collected from a healthy donor.

2.3.4.1 Lymphoprep separation of peripheral blood mononuclear cells

Blood was diluted in PBS (1:3) and mixed well. Two volumes diluted blood was overlaid over one volume of Lymphoprep (Ficoll-PaqueTM PLUS, Lymphoprep, Norway). The samples were centrifuged at 300 x g for 20 min at room temperature to separate mononuclear cells from the other blood constituents. The inter-phase layer was collected, diluted 1/10 in PBS and centrifuged at 300 x g for 10 min at room temperature. The cells were then washed with cold PBS and centrifuged at 220 x g for 10 min at 4°C. The mononuclear cells were subsequently counted using a haemocytometer. Cells were washed with PBS at 220 x g for 10 min at 4°C and resuspended in the appropriate volume of PBS to obtain the desired cell density.

2.3.4.2 CD4+ T-lymphocyte purification

CD4+ T lymphocytes were purified from peripheral blood mononuclear cells isolated by Lymphoprep centrifugation. CD4+ T-lymphocytes were positively selected using CD4 Micro Beads and a magnetic cell sorter (Miltenyi Biotec, Bergisch Gladbach, Germany) according to the manufacturer's instructions. Briefly, mononuclear cells were resuspended at approximately 2 x 10^7 cells/ml in PBS containing 0.5% bovine serum albumin (BSA- Sigma Chemical Co.) and 2mM EDTA. Mononuclear cells were

incubated with the CD4 Micro Beads for 15 min at 4°C with rotation. Cells were washed by centrifugation at 300 x g. Cells were resuspended in 1ml PBS (0.5% BSA and EDTA) and passed through a MS+ column (Miltenyi Biotec, Bergisch Gladbach, Germany) which retained CD4+ cells. The column was flushed with 1ml PBS (BSA +EDTA) and approximately 5 x 10^6 -1 x 10^7 CD4+ T-lymphocytes were obtained. T-lymphocytes purified by this procedure were always more than 98% CD4+/CD3+ pure (Appendix 1). The eluted fraction of mononuclear cells (predominantly CD8+ population - Appendix 1) was also collected. T-lymphocyte preparations were used fresh in all experiments and added to the cultures grown in DMEM 1% FBS for up to 48 hr.

2.3.5 Cryopreservation

HaCaTs and T-lymphocytes were stored in liquid nitrogen using standard techniques. Cells were centrifuged and resuspended at approximately 5 x 10^6 cells /ml in media containing 25% FBS and 10% DMSO (Sigma Chemical Co.) with constant mixing. Cells were then transferred into cryovials (Nunc, Roskilde, Denmark) and frozen slowly by placing in a polystyrene container kept at -80°C for 24 hr before transferring to liquid nitrogen.

To recover cryopreserved cells, cells were thawed quickly in a 37°C water bath and transferred into a 10ml sterile tube containing 5 ml of fresh media. After mixing well, cells were centrifuged at 220 x g and resuspended in fresh culture media.

2.4 Functional studies co-culture experiments

2.4.1 Mitogen activation of T-lymphocyte

Phorbol 12-myristate 13-acetate (PMA- Sigma Chemical Co.) stocks were prepared in DMSO at a concentration of 10 μg/ml and stored in aliquots at -20°C. 1 ml of this stock solution was added to each ml of cell media and used at a final concentration of 10 ng/ml. Ionomycin (Sigma Chemical Co.) was prepared in DMSO at a concentration of 1 mg/ml and diluted to give 100 μg/ml stock solutions which were stored in aliquots at -20°C. 5 ml of this stock solution was added to each ml of cell media and used at a final concentration of 500 ng/ml.

To activate Jurkat T-lymphocytes for use in co-culture experiments, Jurkat T-lymphocytes were serum starved over-night and incubated with 10 ng/ml PMA for 48 hr in DMEM containing 1% FBS. Primary CD4+ T-lymphocytes were activated with 10 ng/ml PMA and 500 ng/ml ionomycin in DMEM containing 1% FBS (Arnold *et al.* 1999, Trautmann *et al.* 2000c).

2.4.2 Jurkat T-lymphocyte conditioned media

Conditioned medium was prepared by growing 5 x 10^5 Jurkat T-lymphocytes/ml in 25 cm^2 flasks with or without mitogen activation [+/- 10 ng/ml PMA] in DMEM containing 1% FBS and incubated for 48 hr. The conditioned medium was collected, centrifuged and the cell-free supernatant added to HaCaTs immediately. An aliquot of the cell-free

conditioned media was stored at -20°C for cytokine measurements as described in Section 2.11.

2.4.3 Jurkat T-lymphocyte and HaCaT co-culture

Jurkat T-lymphocytes were activated (Section 2.4.10) three days prior culture with HaCaTs. Following activation, Jurkat T-lymphocytes were washed in PBS and 5 x 10^5 Jurkat T-lymphocytes per ml were co-cultured with HaCaTs grown to 70-80% confluence in 12 well plates with fresh DMEM containing 1% FBS for 48hr.

2.4.4 Primary T-lymphocyte co-culture with HaCaTs or NHEKs

Immediately after isolation, primary CD4+ T-lymphocytes (5 x 10^5/ml) were stimulated with PMA (10ng/ml) and ionomycin (500ng/ml) and co-cultured with either HaCaTs in DMEM containing 1% FBS or with NHEK in KBM for 48 hr.

2.5 Flow cytometry

All samples were analysed using an Epic Elite ESP Beckman Coulter flow cytometer. The machine was calibrated daily using BD CaliBRITE beads (BD Biosciences, North Ryde, AU). For keratinocytes, live gating was performed and 10000 events were counted per sample. T-lymphocytes were gated based on size and light scatter properties and 10000 events were counted per sample (see Appendix 2). Data was analysed using Expo32 software (Beckman-Coulter).

2.5.1 Cell viability and apoptosis

Two colour flow cytometry was used to assess keratinocyte or T-lymphocyte viability, apoptosis and necrosis. The adherent HaCaTs or NHEK were collected by incubating with trypsin (0.25%)-EDTA (GIBCO, Auckland, NZ) and pooled with the non-adherent cells. Jurkat and primary T-lymphocyte were collected by centrifugation at 220 x g for 5 min. The cells were washed twice with phosphate-buffered saline pH 7.4 (PBS) and 1 x 10^5 cells/ml were incubated with Annexin V-FITC (1 μg/ml) (BD Biosciences, North Ryde, AU) to detect apoptotic cells and with the nuclear stain propidium iodide (PI - 5 μg/ml) (Sigma Chemicals, Castle Hill, AU) in binding buffer for 15 min at room temperature in the dark. Cells were washed and samples were resuspended in 200ml binding buffer and analysed within 1 hour of staining by flow cytometry. Quadrant markers were set on dotplots of unstained cells and then subsequently applied to dot plots of other samples. T-lymphocytes were gated and size excluded at the beginning of sample analysis.

2.5.2 Cell surface immunofluorescence staining

HaCaT or NHEK cell surface marker staining was performed on adherent cells collected using trypsin (0.25%)-EDTA which were pooled with non adherent cells and 5 x 10^5 cells were transferred into FACS tubes. Jurkat and Primary T-lymphocytes were collected by centrifugation at 220 x g for 5 min and 5 x 10^5 cells were transferred into FACS tubes.

All incubations were performed for 30 min on ice and a washing step was performed after each antibody incubation using PBS wash buffer. Cells were washed with pre-chilled PBS washing buffer (with 2% FBS and 0.09% sodium azide) centrifuged at 220 x g for 5 min at 4ºC and blocked with 10 ml fetal bovine serum for 15 min prior to staining. Duplicate samples were stained in parallel with IgG isotype matched control antibodies (Table 2.1). Three different detection systems were employed to stain for surface antigens as required during this study.

Cells were stained using FITC- or PE- conjugated primary antibodies (Table 2.1). Cells were also indirectly stained, using unlabelled primary antibodies followed by conjugated secondary immunoglobulins (FITC or PE; Table 2.2). All cells were fixed and resuspended in sterile saline solution or washing buffer before been analysed by flow cytometry. Three step high sensitivity staining was performed by incubating cells with primary followed with a biotinylated secondary antibody and subsequently with streptavidin-PE (Sigma Chemical Co.; Table 2.3), fixed and resuspended in sterile saline solution or washing buffer before been analysed by flow cytometry.

After staining, the cells were fixed with 1 ml of a 1 x FACS Lysing Solution (BD Biosciences, North Ryde, AU) and incubated in the dark for 15 min at room temperature. Cells were resuspended in sterile saline solution (0.9% NaCl) or washing buffer and were analysed immediately or stored over-night before analysing by flow cytometry.

2.5.3 Intracellular Immunofluorescence staining

For intracellular staining of keratinocytes, cells were harvested, washed and permeabilised with 1ml of 1 x FACS-Perm solution (BD Biosciences North Ryde, AU) for 15 min at room temperature. Permeabilised cells were blocked with 10ml fetal bovine serum for 10min before staining with primary antibodies. Duplicate samples were stained with IgG isotype matched control antibody. Cells were subsequently incubated with the appropriate biotin-conjugated secondary antibodies followed by incubation with streptavidin-PE in the dark. Cells were fixed with 1x FACS Lysing Solution, resuspended in sterile saline or wash solution and analysed by flow cytometry.

2.6 DNA fragmentation studies

2.6.1 HOECHST staining

HaCaTs or NHEKs plated on 12 well tissue culture plates were washed twice with PBS, and fixed with 4% formaldehyde in PBS for 15 min at room temperature. Cells were washed again with PBS before staining with 500ml of 1 μg/ml HOECHST 33342 dye (Sigma Chemicals Co.) in PBS for 15 min in the dark. Cells were washed and staining for nuclear fragmentation was evaluated using a Nikon inverted fluorescent microscope fitted with a DAPI filter.

2.6.1.1 DNA ladder

For the evaluation of DNA fragmentation, adherent cells were scraped and together with non-adherent cells were centrifuged at 300 x g for 7 min at room temperature. Cell

pellets were washed twice with 1 ml cold PBS at 350 x g for 5 min. Cells were incubated in 50 ml of cell lysis buffer for 30 min at 4°C. Cell debris and high-molecular-weight DNA were precipitated by centrifugation at 12,000 x g for 30 min at 4°C. Supernatants containing fragmented DNA were carefully collected and then treated with proteinase K (0.2 g/L) at 50°C for 1 hr followed by 2 g/L RNAse A at 50°C for a further hour. Samples were incubated with pre-warmed loading buffer for 10 min before running on a low melting point agarose gel (see Section 2.6.2 b) containing 1 ml/ml ethidium bromide (Sigma Chemicals Co.).

2.6.1.2 Agarose gel electrophoresis

DNA degradation from samples was assessed by gel electrophoresis. The gel was made by adding 1.5% agarose in TAE buffer (low melting point agarose gel) with ethidium bromide. The gel was melted and poured onto gel tank and allowed to cool. The gel was placed in talk with TAE running buffer and the warm samples as well as a negative control containing melted loading buffer were loaded into wells. Electric current was applied at 100 Volts for 1.5-2 hr. Gels were examined and photographed under ultraviolet light.

2.7 Caspase activity assay

For the evaluation of caspase activity, protein was extracted by lysing the cells with cold NP40 lysis buffer on ice for 15 min. The cells were scraped and colleted into centrifuge

tubes and the insoluble material pelleted at 13400 x g for 15 min at 4°C.

Caspase 3, 8 and 9 activity was measured in protein extracts by measuring the capacity of the sample to cleave a substrate specific for each caspase, resulting in the release of the fluorogen AFC. The peptides included caspase 3 substrate IV (DEVD-AFC), caspase 8 substrate II (IETD-AFC) and caspase 9 substrate I (LEHD-AFC), all from CalBiochem, La Jolla, CA. Triplicate samples containing a 50 ml aliquot of the cell lysate was tested for caspase activity by incubation with 1ml of protease buffer containing 8 μM of the relevant fluorescent substrate for 24 hr at room temperature in the dark. The release of AFC was quantified by measuring the fluorescent emission at 490nm (excitation 400nm) for caspases 3 and 8 and at 460nm (excitation 400nm) for caspase 9 using a Perkin-Elmer LS50 spectrofluorimeter. A fluorescence unit of 1 was determined as the equivalent to the amount of caspase required to produce 1pmol of AFC/min at 25°C.

2.8 Western blotting

Protein for western blot analysis was obtained by incubating the cells in lysis buffer containing 10% SDS, for 15 min on ice. The wells were scraped and the cell material passed through a 16G needle 5 times. The insoluble material was pelleted at 13,400 x g for 5 min at 4°C and soluble supernatant collected. The protein concentration of samples was calculated using the Bradford method (see Section 2.8.1). Equal amounts of protein were loaded per well and electrophoresed through a 15% SDS polyacrylamide gel (Bio-Rad Hercules, US) at 60mA for 90 min (see Section 2.8.1). The proteins were

transferred onto a Hybond nitrocellulose membrane (Amersham Life Sciences, Sydney, AU). The membranes were equilibrated with cold transfer buffer for 15 min before wet transfer. The wet apparatus was assembled as per the manufacturer's instructions (Bio-Rad Hercules, US). The tank was filled with cold transfer buffer and run at a constant Amperage (900mA) for 30 min. When finished the membranes were stained with Red Ponceau (Sigma Chemicals Co.) to monitor protein transfer and protein loading.

The membranes were blocked with 2% powdered skim milk in PBST for 30 min at room temperature and then incubated with primary antibody in 1% powdered skim milk in PBST overnight at 4°C. Membranes were washed three times for 5 min with wash buffer and incubated with secondary HRP IgG in 1% powdered skim milk in PBST for 1 hr at room temperature. Membranes were washed and then soaked for 2 min in ECL Western Blot reagents (Amersham Life Sciences, Sydney, AU) and bands detected by autoradiography (ECL film-Amersham Life Sciences, AU). Rainbow molecular weight markers (Amersham Life Sciences, Sydney, AU) were used for the determination of protein size.

2.8.1 Protein quantification - Bradford Assay

Protein concentration was calculated using the Bradford method as per the manufacturer's instructions (Bio-Rad Hercules, US). Briefly, various concentrations of BSA protein (Sigma Chemicals Co.) were made up in PBS. For establishing a standard curve, 100ml of each dilution of BSA protein was added to 900ml Bradford reagent, incubated for 5 min at room temperature and the absorbance measured at 595 nm. For

samples, 10 ml of sample and 990 ml Bradford reagent were incubated for 5 min at room temperature and the absorbance measured at 595 nm. The standard curve was used to calculate protein concentration of samples.

2.8.2 SDS-PAGE Separating Gels

The resolving gel consisted of 15% bis/acrylamide, 1.5 M Tris-HCl pH 8.8, 0.4% SDS, with 50 ml of 10% ammonium persulfate solution and 10 ml of TEMED. Once the resolving gel had polymerized, the upper stacking gel was loaded. The stacking gel was prepared with 5% acrylamide, 0.5 M Tris-HCl pH 6.8, 0.4% SDS with 10 ml of 10% ammonium persulfate solution and 1 ml of TEMED and allowed to polymerize for 15 min with a comb inserted for loading samples. Samples were loaded and electrophoresed initially at 20 mA constant current. After 10-15 min, the current was increased to 30 mA for approximately 2 hr.

2.9 Slot blot

Soluble FasL (sFasL) expression in conditioned media was determined by Slot Blot analysis. 100ml of conditioned media was loaded onto Hybond nitrocellulose membrane (Amersham Life Sciences, Sydney, AU) in a slot blot apparatus (Bio-Rad, North Ryde, NSW). The slot blot was assembled as per the manufacturer's instructions and connected to a vacuum pump to draw the samples through the slots onto the membrane. Membranes were allowed to dry and then blocked with 2% powdered skim milk in PBST for 30 min at room temperature. Membranes were incubated with primary

antibody in 1% powdered skim milk in PBST overnight at 4°C. The membranes were washed 3 times with wash buffer and then incubated with secondary -HRP antibody in 1% powdered skim milk in PBST for 2 hr at room temperature. The signal was detected using ECL Western Blot reagents (Amersham Life Sciences, Sydney, AU) and X-ray film (Fujifilm, Tokyo, Japan).

2.10 Cytospins

Non adherent cells were washed twice in cold PBS containing 2% FBS and resuspended in 100 ml of cold PBS containing 1% BSA. The slides and filters were placed into appropriate slots in the cytospin. Cell suspensions were aliquoted into the appropriate wells and centrifuged at 300 x g for 10 min. The filters were removed from the slides and allowed to dry. Slides were stained with HOESCHT 33342 nuclear stain and fixed as described in Section 2.6.1. The slides were dried in a desiccation chamber for 1 hr before analysis as described in Section 2.6.1.

2.11 Quantification of cytokines

The conditioned media of samples and controls was collected and the inflammatory cytokines; IFNγ and TNFα released determined by solid-phase sandwich ELISAs.

Microtiter plates (384-wells; Nunc, Roskilde, Denmark) were coated with a monoclonal anti-human IFNγ antibody (R&D Systems, Minneapolis, US) in carbonate buffer pH 5.5 or anti-human TNFα antibody (BD Pharmingen, San Diego, CA) in phosphate buffer pH

5.5 at 4°C overnight. Plates were washed with PBS and wells blocked with 30 ml of 2.5% BSA/PBS for 1 hr at room temperature with agitation. Various concentrations of standard cytokine protein were prepared with DMEM containing 1% FBS and 20 ml of each standard/well loaded on the plate. The standard curve and 20 ml of neat supernatant samples were incubated on plates for 3 hr with agitation. The sensitivity of the IFNγ ELISA was < 1 pg/ml (recombinant IFNγ standards; Sigma, St. Louis, MO). The sensitivity of the TNFα ELISA was < 5 pg/ml (recombinant TNFα standards; kindly provided by Dr. Mark DeNickilo, TGR Biosciences). Plates were washed with PBS and the standard curve and samples incubated with 20 ml of either a biotinylated goat anti-IFNγ (R&D Systems, Minneapolis, US) or a biotinylated anti-human TNFα (BD Pharmingen, San Diego, CA) antibodies for 2 hr with agitation. Plates were washed and all wells incubated with 20 ml of a 1/1000 dilution of Europium streptavidin (Delfia, Zaventen, Belgium) for 1 hr. ELISAs were developed after 10 min incubation with enhancer solution (Delfia, Zaventen, Belgium). Optical density was measured at emission 620 nm/excitation 340 nm using a Wallac Victor2V 1420 multi Label HTS Counter (Perkin Elmer Life Sciences).

2.12 Statistics

Each experiment was performed at least three times. Results are expressed as mean ± SEM. Apoptosis and caspase activity data was analysed by one-way analysis of variance (ANOVA) followed by post-hoc t-test using Dunnett's method (multiple comparisons versus the untreated control) using Sigma-Stat software. Data was considered to be statistically significant when $p<0.05$.

CHAPTER 3

3 SODIUM BUTYRATE INDUCED HACAT APOPTOSIS

3.1 Introduction

The main objective of this chapter was to establish methodologies for measuring apoptosis of human keratinocytes. The human keratinocyte cell line HaCaT was used in these studies. HaCaTs are non-tumorigenic epithelial cells derived from adult human skin (Boukamp *et al.* 1988) which demonstrates highly preserved epidermal characteristics and normal differentiation, making them suitable cells for studying apoptosis and keratinocyte differentiation *in vitro* (Boukamp *et al.* 1988, Ryle *et al.* 1989).

The studies in this chapter characterise the effect of sodium butyrate on HaCaTs. Sodium butyrate is a well known inducer of cell cycle arrest and apoptosis in epithelial cells (Chai *et al.* 2000, Litvak *et al.* 2000, Medina *et al.* 1997, Zhu & Otterson 2003). It is a short chain fatty acid which is produced by anaerobic bacterial fermentation of insoluble fiber in the colon (D'Argenio & Mazzacca 1999) (Figure 3.1 a). It acts as a physiological regulator of homeostasis for colonic epithelial cells by regulating the

balance between proliferation, differentiation and apoptosis (Cai *et al.* 2004, Chopin *et al.* 2004, Cuff & Shirazi-Beechey 2004, Tabuchi *et al.* 2002).

Sodium butyrate is a potent histone deacetylase inhibitor (HDI; Figure 3.1 b) (Monneret 2005) that targets nuclosomes and results in increased acetylation. Histone hyper-acetylation results in a relaxed chromatin structure that influences the transcription of proteins involved in cell cycle regulation and growth arrest such as p21 (Burgess *et al.* 2001, Hitomi *et al.* 2003). Sodium butyrate has also been shown to induce apoptosis by altering gene expression of proapoptotic members of the Bcl-2 family (Litvak *et al.* 2000). Studies have shown that death receptor signalling through Fas and TRAIL are involved in sodium butyrate induced apoptosis in breast cancer and colon cancer cell lines (Bonnotte *et al.* 1998, Chopin *et al.* 2004, Fan *et al.* 1999). Previous work by Pollanen et al observed that treatment with sodium butyrate resulted in abnormal cell morphology of junctional epithelial cells (Pollanen *et al.* 1997), and others have suggested these morphological changes to be the formation of cornified envelopes in keratinocytes by induction of terminal differentiation (Ford *et al.* 1993, Schmidt *et al.* 1989, Staiano-Coico *et al.* 1989). Given that keratinocyte apoptosis has also been shown to be mediated by death receptors such as Fas and TRAIL (Leverkus *et al.* 1997, Leverkus *et al.* 2003), sodium butyrate was selected as a suitable agent to investigate apoptosis and differentiation of keratinocytes and establish the methods necessary to undertake the studies required by this thesis.

The studies in this chapter characterise the effect of sodium butyrate on HaCaT apoptosis and terminal differentiation. In particular, the mechanisms of apoptosis included events that are characteristic of early and late apoptosis using the following methods:

- Assessment of early and late apoptosis was performed by flow cytometry using Annexin V and propidium iodide (PI) staining. A key characteristic of early apoptosis is the translocation of phosphatidylserine (PS) from the inner to outer membrane leaflet of the plasma membrane. Annexin V binds with high affinity to PS exposed on the cell surface and was used to detect early apoptotic cells. PI is a nuclear stain and was used to detect late apoptotic and necrotic cells.
- Since apoptosis is a morphologically distinct form of cell death, phase contrast microscopy was used to assess apoptotic morphology. This was characterised by cell shrinkage, membrane blebbing and cell fragmentation into apoptotic bodies.
- HOECHST 33342 staining was employed to assess chromatin condensation and nuclear fragmentation.
- Mechanisms likely to be involved in mediating HaCaT apoptosis were also investigated including the Fas pathway which was examined by assessing membrane and cytoplasmic Fas expression.
- Activation of the caspase cascade is important for mediating the induction of apoptosis via death receptors (Barnhart *et al.* 2003). Caspase activity was measured using fluorescent caspase activity assays specific for caspases 3, 8 and 9.

- Keratinocyte differentiation was investigated by assessing the intracellular expression of keratin 14 (K14; basal cell marker), keratin 10 (K10; suprabasal cell marker) and involucrin (terminal differentiation marker) by flow cytometry.

Figure 3.1

a)

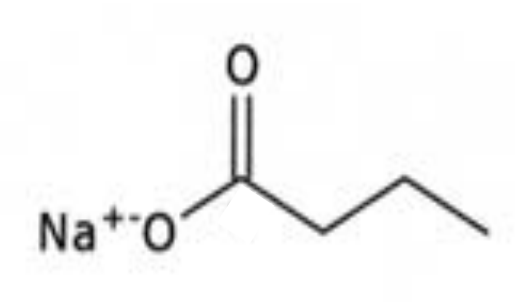

b)

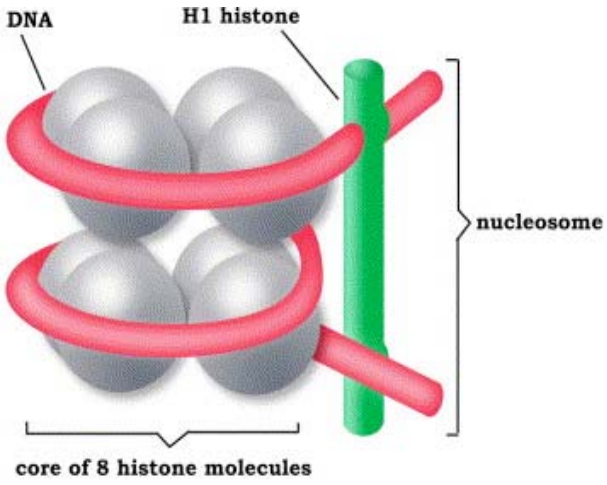

NUCLEOSOME

Figure 3.1- (a) Molecular structure of sodium butyrate. (b) Nucleosome; target for histone deacetelase inhibitors. Picture from Monneret et al., 2005.

3.2 Methods

3.2.1 Butyrate treatment of HaCaT

Sodium butyrate (Sodium butyrate - BDH, Poole, England) was dissolved in DMEM containing 10% FBS at a stock concentration of 40mg/ml and stored at 4°C. HaCaTs were cultured in DMEM containing 10% FBS and were grown to 70-80% confluence in 6 well plates (unless otherwise indicated) before treatment with sodium butyrate. HaCaTs were treated with doses ranging from 0.08-0.8 mg/ml sodium butyrate for up to 72 hr in DMEM containing 10% FBS. HaCaTs controls were left untreated in DMEM containing 10% FBS.

3.2.2 Measurements of apoptosis

Apoptosis of HaCaTs was measured by flow cytometry (Annexin V/PI staining) as described in Methods section 2.5.1. Nuclear fragmentation was assessed by HOECHST 33342 dye staining and DNA Ladder as described in Methods section 2.6.1 and 2.6.2 respectively. Surface Fas expression was examined by flow cytometry (section 2.5.2). Fas, caspase 3 and PARP whole cell protein expression was analysed by Western blot (section 2.8). Caspase activity assays were performed as described in Methods section 2.7.

3.2.3 3.2.3 Measurements of differentiation

Differentiation marker expression of HaCaTs were measured by intracellular staining and analysed by flow cytometry as described in Methods section 2.5.3.

3.3 Results

3.3.1 Induction of HaCaT apoptosis by Sodium butyrate

HaCaTs were incubated with increasing concentrations of sodium butyrate for 24 hr and assessment of apoptosis was performed by Annexin and PI staining. Early apoptotic cells were identified by positive Annexin V staining on the cell membrane. Cells stained with Annexin V and the viability dye PI were regarded as in late apoptosis. Cells stained with PI only were considered to be necrotic. As shown in the representative dot plot in Figure 3.2, most HaCaTs incubated under control conditions (10% FBS) were negative for Annexin V or PI staining and were considered to be viable cells (Figure 3.2a). However when the cells were treated for 24 hr with increasing concentrations of sodium butyrate (0.08, 0.4 and 0.8mg/ml), there was a concomitant increase in cells induced to undergo apoptosis as shown by the greater number of cells in the AE (Annexin V positive/PI negative) and late apoptotic quadrants (Annexin V positive/PI positive; Figure 3.2 b-d). Despite the effect of butyrate on apoptosis, there was only a slight increase in the number of necrotic cells (N; Annexin V negative/PI positive - Figure 3.2 a-d).

The combined results from three independent experiments showed the percentage of apoptotic cells (EA and LA) increased significantly when HaCaTs were treated with 0.4 and 0.8mg/ml butyrate for 24hr ($p<0.05$; Figure 3.2 e). Compared to 8% of cells in control cultures, 46% of cells treated with 0.8mg/ml butyrate were apoptotic with a

concomitant decrease in the percentage of viable cells also found to be significant ($p<0.05$). The temporal induction of apoptosis was investigated using the most effective concentration of sodium butyrate (0.8mg/ml). Apoptosis was significantly increased by 18hr, with 66% of the total cell population found to be apoptotic after 72hr ($p<0.05$; Figure 3.3). Although necrosis did not change in the first 48hr, 15% of cells were necrotic after 72hr however this was not significantly different when compared to controls (Figure 3.3).

3.3.2 Sodium butyrate induced morphological features of apoptosis and nuclear fragmentation

Analysis of HaCaT cell morphology demonstrated that sodium butyrate treated cells appeared shrunken, displayed fewer intercellular connections, and a greater number of cells were detached from the culture plate after 24hr (Figure 3.4 b and c) compared to control cultures (Figure 3.4 a). Apoptotic bodies were also evident (Figure 3.4 c arrow). The effect of sodium butyrate on nuclear fragmentation was assessed in parallel cultures using the HOESCHT 33342 nuclear stain. Figure 3.4 d shows minimal nuclear staining in controls, whereas HaCaTs treated with 0.8mg/ml sodium butyrate showed increased staining representing nuclear condensation and fragmentation (Figure 3.4 e and f respectively).

The detached cells from experiments described in Figure 3.4 were collected onto slides by cytospins (Methods Section 2.10) and stained for nuclear fragmentation. Figure 3.5 demonstrated that a higher number of detached cells were collected from sodium

Figure 3.2

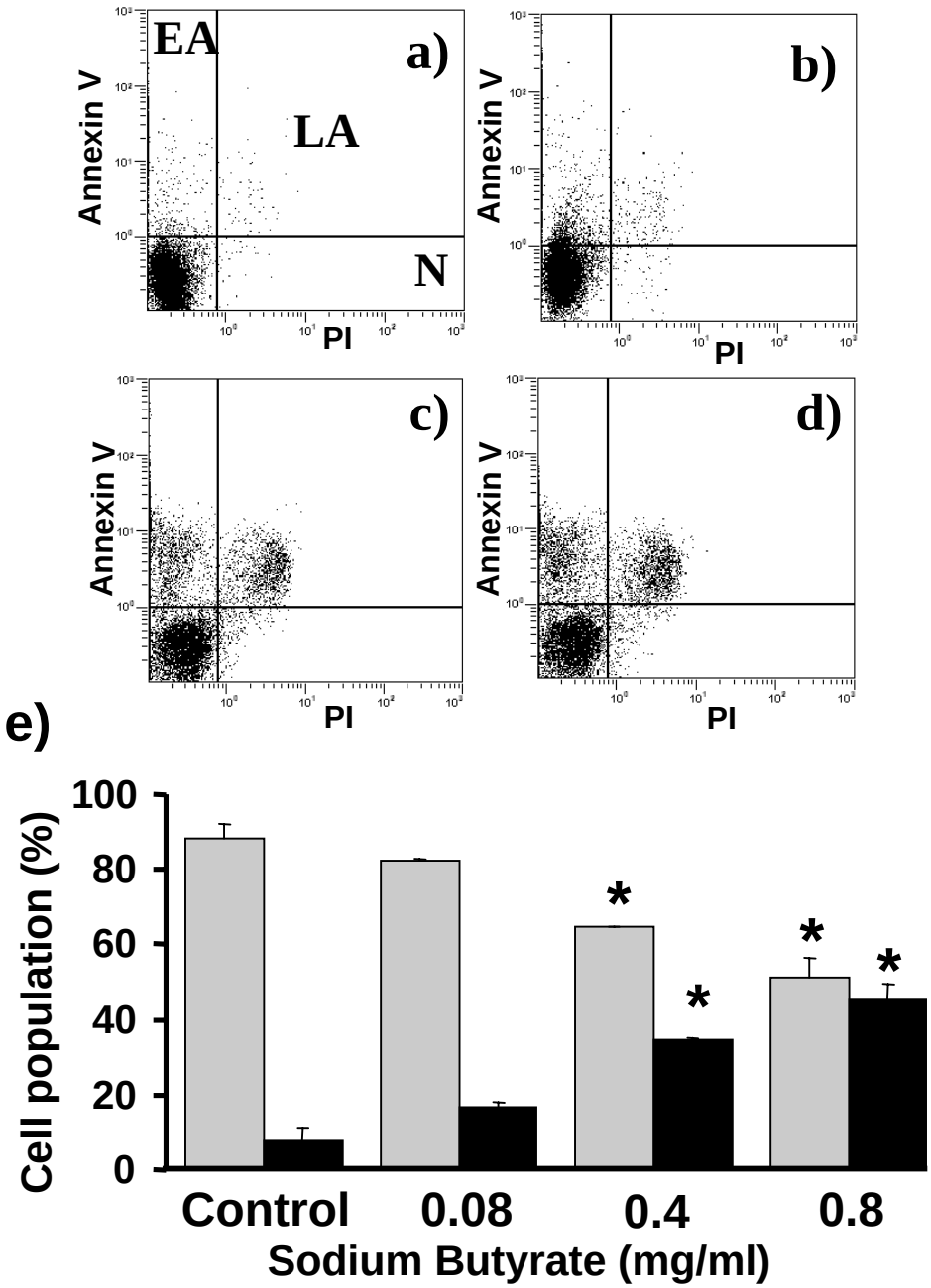

Figure 3.2- Effect of sodium butyrate on HaCaT apoptosis. a) Representative dot plot of Annexin V and propidium iodide (PI) stained control HaCaTs after 24hr. b-d) HaCaTs treated with 0.08, 0.4 and 0.8mg/ml sodium butyrate respectively for 24hr. Unstained cells (Annexin V negative/PI negative) were considered viable, Annexin V positive/PI negative cells were considered early apoptotic (EA), Annexin V positive/PI positive cells were considered late apoptotic (LA) and Annexin V negative/PI positive cells represented the necrotic population (N). e) Collated data from 3 separate experiments (n=3) showing the effect of sodium butyrate (0.08-0.8mg/ml) on HaCaT viability (grey bar) and apoptosis ([EA + LA]; black bar). Bar graphs show the parameters measured as a percentage of the total cell population with the data presented as mean±SEM. Data was analysed using one-way analysis of variance (ANOVA) and post-hoc t-test with significant differences compared to controls shown (*$p<0.05$).

Figure 3.3

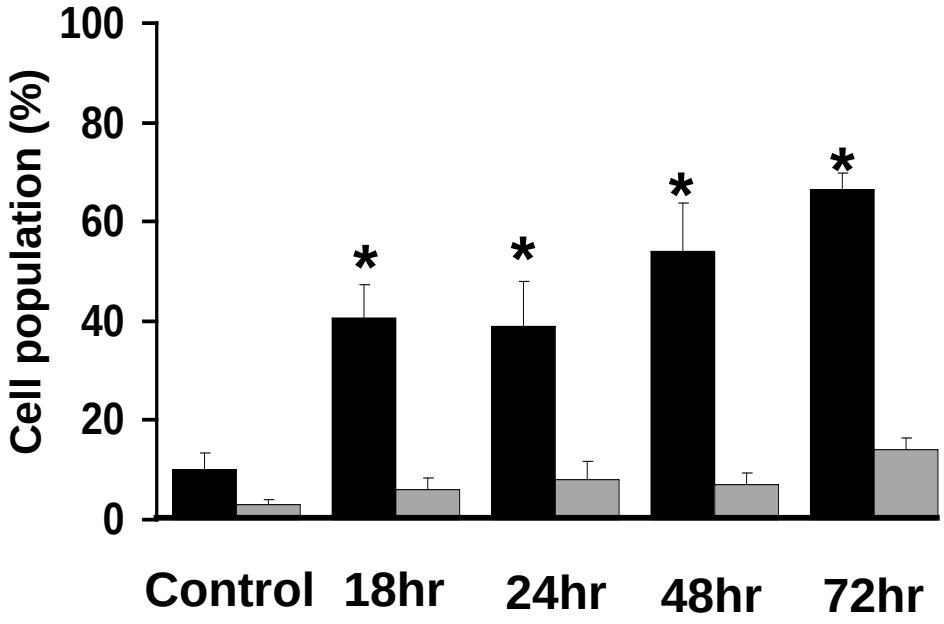

Figure 3.3- Time response effect of sodium butyrate on HaCaT apoptosis and necrosis. HaCaTs were treated with 0.8mg/ml sodium butyrate for up to 72hr and the combined data from 3 separate experiments (n=3) presented showing the effect on apoptosis (black bar) and necrosis (grey bar). Control cells were incubated in the absence of sodium butyrate for 72hr. Bar graphs show the parameters measured as a percentage of the total cell population with the data presented as mean±SEM. Data was analysed using one-way analysis of variance (ANOVA) and post-hoc t-test with significant differences compared to controls shown (*$p<0.05$).

Figure 3.4

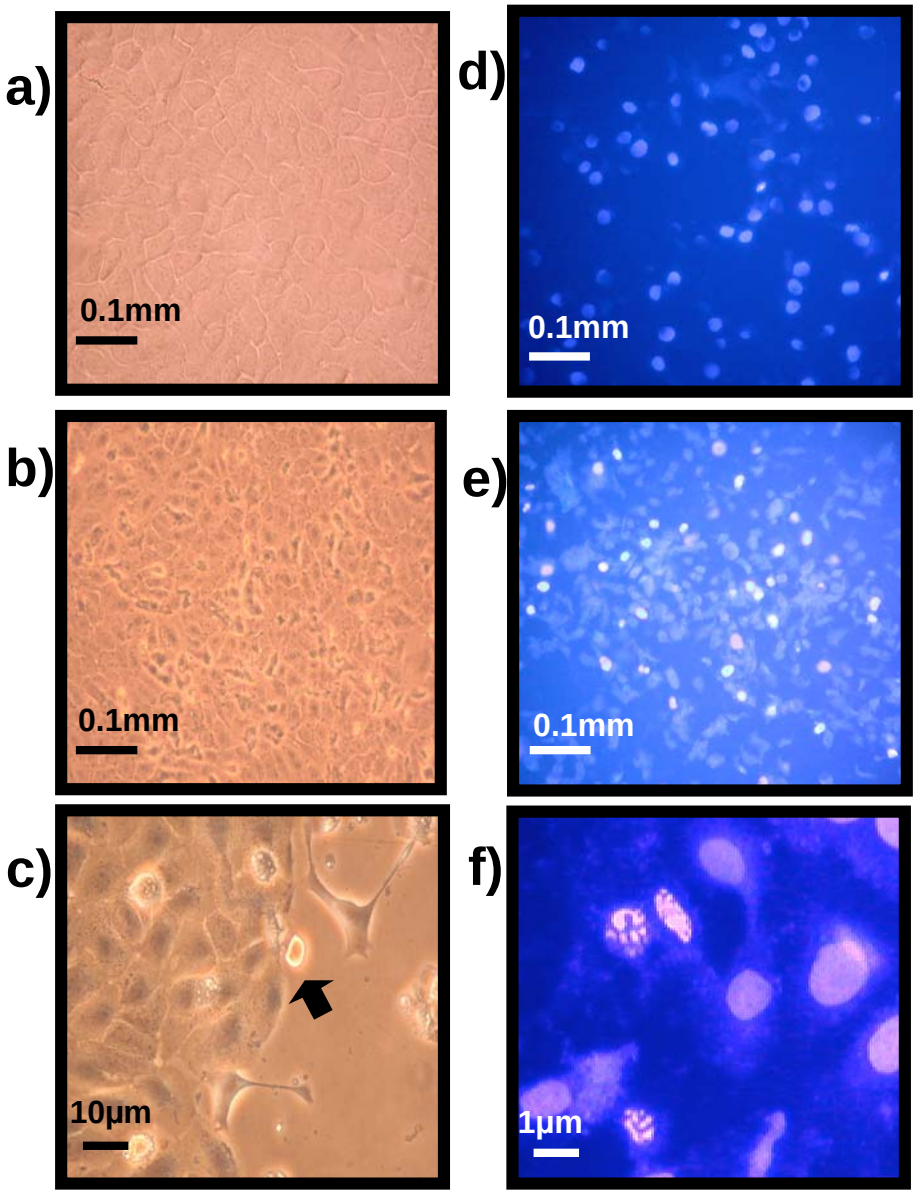

Figure 3.4– Effect of sodium butyrate on HaCaT morphology and nuclear fragmentation. Phase contrast microscopy of control HaCaTs incubated with 10% FBS (a) and cells treated with 0.8mg/ml sodium butyrate for 24hr (b and c) arrow points to an apoptotic body. HOESCHT fluorescent stain was used to detect condensed chromatin and nuclear fragmentation of (d) control HaCaT cells, (e) and (f) HaCaTs treated with 0.8mg/ml sodium butyrate for 24hr.

butyrate treated samples compared to control samples, all the detached cells showed positive HOESCHT 33342 staining (Figure 3.5 a and b respectively).

The cleavage of chromatin into small DNA fragments is a hallmark of apoptosis and can be observed as a DNA ladder (Methods Section 2.6 a). Compared to the DNA from control cells, which were found to be intact, sodium butyrate dose dependently induced DNA degradation however, no distinct DNA ladder pattern was observed (Figure 3.5 c). A parallel experiment with Jurkat T-lymphocytes treated with 0.8mg/ml sodium butyrate under the same conditions produced the expected DNA ladder pattern (Figure 3.5 c).

3.3.3 Activation of the caspase cascade by sodium butyrate treated HaCaTs

The activity of initiator caspases 8 and 9 as well as the downstream effector caspase 3 was measured in HaCaTs treated with Sodium butyrate. Given that the temporal profile of activity is different for each caspase, the response to butyrate (0.8mg/ml) was examined at time points from 0 hr up to 72 hr. Sodium butyrate induced caspase 8 activity by 3 hr with this reaching a significant 2-3-fold increase over untreated control levels after 8 hr (Figure 3.6 a). Caspase 8 activity gradually declined after 8hrs, returning to basal levels by 48hrs. Caspase 3 activity on the other hand was elevated by 6 hr and reached a significant three-fold increase after 18 hr with a peak of more than 4-fold observed at 24 hr (Figure 3.6 a). Although caspase 3 activity declined after 24 hr, it was still elevated at 48 hr but was undetectable by 72hr. This may be due to increased protease levels within the cultures as the total protein content of extracts from butyrate

treated cells was also reduced between 24 and 72 hr (data not shown). Caspase 9 was not activated at any time by sodium butyrate (Figure 3.6 a).

Having established the time of maximal activity for caspases 8 and 3 at the concentration of sodium butyrate found to induce the most apoptosis, the dose effect of sodium butyrate on caspase activity was investigated at these time points (8 hr and 24 hr respectively). Consistent with the apoptosis data, Sodium butyrate was shown to increase caspase 8 activity in a dose dependent manner in HaCaTs; although a significant increase was only observed when the 0.8mg/ml dose was used (Figure 3.6 b). Caspase 9 activity has been reported to peak between 6-9 hr (Sitailo *et al.* 2002). The effect of sodium butyrate on caspase 9 activity was examined at 8 hr, however sodium butyrate did not induce caspase 9 activity at any dose tested (Figure 3.6 b).

Caspase 3 proteolytic activity is dependent on the cleavage of the 35kDa pro-caspase 3 precursor to a 17kDa active caspase 3 fragment. Western blot analysis showed that sodium butyrate dose dependently decreased pro-caspase 3 in HaCaTs after 24 hr (Figure 3.7 a). Consistent with other reports however (Denning *et al.* 1998, Liu *et al.* 2000), an increase in the 17kDa fragment was not observed. Cleavage of pro-caspase 3 to the active 17kDa fragment was confirmed however by the assessment of PARP, a known protein substrate of caspase 3 (Decker & Muller 2002, Hong *et al.* 2004). Figure 3.7 b demonstrates that sodium butyrate induced cleavage of PARP from the 113kDa pro-form to the 89kDa fragment in a dose-dependent manner.

Figure 3.5

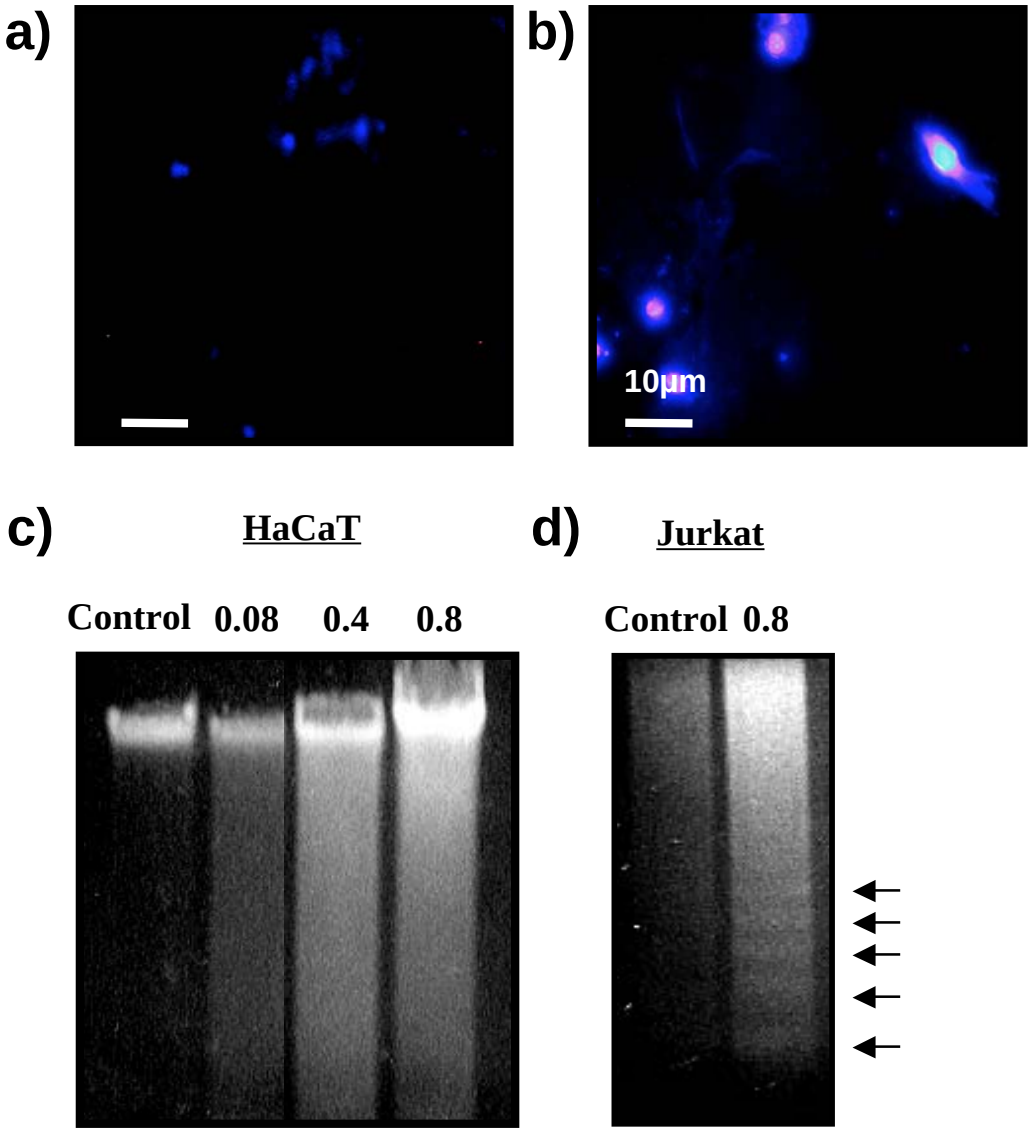

Figure 3.5– Effect of sodium butyrate on DNA fragmentation. Non adherent HaCaTs were collected from control HaCaT (a) and HaCaTs treated with 0.8mg/ml sodium butyrate for 24hr (b) and stained with HOESCHT to detect condensed chromatin and nuclear fragmentation. Representative DNA ladder of control HaCaTs and HaCaTs incubated with 0.08, 0.4 and 0.8mg/ml sodium butyrate for 24hr. (c) DNA ladder of Jurkat T-lymphocytes in control conditions (10% FBS) or (d) treated with 0.8mg/ml sodium butyrate for 24hr (arrows indicate DNA ladder bands).

Figure 3.6

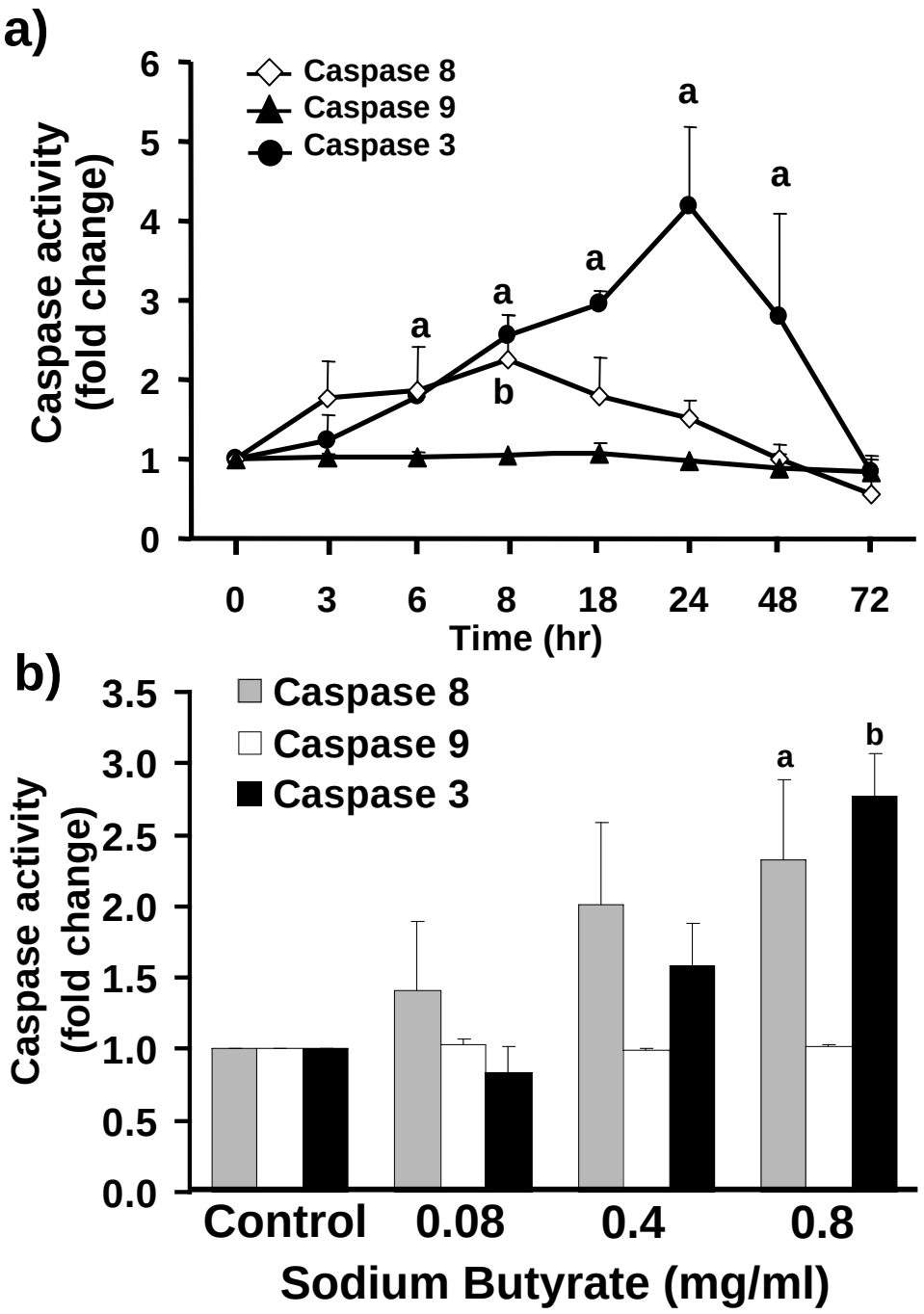

Figure 3.6– Effect of sodium butyrate on caspase activity. (a) The activation of HaCaT caspase 8 (open diamonds), 9 (closed triangles) and 3 (closed circles) was measured using different fluorogenic substrates. The change in relative fluorescence units at various time points after treatment with 0.8mg/ml of sodium butyrate was measured and control cells were left untreated over 72hr. (b) Caspase 8 (grey bars) and caspase 9 (white bars) activity of HaCaTs was measured after 8hrs and caspase 3 activity (black bars) was measured after 24hr of treatment with 0.08, 0.4and 0.8mg/ml doses of sodium butyrate. Data is presented as the mean±SEM of 3 independent experiments and was analysed using one-way analysis of variance (ANOVA) and post-hoc t-test with significant differences compared to controls shown (caspase 3, **a**; caspase 8, **b**; *p<0.05).

Figure 3.7

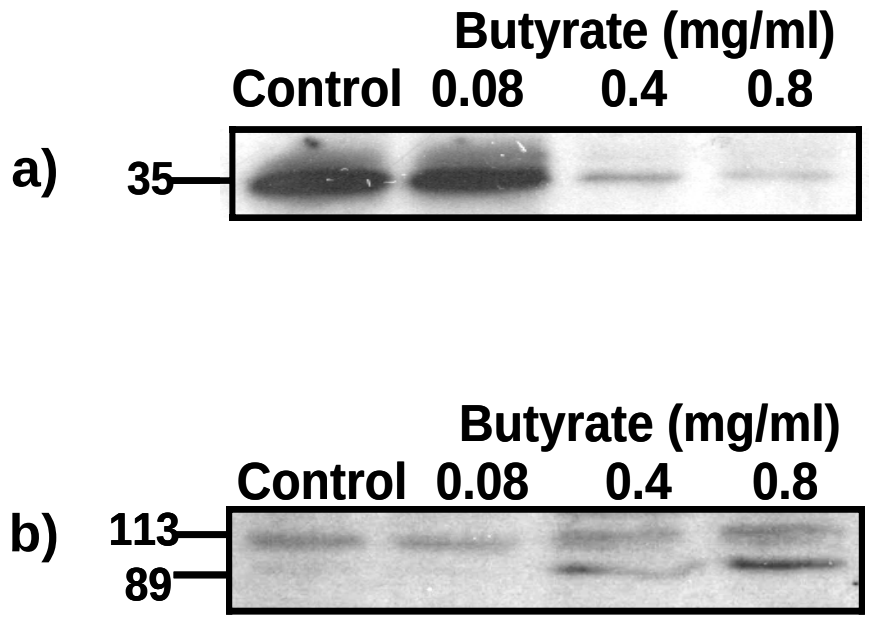

Figure 3.7– Effect of sodium butyrate on caspase 3 and PARP cleavage. (a) Western Blot shows pro-caspase 3 (35kDa) protein expression of control and HaCaTs treated with 0.08, 0.4 and 0.8mg/ml sodium butyrate for 24hr. (b) PARP cleavage was measured in whole cell lysates from the cells described in, the lower band 89kDa is the cleaved product from caspase 3 activity. The data presented are representative of 3 separate experiments.

3.3.4 Sodium butyrate induced Fas expression HaCaTs.

The caspase cascade is often activated by the death receptor Fas, hence, the effect of sodium butyrate on Fas expression by HaCaTs was investigated using flow cytometry and western blot analysis. As shown in Figure 3.8 a, HaCaTs treated with sodium butyrate for 24hr showed an increase in the level of Fas surface expression with this represented by the mean fluorescence intensity (MFI) of Fas staining increasing from 0.7 to 1.3.

Expression of the heterogenous forms of Fas were also investigated by western blot analysis which showed the higher molecular weight Fas fragment (50kDa) was elevated in sodium butyrate treated HaCaTs compared to controls (Figure 3.8 b). This observation was consistent with the flow cytometry data shown in Figure 3.8 a and other studies associating this form of Fas with increased susceptibility to Fas-mediated death (Park *et al.* 2003). Fas and downstream activation of caspases was confirmed with down regulation of pro-caspase 3 by sodium butyrate (Figure 3.8 c).

3.3.5 Caspase 3 inhibitor did not inhibit butyrate induced apoptosis

A membrane permeable caspase 3 inhibitor DMQD-CHO (Ghayur *et al.* 1996, Hirata *et al.* 1998) was used to determine if inhibiting activation of caspase 3 could protect cells from sodium butyrate induced apoptosis. Pre-treating HaCaTs for 24hr with the caspase 3 inhibitor decreased sodium butyrate induced caspase 3 activity in a dose dependent

Figure 3.8

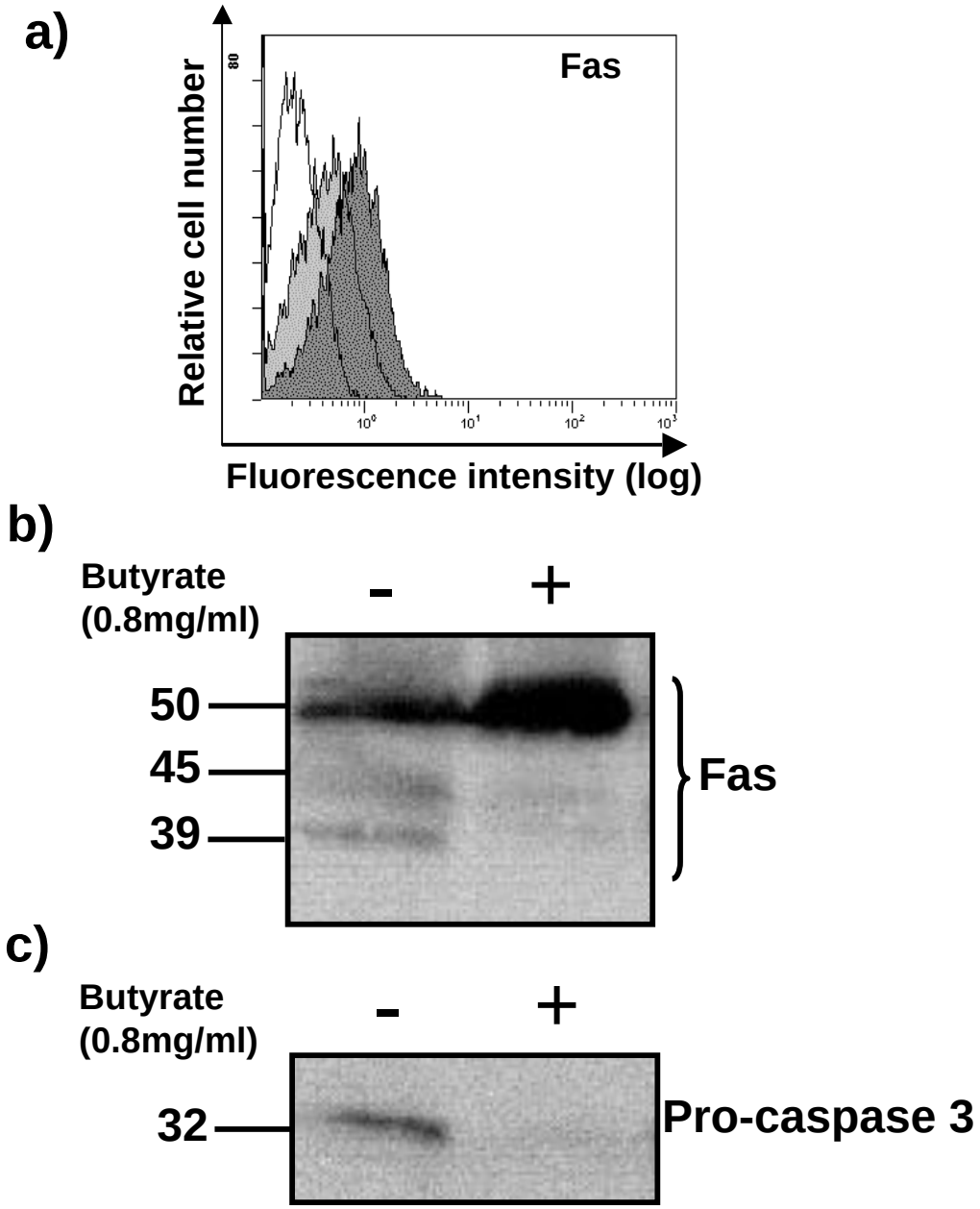

Figure 3.8– Effect of sodium butyrate on HaCaT Fas expression. Surface Fas expression of HaCaTs was analysed by flow cytometry. (a) The grey filled histogram shows the Fas staining of untreated HaCaT controls and dark grey filled histogram shows the Fas staining of 24hr sodium butyrate (0.8mg/ml) treated HaCaTs. Unfilled histogram represents staining of an isotype-matched control Ab. (b) The 3 bands of the Fas protein were detected by the Fas Ab using western blot from whole cell lysates of control cells and cells treated with 0.8mg/ml sodium butyrate for 24hr. (c) The membrane from (b) was also probed for the expression of pro-caspase 3 protein.

Figure 3.9

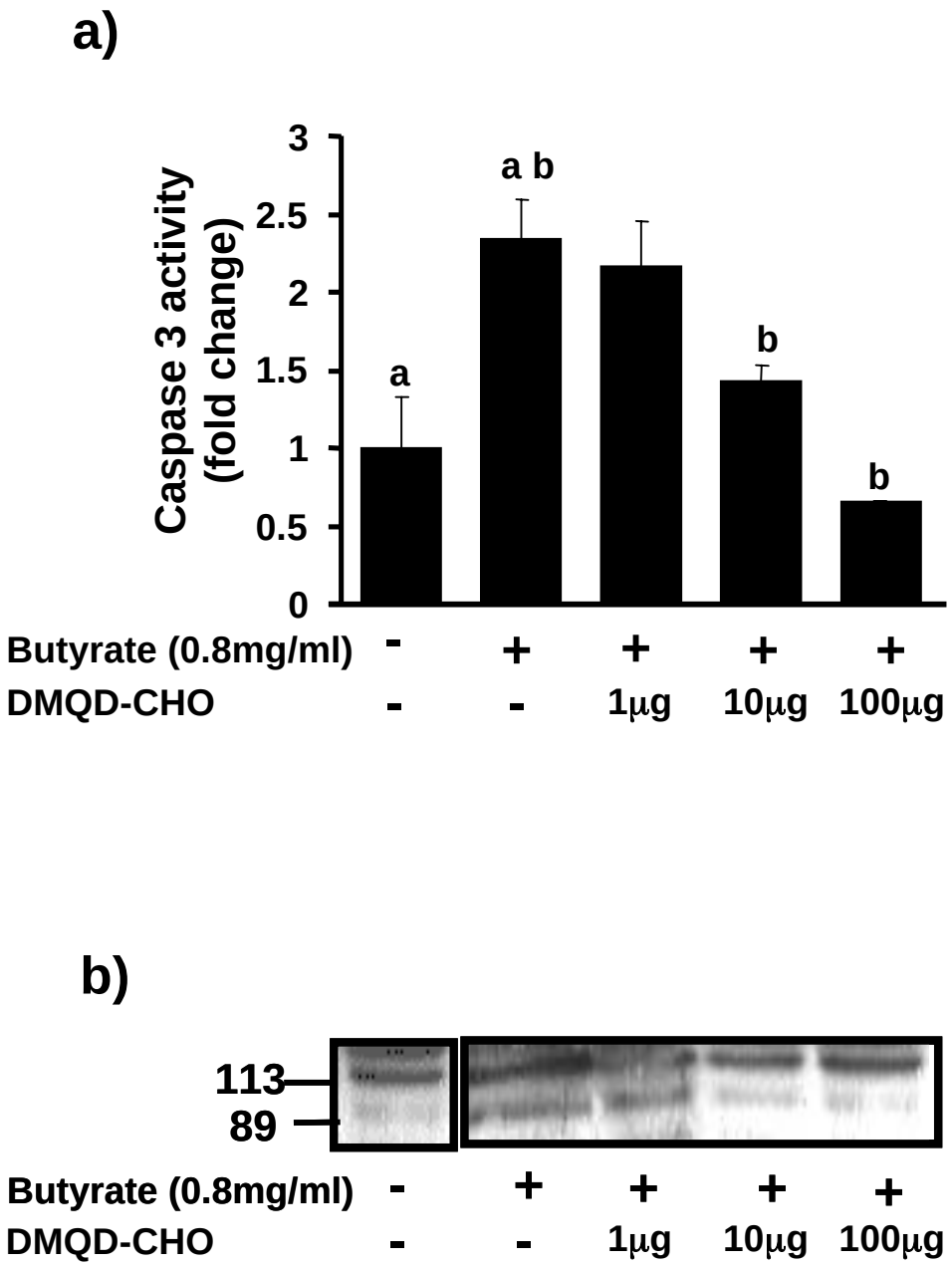

Figure 3.9– Effect of caspase 3 inhibitor on sodium butyrate induced caspase 3 activity and PARP cleavage. (a) The activation of caspase 3 was measured in HaCaT cells pretreated for 24hrs with 1-100ug/ml of a caspase 3 inhibitor DMQD-CHO, before incubation with 0.8mg/ml sodium butyrate for 24hrs. Values were normalised to the activation of control non-sodium butyrate treated samples and represent the mean of 5 independent experiments ± SEM *p<0.05. (b) A representative western blot of PARP cleavage expression on HaCaT cells pretreated with 1-100ug/ml of specific caspase 3 inhibitor, before incubation with 0.8mg/ml sodium butyrate for 24hr.

Figure 3.10

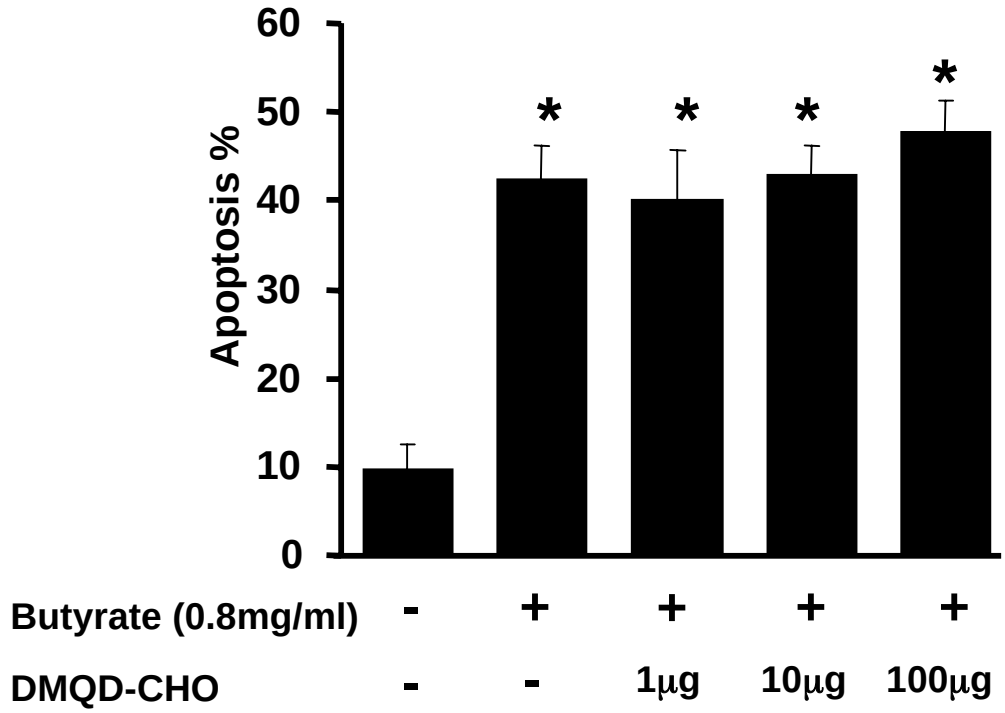

Figure 3.10– Effect of caspase 3 inhibitor on sodium butyrate induced HaCaT apoptosis. HaCaT cells were pretreated with 3 different doses of a caspase 3 inhibitor DMQD-CHO (1-100 μg/ml), before incubation with 0.8mg/ml sodium butyrate for 24hr. Cells were stained with Annexin V and PI and analysed by flow cytometry. Values represent the mean percentage of apoptotic cells ± SEM of 5 independent experiments.

manner. The activity was significantly reduced by 100ug/ml of the inhibitor ($p<0.05$ Figure 3.9 a). The reduction in sodium butyrate induced caspase 3 activity was confirmed by the ability of DMQD-CHO to prevent sodium butyrate mediated PARP cleavage (Figure 3.9 b).

Although pre-treatment of HaCaTs with DMQD-CHO blocked sodium butyrate induced caspase 3 activity and PARP cleavage, this inhibitor was unable to prevent the significant increase in Annexin V staining induced by sodium butyrate measured by flow cytometry (Figure 3.10). Cells examined using phase contrast microscopy however showed that the apoptosis related morphological changes induced by sodium butyrate compared to control, such as cell shrinkage and detachment from the culture plate (Figure 3.11 a and b), were reduced by DMQD-CHO (Figure 3.11 c). DMQD-CHO also decreased nuclear fragmentation seen with sodium butyrate treated HaCaTs (Figure 3.11 d - f).

3.3.6 Sodium butyrate did not induce HaCaT differentiation

To determine if sodium butyrate induced apoptosis was associated with terminal differentiation of HaCaTs, the intracellular expression of differentiation markers was examined by flow cytometry. The expression of keratin 14 (K14; basal cell marker), keratin 10 (K10; suprabasal cell marker) and involucrin (terminal differentiation marker) was assessed. Sodium butyrate did not change the percentage of cells expressing the basal cell marker K14, K10 or involucrin compared to control cells (Figure 3.12 a-c).

Figure 3.11

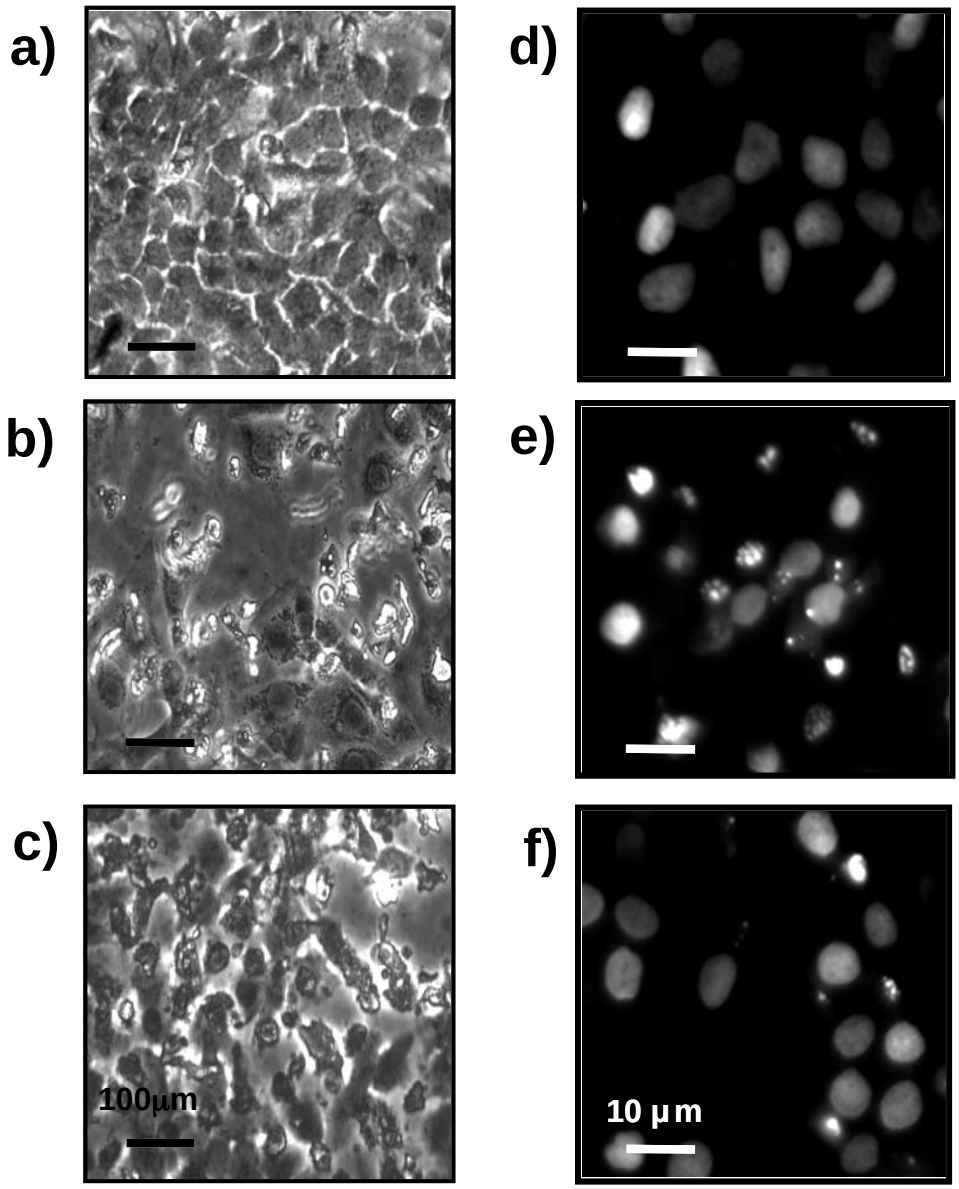

Figure 3.11– Effect of caspase 3 inhibitor on sodium butyrate induced HaCaT apoptosis morphology and nuclear fragmentation. HaCaT morphology was assessed on cultures prior to flow cytometry while chromatin condensation and DNA fragmentation was assessed in parallel cultures using the HOESCHT 33342 fluorescent stain. Phase contrast microscopy of (a) control HaCaT cells, (b) cells treated with 0.8mg/ml sodium butyrate for 24hr and (c) HaCaTs pretreated for 24hr with 100ug DMQD-CHO before incubation with 0.8mg/ml sodium butyrate for 24hrs. Nuclear fragmentation viewed by HOESCHT fluorescent stain of (d) control HaCaT cells, (e) HaCaTs treated with 0.8mg/ml sodium butyrate and (g) HaCaTs pretreated for 24hr with 100ug DMQD-CHO before incubation with 0.8mg/ml sodium butyrate for 24hrs.

Figure 3.12

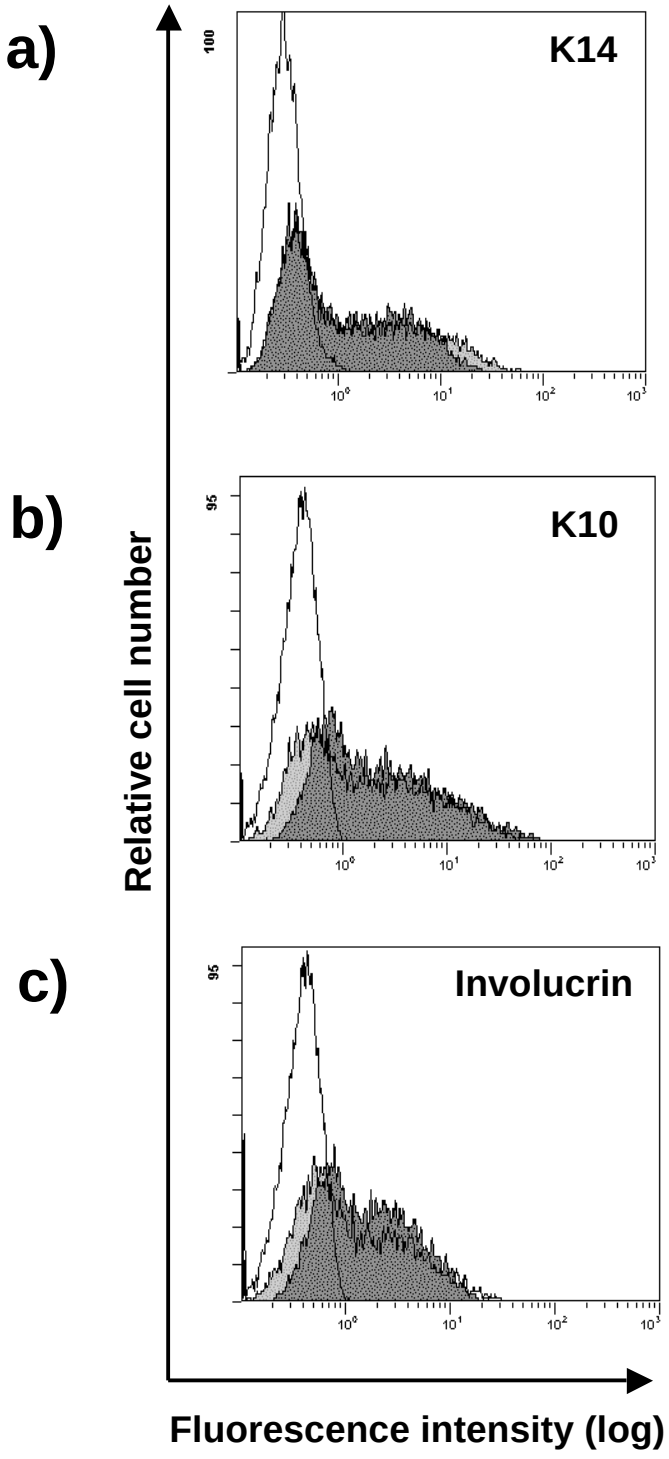

Figure 3.12– Effect of sodium butyrate on keratinocyte differentiation. The intracellular expression of keratinocyte differentiation markers was assessed by flow cytometry. a) representative histogram of keratin 14 expression, b) keratin 10; c) involucrin. In each panel the light grey histogram shows staining in control HaCaTs and the overlaying dark grey histogram staining in HaCaTs treated for 24 hours with sodium butyrate (0.8mg/ml). The unfilled histogram is the negative control (isotype-matched Ab).

This result indicated that sodium butyrate did not modulate the normal progression of the HaCaTs through the phases of differentiation.

3.4 Summary

The objective of this chapter was to determine the most effective assessment of keratinocyte apoptosis. The findings from the studies in this Chapter showed that apoptosis can be readily detected in HaCaT keratinocytes treated with sodium butyrate. Annexin V staining, as well as morphology and nuclear fragmentation appear to be the most reliable methods for detecting apoptosis of HaCaTs. The results also suggest that the assessment of Fas and subsequent caspase 3 activation is important for examining the mechanism of apoptosis in HaCaTs. In addition, the studies performed in this chapter have characterised a novel aspect of the effect of sodium butyrate has on keratinocyte apoptosis. Despite not been directly relevant to the aim of this thesis, these outcomes will be discussed, nonetheless with this discussion providing details that help validate the focus on the mechanisms in subsequent chapters.

Consistent with other studies using intestinal epithelial cell lines (Jones *et al.* 2004), similar concentrations of sodium butyrate reduced HaCaT viability. This decrease in HaCaT viability was accompanied by a significant increase in apoptotic cells as identified by Annexin V staining and characteristic morphological changes. Changes in cell morphology including cell shrinkage, cellular detachment from the culture plate and apoptotic body formation was consistent with apoptosis. Apoptosis was confirmed by

the increase in the number of condensed and fragmented nuclei observed by 24 hr in sodium butyrate treated cells using HOESCHT 33342 dye. These observations were similar to those from studies in gastric cancer cell lines (Litvak *et al.* 2000). Although nuclear fragmentation was evident in sodium butyrate treated cells, DNA fragmentation visualised by gel electrophoresis demonstrated no ladder pattern characteristic of fragmentation in butyrate treated cells. Instead the DNA appeared degraded. This is inconsistent with results obtained using the HOESCHT 33342 stain, which indicated fragmentation of the nucleus occurred following sodium butyrate treatment. Degradation of DNA or smearing has also been associated with necrosis, although this appears unlikely given the low levels of PI staining detected by flow cytometry. However when the same experiment was performed in Jurkat T-lymphocytes, a typical ladder DNA pattern was observed with sodium butyrate treatment. The reason for the HaCaT smears is still unclear, given that others have shown a distinct ladder pattern by HaCaTs exposed to UVA-350-400 mJ/cm2 and UVB-30 mJ/cm2 (Banerjee *et al.* 2005). Nonetheless, the data presented suggests that PS turnover detected by Annexin V staining and PI staining for necrotic cells are adequate measures for detecting different stages of apoptosis. In addition HOESCHT 33342 staining for nuclear fragmentation appears a more reliable indicator of HaCaT apoptosis induced by sodium butyrate.

The death receptor pathway Fas/CD95 was investigated as it has been shown to play an important role in UV radiation induced apoptosis of keratinocyte, sodium butyrate induced tumour cell apoptosis (Bonnotte *et al.* 1998, Chopin *et al.* 2004, Hernandez *et al.* 2001, Rosato *et al.* 2003) and Fas has also been shown to be implicated in T-

lymphocyte induced keratinocyte apoptosis in inflammatory skin disorders (Bang *et al.* 2002, Leverkus *et al.* 1997, Mammone *et al.* 2000b, Takahashi *et al.* 2001, Trautmann *et al.* 2000c). The effect of sodium butyrate on Fas expression by keratinocytes has not been previously investigated and the results obtained from these studies suggest a central role for Fas as sodium butyrate increased surface expression of Fas by HaCaTs.

The caspase cascade mediates the death receptor signal, and its activation leads to downstream apoptotic events resulting in overall cell execution (Barnhart *et al.* 2003). In order to further characterise the apoptotic pathway activated by sodium butyrate in HaCaTs, the activation of caspases from the extrinsic and intrinsic pathways was examined. It has been shown that sodium butyrate induced both the intrinsic and extrinsic caspase pathways in colon cancer cell lines (Rosato *et al.* 2003). The increase in caspase 8 activity by sodium butyrate supports the view that Fas mediates sodium butyrate induced keratinoctye apoptosis. Activation of Fas results in the recruitment of adapter protein Mort1 to the Fas death domain (FADD). A protein complex known as the death-inducing signalling complex (DISC) is formed when inactive caspase 8 is recruited to FADD, resulting in activation of caspase 8 and initiation of caspase-mediated apoptosis (Barnhart *et al.* 2003, Kuwana *et al.* 1998). The results from this chapter indicated that sodium butyrate induced HaCaT apoptosis, exclusively via the extrinsic pathway and specifically by activating caspase 8 followed by caspase 3, resulting in PARP cleavage. There was no concomitant caspase 9 activation. This differs to the caspase profile seen in UV induced keratinocyte apoptosis, which requires

activation of caspase 9 and the mitochondrial pathway (Barnhart *et al.* 2003, Sitailo *et al.* 2002).

The specific caspase 3 inhibitor DMQD-CHO was able to diminish sodium butyrate induced caspase 3 activity, inhibit PARP cleavage and decrease the number of HaCaT-keratinocytes with fragmented nuclei and those lifting off the culture plate. These results show from a biological viewpoint that DMQD-CHO appeared to suppress apoptosis in HaCaTs, consistent with studies in a Pre-B leukaemia cell line ALL-697 where DMQD-CHO also decreased chromatin condensation and inhibited PARP cleavage (Zhang *et al.* 1999). The results demonstrated however, DMQD-CHO did not prevent the translocation of PS to the outer membrane leaflet as measured by Annexin V staining.

PS translocation is an early event in apoptosis and, somewhat controversially, is generally considered to be linked to activation of the initiator caspase 8 and the cleavage of plectin, a major cross-linking protein involved in apoptosis-induced reorganization of the actin cytoskeleton (Barnhart *et al.* 2003, Stegh *et al.* 2000b). Others have reported that Annexin V staining induced by death receptors can be decreased by inhibiting effector caspases using z-VAD-fmk (Griffith *et al.* 2000, Maianski *et al.* 2003), however this is a relatively non specific inhibitor that can inhibit initiator caspases as well as effector caspases (Schotte *et al.* 1999). Our finding that an increase in caspase 8 activity preceded the activation of caspase 3 together with the inability of DMQD-CHO to prevent PS exposure lends support to the view, at least in keratinocytes, that the initiator caspases are indeed responsible for this event and that inhibition of effector caspases

does not decrease Annexin V staining (Cummings *et al.* 2004, Drenou *et al.* 1999). Thus it appears in keratinocytes that the early apoptotic related changes in cell membrane symmetry are controlled by upstream initiator caspases (Hirata *et al.* 1998), with caspase 3 mediating chromatin condensation and DNA fragmentation (Hirata *et al.* 1998, Liu *et al.* 1997) and blockade of caspase 3 being capable of limiting the progression of apoptosis but not preventing its initiation. This result also indicated that Annexin V staining maybe a more sensitive indicator of apoptosis than the measurement of caspase 3 activity.

Another possible reason the caspase inhibitor did not prevent apoptosis is that sodium butyrate may have induced terminal differentiation, a process that has been shown to also activate caspase 3 (Weil *et al.* 1999). Sodium butyrate has been reported to promote differentiation in colon cells (Cai *et al.* 2004) and has also been shown to induce terminal differentiation and formation of cornified envelopes in keratinocytes (Ford *et al.* 1993, Schmidt *et al.* 1989, Staiano-Coico *et al.* 1989). In contrast to these reports, sodium butyrate did not alter the intracellular expression of keratinocyte markers in HaCaTs that are normally associated with basal cells (K-14), cells committed to a differentiation path (K-10) or becoming terminally differentiated (involucrin). These data suggested that sodium butyrate induced apoptosis was induced in keratinocytes in a manner distinct from terminal differentiation.

From the results presented in this Chapter, the following conclusions can be drawn:

- Annexin V staining, as well as cellular morphology and staining for nuclear fragmentation appear to be the most reliable methods for detecting apoptosis of HaCaTs.
- The assessment of Fas and subsequent caspase 3 activation is important for examining the mechanism of apoptosis in HaCaTs.

Given that sodium butyrate induced Fas activation of caspase 8 and 3, leading to PARP cleavage and apoptosis (Figure 3.13), appears to act at a point that bypasses the protection provided by anti-apoptotic proteins known to be important in malignant cell survival (Raisova *et al.* 2001, Zhu & Otterson 2003). These findings give support to the view that HDI's such as Sodium butyrate may be useful treatments for epidermal disorders such as psoriasis or cutaneous malignancies where the activation of keratinocyte cell death appear dysregulated.

Figure 3.13

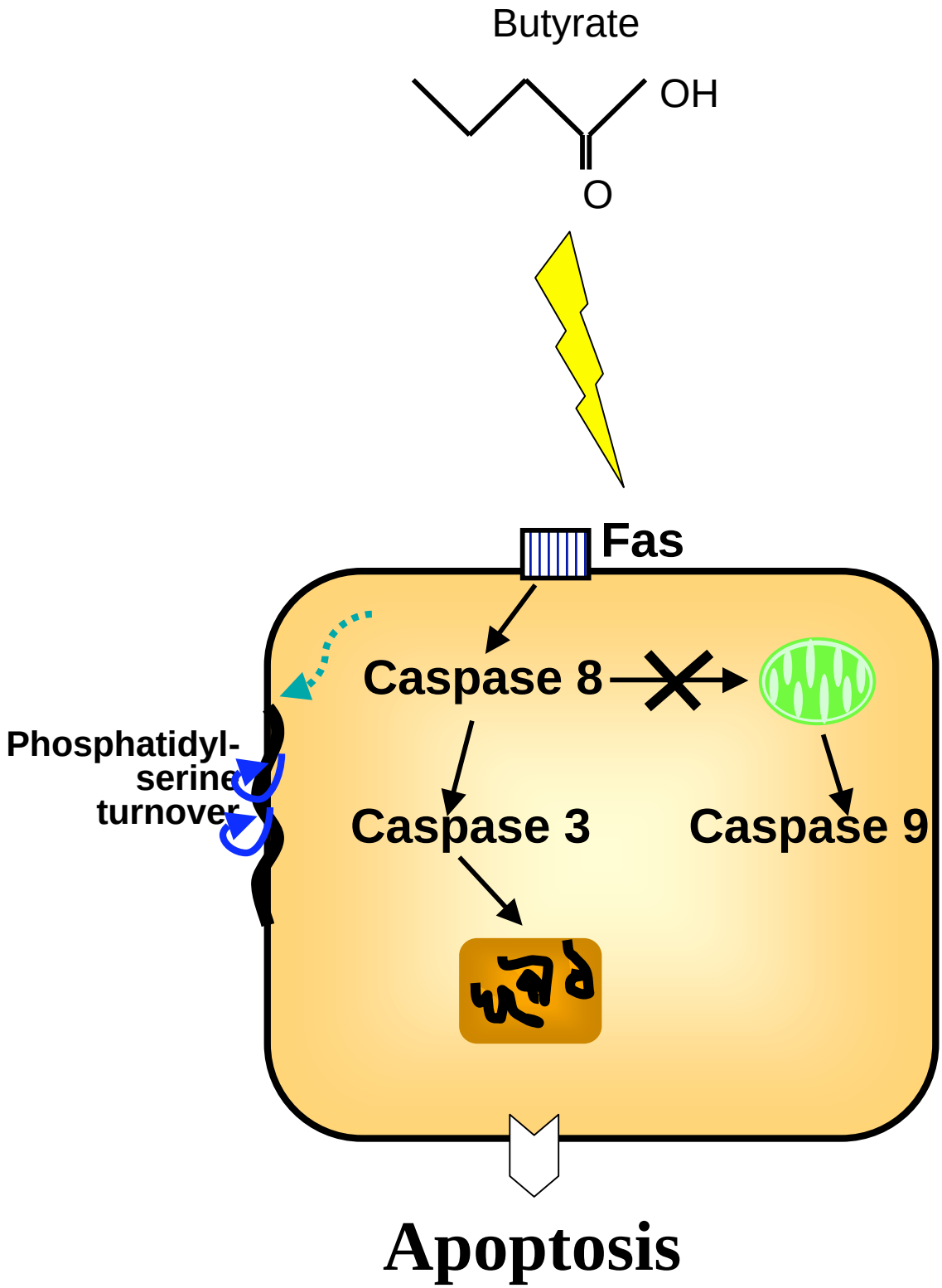

Figure 3.13. Sodium butyrate induced Fas mediated HaCaT apoptosis.

CHAPTER 4

4 JURKAT INDUCED HACAT APOPTOSIS

4.1 Introduction

To satisfy the overall objective of this thesis, a cell co-culture model was required to allow T-lymphocyte induced apoptosis of keratinocytes to be studied *in vitro*. Using the methods for measuring keratinocyte apoptosis described in Chapter 3, the studies in this chapter aimed to establish optimum conditions for the induction of keratinocyte apoptosis by T-lymphocytes and to characterise the major mechanisms involved.

This chapter reports studies performed using Jurkat and HaCaT cell lines with the specific aims as follows:

1. Establish the effects of Jurkat T-lymphocytes on HaCaT apoptosis

CD4+ T-lymphocytes or T-lymphocytes are the primary inducers of keratinocyte apoptosis resulting in the development of skin lesions and impaired epidermal integrity in atopic skin (Campa *et al.* 1990, Werfel T 2002). Studies were performed to identify conditions necessary for Jurkat T-lymphocytes to induce HaCaT apoptosis in co-culture. Moreover, given that it has been demonstrated that soluble factors released by activated

Primary T-lymphocytes are capable of inducing keratinocyte apoptosis (Trautmann *et al.* 2000a), studies in this chapter also investigated the effect of soluble factors released by Jurkat T-lymphocytes on HaCaT apoptosis.

2. Characterise the involvement of the Fas pathway and the effect of inflammatory cytokine IFNγ on Jurkat induced keratinocyte apoptosis

It has been suggested that keratinocyte apoptosis induced by T-lymphocytes in AE is mediated by Fas, with inflammatory cytokines such as interferon γ (IFNγ), shown to be required by T-lymphocytes to induce apoptosis of keratinocytes via upregulation of both Fas and Fas ligand (FasL) (Arnold *et al.* 1999, Trautmann *et al.* 2000c).

3. Investigate the involvement of adhesion molecules

Studies will investigate the expression of adhesion molecules given that these have been suggested to assist in the development of the AE lesions by retaining T-lymphocytes in the skin (Nickoloff *et al.* 1993).

4.2 Methods

Given that standard growth media used for HaCaTs and Jurkat culture (10% FBS) contains growth factors which may interfere with the induction of keratinocyte apoptosis by Jurkat T-lymphocytes (Reinartz *et al.* 1996), preliminary experiments were performed to titrate the FBS concentrations. These showed that 1% FBS did not compromise the cell survival in the culture periods (Appendix 3). All experiments in this and subsequent chapters were thus performed using 1% FBS supplemented media (basal media).

4.2.1 Jurkat conditioned media

Jurkat T-lymphocytes were serum starved overnight and 5 x 10^5 per ml Jurkat T-lymphocytes were cultured in 25-mm flasks with or without mitogen (10ng/ml PMA) in basal media for 48hrs. Cell-free conditioned media which was obtained by centrifugation and added immediately to HaCaTs in 6 well plates and incubated for 48hrs. HaCaT controls were incubated in basal media.

4.2.2 Jurkat T-lymphocyte and HaCaT co-cultures

Three days prior to culture with HaCaTs, Jurkat T-lymphocytes were serum starved overnight and then activated with PMA (10ng/ml) for 48hrs in DMEM containing 1% FBS. HaCaTs were grown to 70-80% confluence in 12 well plates before being cultured with 5 x 10^5 Jurkat T-lymphocytes for 48hrs. Jurkat T-lymphocytes were washed in PBS prior to co-culture and HaCaT controls contained PMA (10ng/ml). In some experiments

100ng/ml recombinant IFNγ (Sigma Chemical Co.) was added to HaCaT control cultures or HaCaT/Jurkat T-lymphocytes co-cultures for 48hrs.

4.2.3 Assessment of HaCaT apoptosis

Annexin and PI staining was used to assess HaCaT apoptosis by flow cytometry as described in Methods section 2.5.1. Conditioned media containing Jurkat T-lymphocytes and non-adherent T-lymphocytes was combined with adherent HaCaTs collected by incubating with trypsin (0.25%)-EDTA. Quadrant markers were set on dotplots of unstained cells (viable cell population) and a gate was used to size exclude Jurkat T-lymphocytes as seen in Appendix 2. For HOECHST 33342 staining of HaCaTs after co-cultures, Jurkat T-lymphocytes were removed by washing twice with PBS (Methods Section 2.6.1).

4.2.4 Mechanistic assessments

Surface Fas and ICAM-1 expression by HaCaTs as well as FasL and CD25 expression by Jurkat T-lymphocytes was examined by flow cytometry (section 2.5.2). Western blot analysis for Fas and PARP expression was performed on adherent HaCaTs after washing wells with PBS twice in order to remove Jurkat T-lymphocytes before protein extraction (Methods section 2.8). HaCaT caspase activity 3 assays were performed as described in Methods section 2.7.

4.3 Results

4.3.1 Jurkat activation

To determine whether activation of Jurkat T-lymphocytes was required to achieve optimal HaCaT apoptosis, the effect of mitogen activation of Jurkat T-lymphocytes was investigated. Figure 4.1 a and b demonstrate that incubation of Jurkat T-lymphocytes with PMA (10ng/ml) for 48hrs resulted in an increase in Jurkat aggregation, which is an indicator of T-lymphocyte activation and consistent with an increase in CD25 or IL-2 receptor expression (Figure 4.1 c). CD25 expression is a well accepted marker of T-lymphocyte activation. Figure 4.1 d demonstrates that incubation of Jurkat T-lymphocytes with PMA (10ng/ml) for 48hrs resulted in increased FasL expression (MFI from 0.2 to 0.9). An increase in soluble FasL (sFasL) was also detected in the conditioned media from PMA stimulated Jurkat T-lymphocytes by dot blot analysis (Figure 4.1 d –insert; Method described in Section 2.9). This confirms preliminary studies which showed that PMA (10ng/ml) was more potent at stimulating Jurkat T-lymphocytes than PHA or ConA (Appendix 4).

4.3.2 Jurkat co-culture induced HaCaT apoptosis

The results from Section 4.3.1 indicate that activated Jurkat T-lymphocytes have the capacity to induce apoptosis via Fas, given that activated Jurkat T-lymphocytes express the death inducing ligand; FasL on the cell surface and also released sFasL into the

conditioned media (Figure 4.1 d). To determine whether Jurkat T-lymphocytes could induce HaCaT apoptosis, HaCaTs were incubated with unactivated or mitogen activated Jurkat T-lymphocytes (PMA 10ng/ml) for 48hr. As shown in the representative dot plot in Figure 4.2 a, most HaCaTs incubated under control conditions (1% FBS) were negative for Annexin or PI staining. HaCaTs co-cultured with unactivated Jurkat T-lymphocytes were also negative for Annexin or PI staining (Figure 4.2 b). However, when HaCaTs were co-cultured with activated Jurkat T-lymphocytes for 48hrs, there was a marked increase in apoptotic cells as shown by the increase in cells found in the EA and LA quadrants (Figure 4.2 c).

To investigate whether Jurkat-induced HaCaT apoptosis was mediated by direct cell-cell interaction between HaCaTs and Jurkat T-lymphocytes or by factors secreted into the conditioned media, HaCaTs were either incubated for 48hrs with conditioned media from Jurkat T-lymphocytes (-/+ PMA 10ng/ml activation), or co-cultured with Jurkat T-lymphocytes (-/+ PMA 10ng/ml activation). Figure 4.2 d shows the collated data from 3 independent experiments and demonstrates that Jurkat conditioned media (grey bars; Figure 4.2 d) from activated or inactivated cells did not induce apoptosis of HaCaTs compared to controls. Whilst there was no significant increase in apoptosis when HaCaTs were co-cultured with unactivated Jurkat T-lymphocytes, there was a significant increase in HaCaT apoptosis when they were co-cultured with PMA activated Jurkat T-lymphocytes ($p<0.05$; Figure 4.2 d -black bars).

Figure 4.1

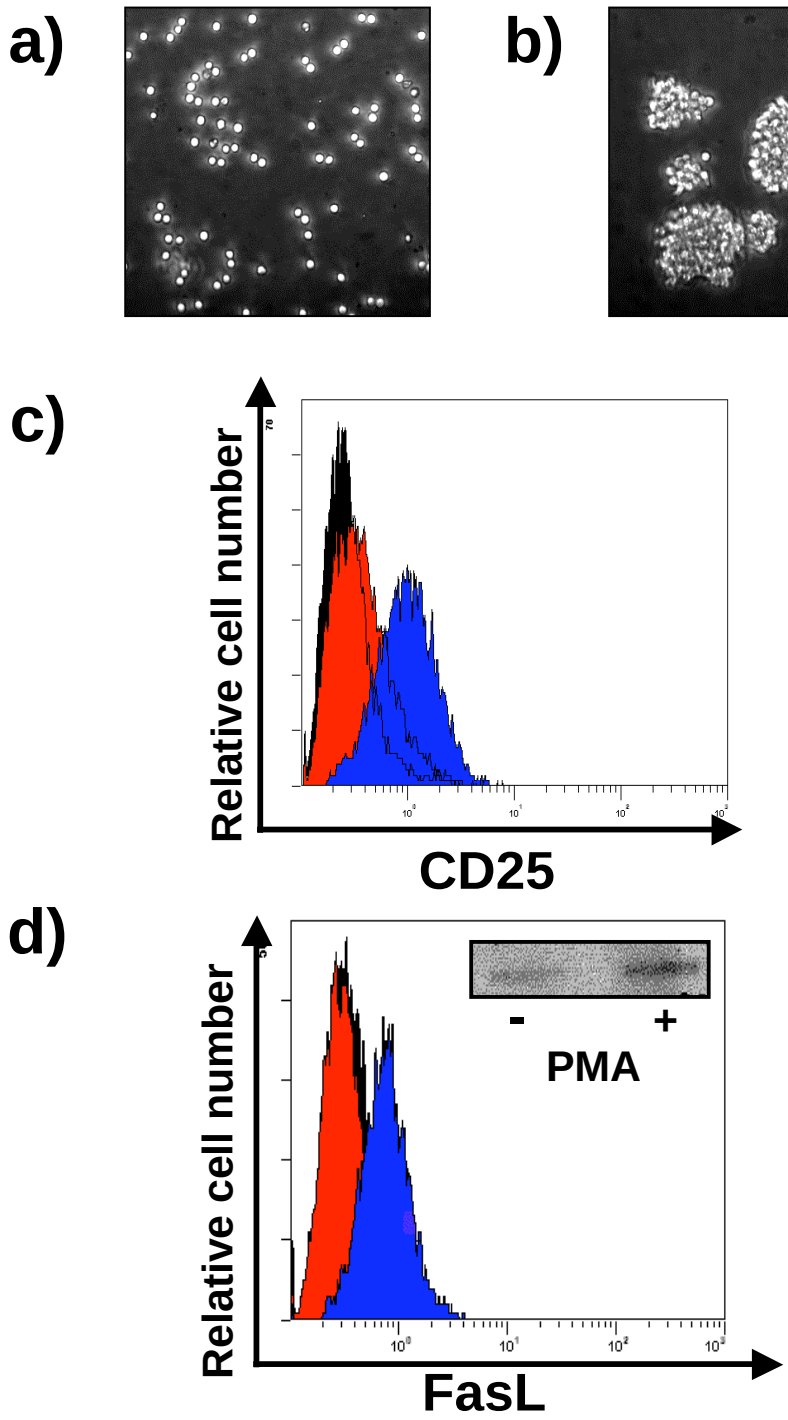

Figure 4.1 Effect of PMA on Jurkat activation and FasL expression. (a) Phase contrast microscopy of unactivated Jurkat T-lymphocytes or (b) PMA activated Jurkat T-lymphocytes in culture media. CD25 and FasL expression by Jurkat T-lymphocytes was analysed using flow cytometry. (c) CD25 expression by unactivated (red histogram) or PMA activated Jurkat T-lymphocytes(blue histogram). (a) FasL expression of unactivated (red histogram) or PMA (10ng/ml) activated Jurkat T-lymphocytes (blue histogram). (a-insert) Dot blot of sFasL present in conditioned media from unactivated "-" or PMA activated "+" Jurkat T-lymphocytes. The black histograms represents staining of an isotype-matched control Ab.

Figure 4.2

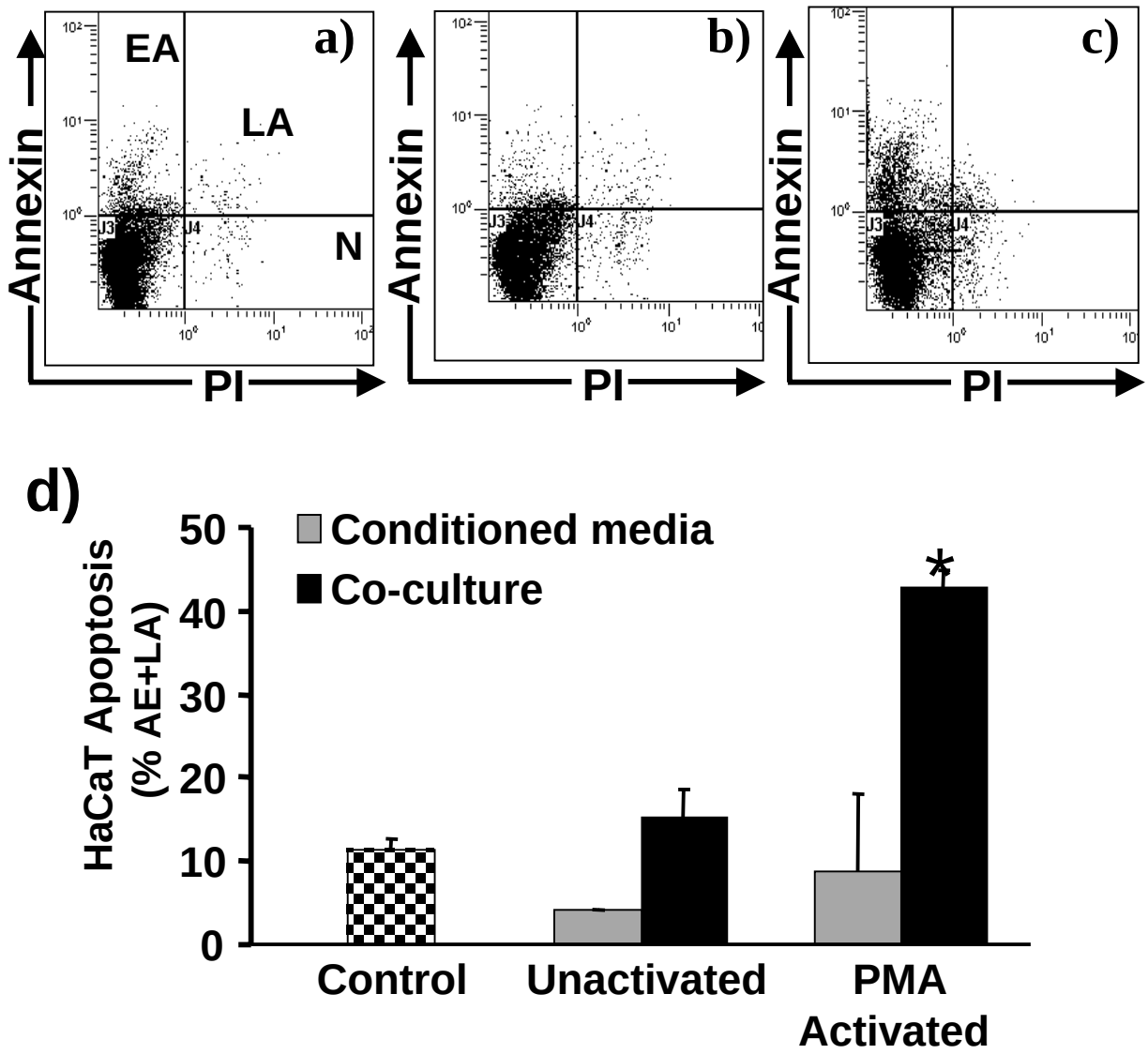

Figure 4.2 Effect of Jurkat conditioned media and Jurkat co-culture on HaCaT apoptosis. (a) Representative dot plots of Annexin V and propidium iodide (PI) stained HaCaT controls or (b) HaCaTs co-cultured with un-activated Jurkat T-lymphocytes or (c) HaCaTs co-cultured with PMA activated Jurkat T-lymphocytes after 48hrs. Annexin V and PI negative cells were considered viable (V), the annexin V positive / PI negative cells were considered early apoptotic (EA), annexin V and PI positive cells were considered late apoptotic (LA) and PI positive / Annexin V negative cells were the necrotic population (N). (d) HaCaT controls (black and white bars), HaCaTs incubated for 48hr with conditioned media from Jurkat (grey bars;+/- activation) or co-culture with Jurkat T-lymphocytes (black bars;+/- activation) were stained with Annexin V and PI and the apoptotic population [EA + LA] was determined. Bar graphs represent the mean ± SEM cell percentage from 3 separate experiments. The data was analysed using one-way analysis of variance (ANOVA) and considered significant at *$p<0.05$.

Figure 4.3

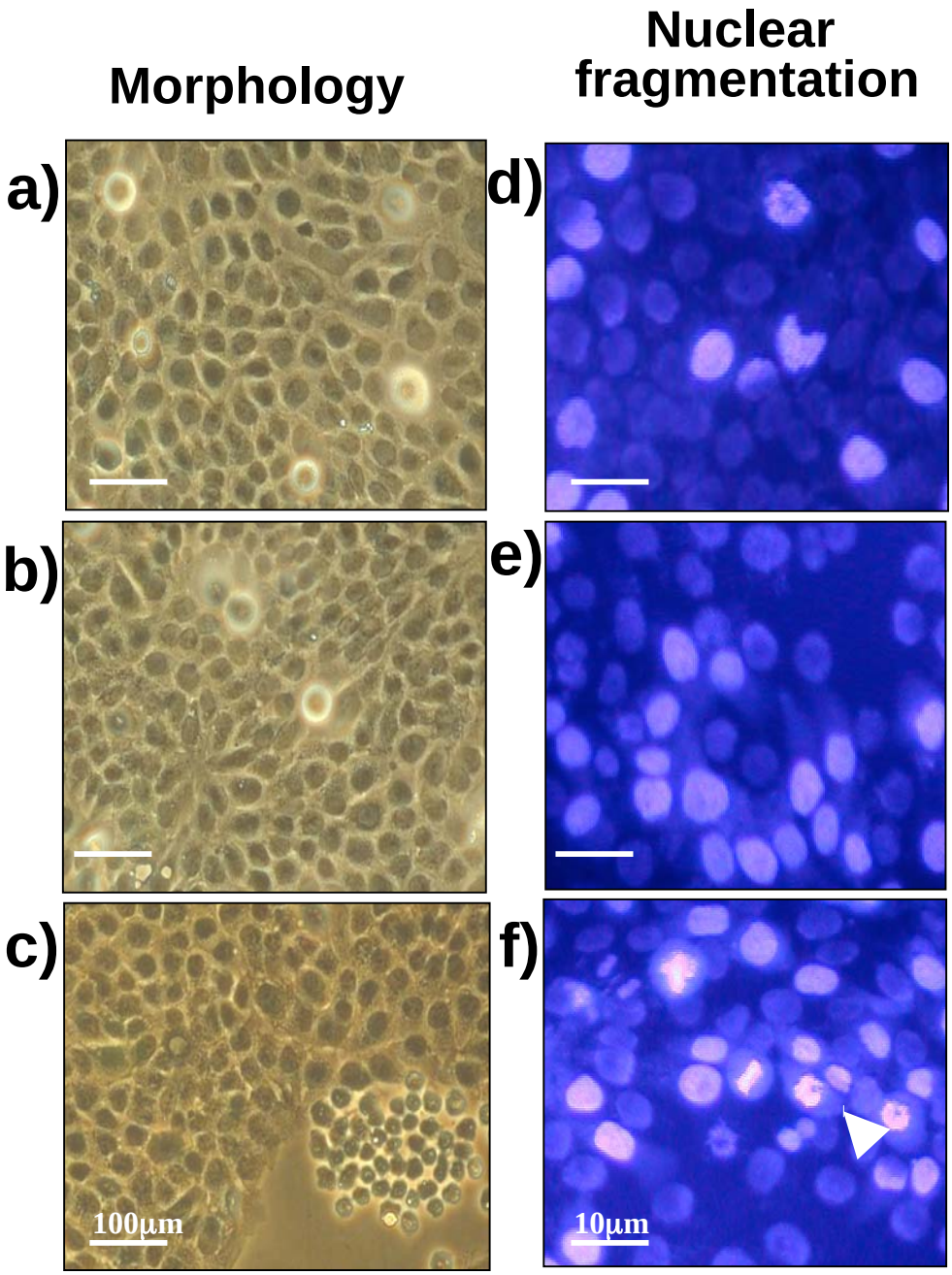

Figure 4.3 Effect of Jurkat conditioned media and Jurkat co-culture on HaCaT morphology and nuclear fragmentation. (a) Phase contrast microscopy of HaCaT controls after 48hr incubation, (b) HaCaTs incubated with conditioned media from PMA activated Jurkat T-lymphocytes for 48hrs and (c) HaCaTs co-cultured with PMA activated Jurkat T-lymphocytes for 48hrs. HOESCHT fluorescent stain was used to detect condensed and fragmented chromatin of (d) control HaCaTs (e) HaCaTs incubated with conditioned media from PMA activated Jurkat T-lymphocytes for 48hrs and (f) HaCaTs co-cultured with PMA activated Jurkat T-lymphocytes for 48hrs, arrows point to fragmented nuclei.

The effect of conditioned media from activated Jurkat T-lymphocytes and activated Jurkat T-lymphocytes co-culture on HaCaT morphology was also determined. Representative images in Figure 4.3 demonstrate that conditioned media from PMA activated Jurkat T-lymphocytes did not alter HaCaT morphology and the cells resembled control HaCaTs (Figure 4.3 a and b). However, HaCaTs co-cultured with activated Jurkat T-lymphocytes showed features characteristic of apoptosis. HaCaTs were shrunken and had a granular appearance, with a number of cells observed to have detached from the culture plate (Figure 4.3 c). Compared to controls and HaCaTs incubated with Jurkat T-lymphocyte conditioned media which showed minimal nuclear fragmentation (Figure 4.3 d and e), HaCaTs co-cultured with activated Jurkat T-lymphocytes showed a marked increase in nuclear condensation and fragmentation (arrows - Figure 4.3 f).

4.3.3 Jurkat co-culture induced HaCaT caspase 3 activity

Caspase 3 was found to be important for mediating some characteristics of apoptosis such as nuclear fragmentation when HaCaTs were treated with sodium butyrate (Chapter 3, Section 3.3.5). Figure 4.4 demonstrates that conditioned media (+/- activated Jurkat T-lymphocytes) did not induce HaCaT caspase 3 activity. Similar to conditioned media, there was no significant increase in caspase 3 activity in HaCaTs co-cultured with unactivated Jurkat T-lymphocytes. Activated Jurkat T-lymphocytes however, significantly induced caspase 3 activity by 2.5-fold over control levels ($p<0.05$; Figure 4.4).

The effect of a specific caspase 3 inhibitor (DMQD-CHO) on Jurkat co-culture induced HaCaT caspase 3 activity was investigated. HaCaTs were pre-incubated with DMQD-CHO (100ug/ml) 24hrs before co-culture. Figure 4.5 a demonstrates that Jurkat induced caspase 3 activity of HaCaTs was prevented by DMQD-CHO. When PARP expression was examined, Figure 4.5 b shows that Jurkat co-culture induced cleavage of the 113kDa pro-form of PARP to the 89kDa fragment and this cleavage was prevented by DMQD-CHO (Figure 4.5 b).

4.3.4 Jurkat induced HaCaT apoptosis by Fas

Interaction of FasL with the death receptor Fas is important for initiating caspase 3 mediated cell death (Arnold *et al.* 1999, Barnhart *et al.* 2003). Fas expression was found to also be important for mediating sodium butyrate induced apoptosis in HaCaTs (Chapter 3, section 3.3.4). To investigate the involvement of Fas in Jurkat T-lymphocyte induced HaCaT apoptosis, HaCaT Fas expression was examined after 48hr incubation with Jurkat conditioned media or with Jurkat T-lymphocytes. Jurkat conditioned media did not increase HaCaT Fas expression compared to HaCaTs controls (green and yellow histograms; Figure 4.6 a and b). However, Figure 4.6 c demonstrates that co-culture with Jurkat T-lymphocytes caused a marked upregulation of HaCaT Fas expression (red histogram- MFI: from 0.5 to 1.2). The increase in HaCaT Fas expression induced by Jurkat T-lymphocytes was confirmed by an increase in Fas protein (45kDa) when cell lysates were assessed by western blot (Figure 4.6 d).

Figure 4.4

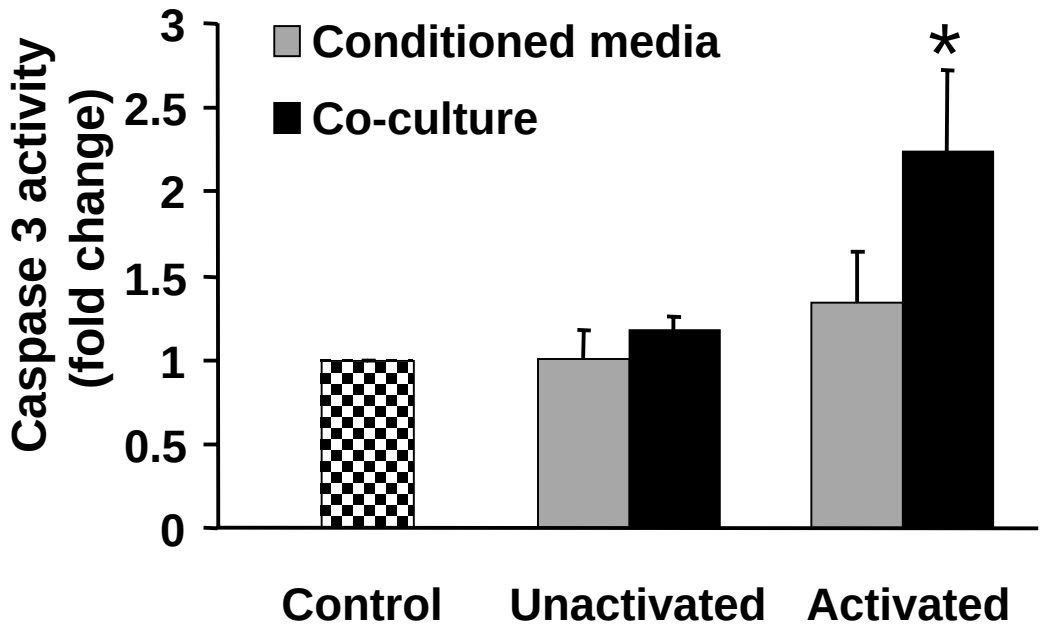

Figure 4.4 Effect of Jurkat conditioned media and Jurkat co-culture on HaCaT Caspase 3 activity. The activation of HaCaT caspase 3 was measured using a caspase 3 specific fluorogenic substrate. Bar graph represents the change in relative fluorescence of control HaCaTs (black and white bar), HaCaTs incubated with conditioned media from Jurkat (grey bars;+/- activation) or co-culture with Jurkat T-lymphocytes (black bars; +/- activation). Values were normalised to the relative caspase 3 activation of HaCaT control samples and represent the mean of 3 independent experiments mean ± SEM. The data was analysed using one-way analysis of variance (ANOVA) and considered significant compared to HaCaT controls as shown as *$p<0.05$.

Figure 4.5

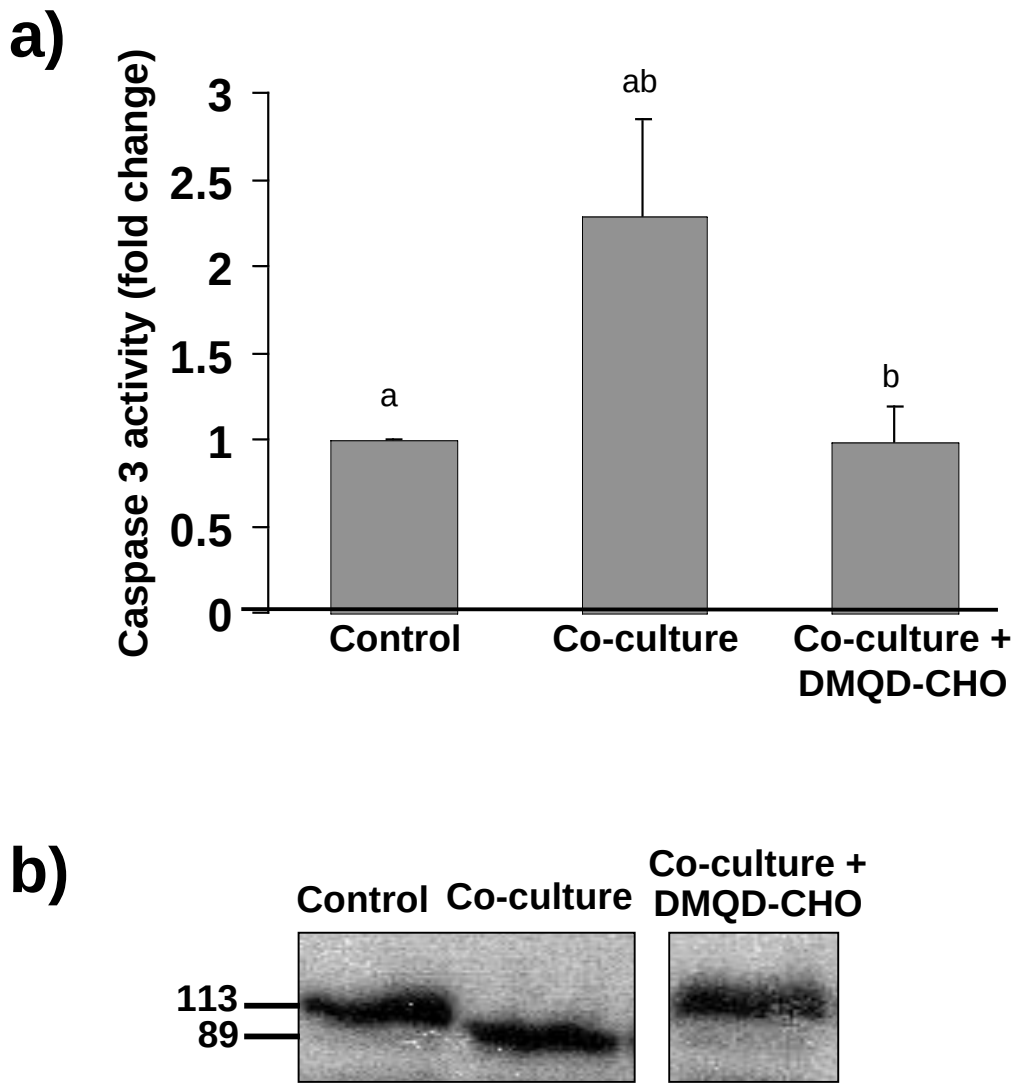

Figure 4.5 Effect of Jurkat T-lymphocytes on HaCaT caspase 3 activity and PARP cleavage. The activation of HaCaT caspase 3 was measured using a caspase 3 specific fluorogenic substrate. (a) Bar graph represents the change in relative fluorescence of control HaCaTs, HaCaTs co-culture with activated Jurkat T-lymphocytes for 48hr and HaCaTs pretreated for 24hrs with 100ug/ml caspase 3 inhibitor (DMQD-CHO) before co-culture with activated Jurkat T-lymphocytes for 48hr. Values were normalised to the relative caspase 3 activation of HaCaT control samples and represent the mean of 3 independent experiments mean ± SEM. The data was analysed using one-way analysis of variance (ANOVA) and post-hoc t-test with significance ($p<0.05$) between treatments shown by the matching symbols ($^{a, b}$). (b) A representative western blot shows PARP cleavage of HaCaTs controls, HaCaTs co-culture with activated Jurkat T-lymphocytes and HaCaTs pretreated with 100ug/ml DMQD-CHO before co-culture with activated Jurkat T-lymphocytes. The 89kDa lower band represents the product of caspase 3 cleavage.

Figure 4.6

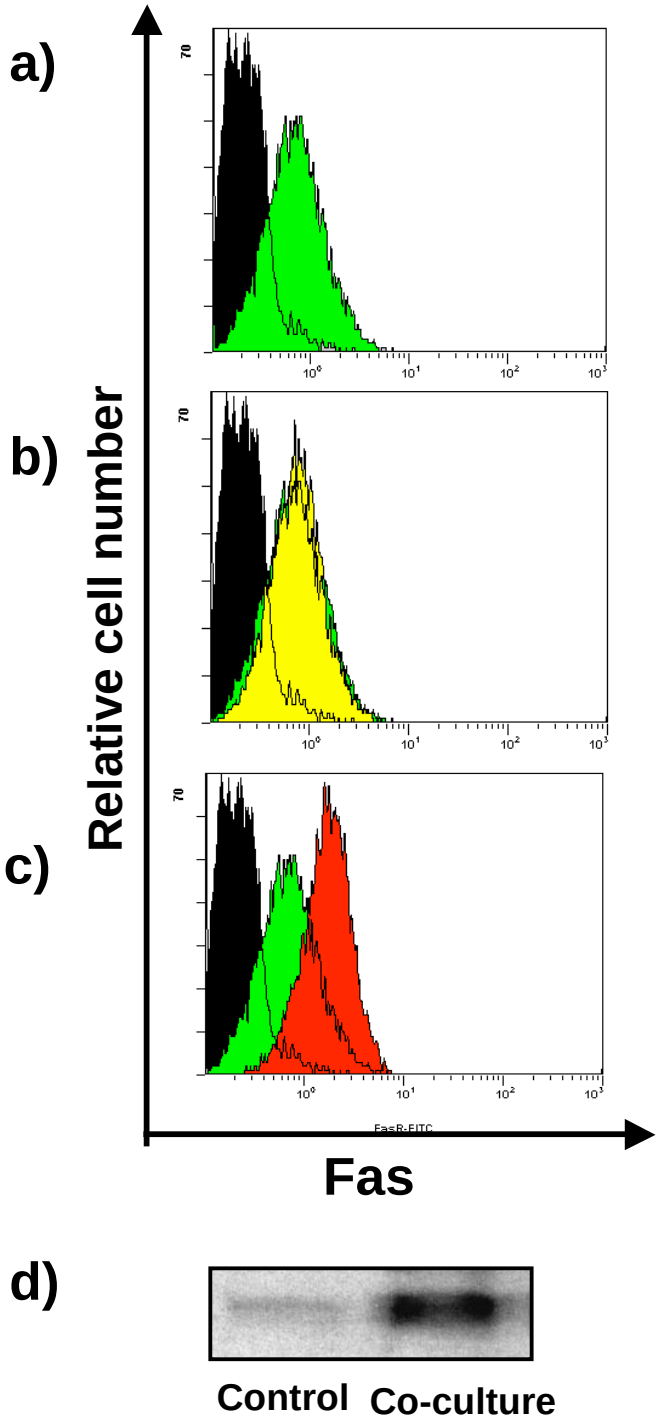

Figure 4.6 Effect of Jurkat conditioned media and Jurkat co-culture on HaCaT Fas expression. Fas expression by HaCaTs after 48hr co-culture was analysed using flow cytometry. (a) Histogram represents expression of Fas by HaCaT controls (green histogram), (b) HaCaTs incubated with Jurkat conditioned media (yellow histogram) and (c) HaCaTs co-cultured with Jurkat T-lymphocytes (green histogram). The black histogram represents staining of an isotype-matched control Ab. Histograms are a representation of 3 separate experiments. (d) Western blot of total Fas expression (45kD) by HaCaT controls and HaCaTs co-cultured with Jurkat T-lymphocytes.

Figure 4.7

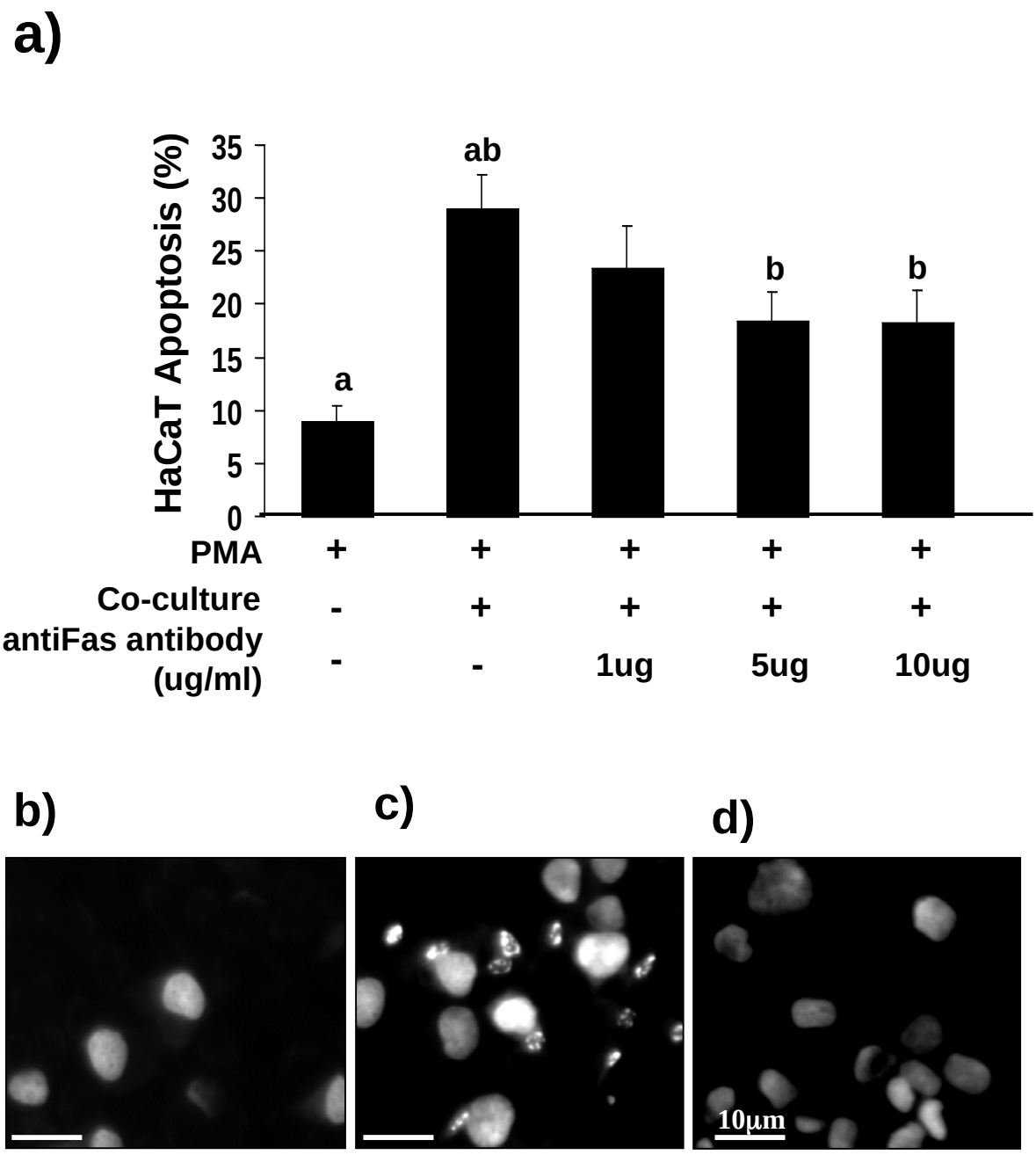

Figure 4.7 Effect of antiFas antibody on Jurkat co-culture induced HaCaT apoptosis. (a) Annexin V and PI staining of HaCaTs were pretreated with 3 different doses antiFas antibody (1-10ug/ml) for 1hr before co-culture with Jurkat T-lymphocytes for 48hr. Values represent the mean percentage of apoptotic cells mean ± SEM of 3 independent experiments *p<0.05. (b) HOESCHT fluorescent staining of HaCaT controls, (c) HaCaTs co-culture with activated Jurkat T-lymphocytes (d) HaCaTs pretreated with 10ug antiFas antibody before co-culture with Jurkat T-lymphocytes.

The direct interaction between Jurkat T-lymphocytes and HaCaTs together with increased Fas and caspase 3 activation appeared to be important for Jurkat T-lymphocytes to induce HaCaT apoptosis. To investigate whether HaCaT apoptosis induced by Jurkat T-lymphocytes was Fas dependent, HaCaTs were pre-treated for 1hr with increasing concentrations of a Fas blocking antibody (1, 5 and 10ug/ml). Figure 4.7 a shows that Jurkat induced HaCaT apoptosis was inhibited dose dependently by the anti-Fas antibody with the 5 and 10ug/ml doses found to have a significantly effect ($P<0.05$;). This result was supported by HOESCHT staining experiments, which demonstrated that the Jurkat co-culture induced HaCaT nuclear condensation and fragmentation seen in Figure 4.7 c, was prevented by 10ug/ml anti-Fas antibody (Figure 4.7 d).

4.3.5 Effect of IFNγ on Jurkat induced HaCaT apoptosis

The studies in this section aimed to investigate the effect of IFNγ on the induction of HaCaT apoptosis by Jurkat co-cultures. Apoptosis and necrosis of HaCaTs incubated with IFNγ (100ng/ml) or co-cultured with Jurkat T-lymphocytes and IFNγ (100ng/ml) was examined by Annexin V/PI staining. Figure 4.8 demonstrates that IFNγ (100ng/ml) significantly increased the number of apoptotic HaCaTs compared to HaCaT controls. The addition of IFNγ (100ng/ml) to co-cultures significantly increased HaCaT apoptosis, increasing it from 27% to 43% apoptotic HaCaTs ($p<0.001$; black bars). The increased HaCaT apoptosis was not associated with a significant increase in necrosis detected by PI staining (grey bars $p<0.05$).

Phase contrast microscopy images of HaCaTs in Figure 4.9 show that compared to untreated controls (Figure 4.9 a and e), IFNγ did not change HaCaT morphology, however it increased nuclear condensation (Figure 4.9 b and f). The addition of IFNγ to co-cultures in Figure 4.9 d, resulted in more profound cell shrinkage, disruption of cell membranes and loss of intercellular connections compared to co-culture alone (Figure 4.9 c). It was evident that IFNγ also increased cell detachment from the culture plate (Figure 4.9 d), as such it was difficult to detect an increase in nuclear condensation by HOESCHT staining, however Figure 4.9 h demonstrated a high incidence of nuclear fragmentation.

4.3.6 Effect of IFNγ on HaCaT Fas expression

The effect of IFNγ on HaCaT Fas expression was investigated. Figure 4.10 a, demonstrates that compared to Fas expression by control HaCaTs (green histogram), IFNγ (100ng/ml) caused a marked increased in HaCaT Fas expression (pink histogram- MFI: from 0.8 to 1.17). The Fas expression level induced by IFNγ was similar to the levels obtained with Jurkat co-culture (Figure 4.6 c). Jurkat co-culture induced HaCaT Fas expression (red histogram- Figure 4.10 b) was shown to be further increased by the addition of IFNγ (purple histogram- MFI: 1.44; Figure 4.10 b).

4.3.7 Jurkat co-culture induced HaCaT ICAM-1 expression.

An observation from the co-culture experiments was an increase in cell-cell adhesion between the Jurkat T-lymphocytes and HaCaTs as seen in Figure 4.3 and 4.9. Since

direct cell interactions appear to be important in mediating Jurkat induced keratinocyte apoptosis, experiments were performed to investigate ICAM-1 expression by HaCaTs co-cultured with Jurkat T-lymphocytes. Compared to HaCaT controls which constitutively expressed surface ICAM-1 (green histogram; Figure 4.11 a), there was a marked increased in HaCaT ICAM-I expression after Jurkat co-culture (red histogram; MFI: from 0.9 to 1.8; Figure 4.11 a). In a separate experiment the effect of INFγ on Jurkat induced ICAM-1 expression was investigated. Figure 4.11 b demonstrates that compared to Jurkat induced ICAM-1 expression (red histogram), the addition of IFNγ further increased Jurkat induced ICAM-1 expression by HaCaTs (purple histogram).

Figure 4.8

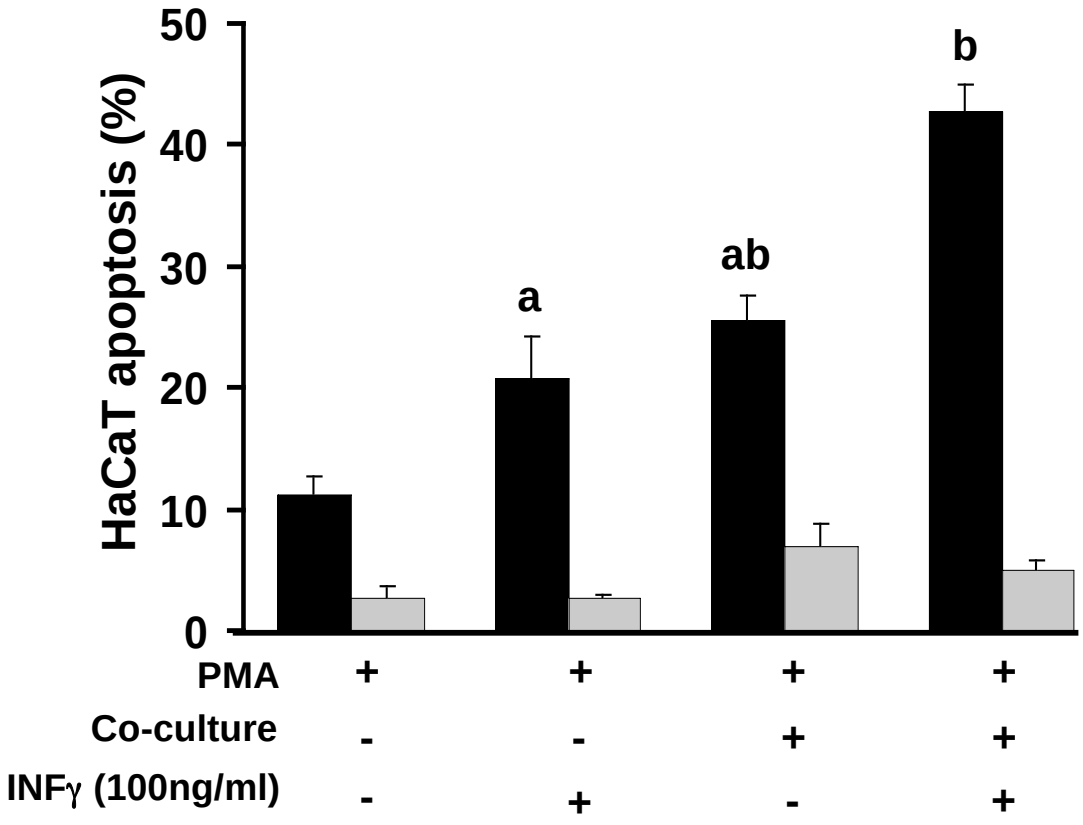

Figure 4.8 Effect of IFNγ on Jurkat induced HaCaT apoptosis. HaCaT apoptosis (black bars) and necrosis (grey bars) was assessed by Annexin V and PI staining of HaCaT controls, HaCaTs incubated with 100ng/ml IFNγ, HaCaT and Jurkat co-culture and HaCaT Jurkat co-culture + IFNγ. The data was analysed using one-way analysis of variance (ANOVA) and post-hoc t-test with significance ($p<0.001$) between treatments shown by the matching symbols (a, b)

Figure 4.9

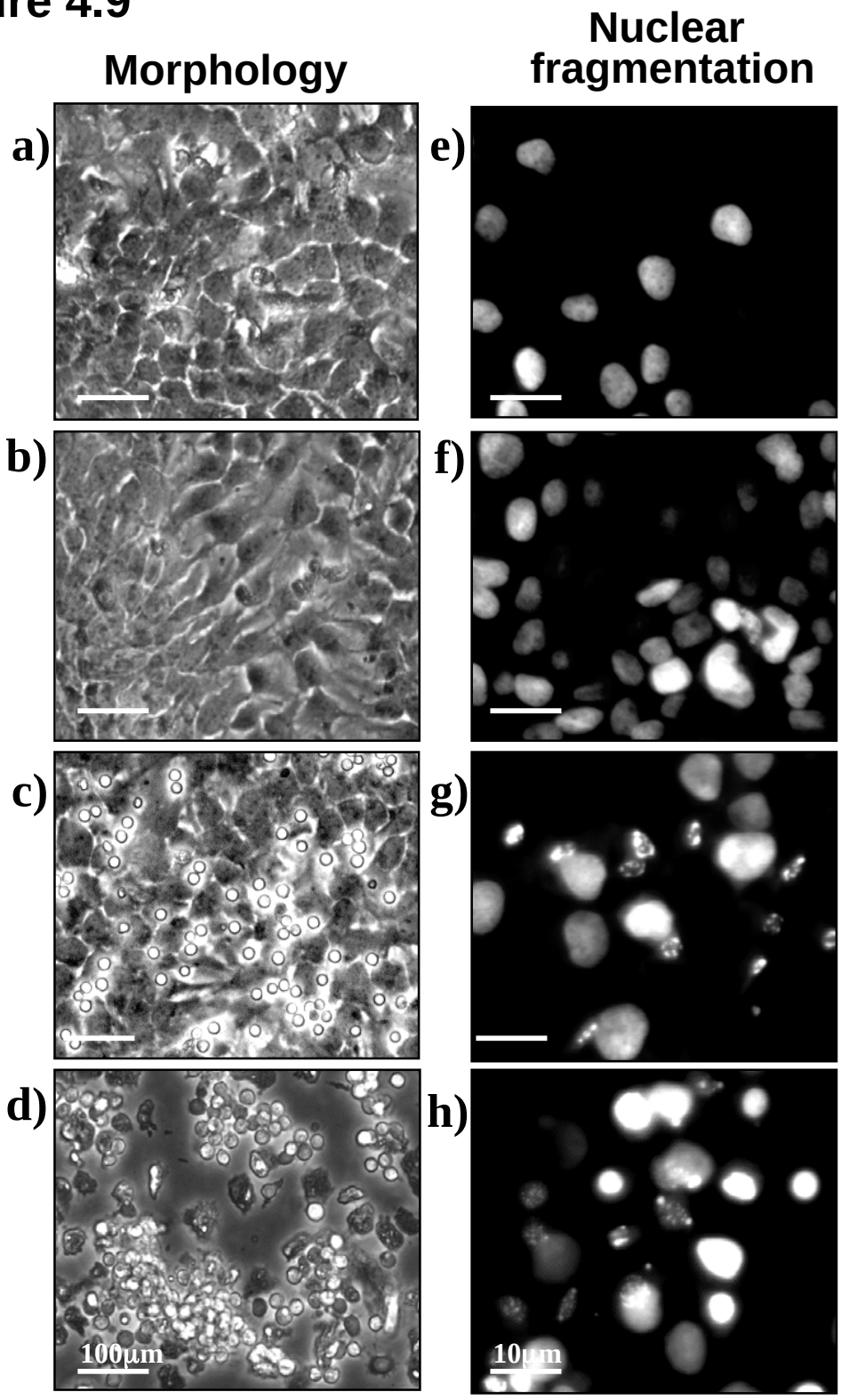

Figure 4.9 Effect of IFNγ on Jurkat induced HaCaT morphology and nuclear fragmentation. Phase contrast microscopy of (a) control HaCaT cells, (b) HaCaTs incubated with IFNγ (100ng/ml), (c) HaCaTs-Jurkat co-culture and (d) HaCaTs-Jurkat co-culture + IFNγ. HOESCHT fluorescent staining by (e) control HaCaTs, (f) HaCaTs incubated with IFNγ, (g) HaCaTs-Jurkat co-culture and (h) HaCaTs-Jurkat co-culture + IFNγ. Pictures are a representation of 4 separate experiments.

Figure 4.10

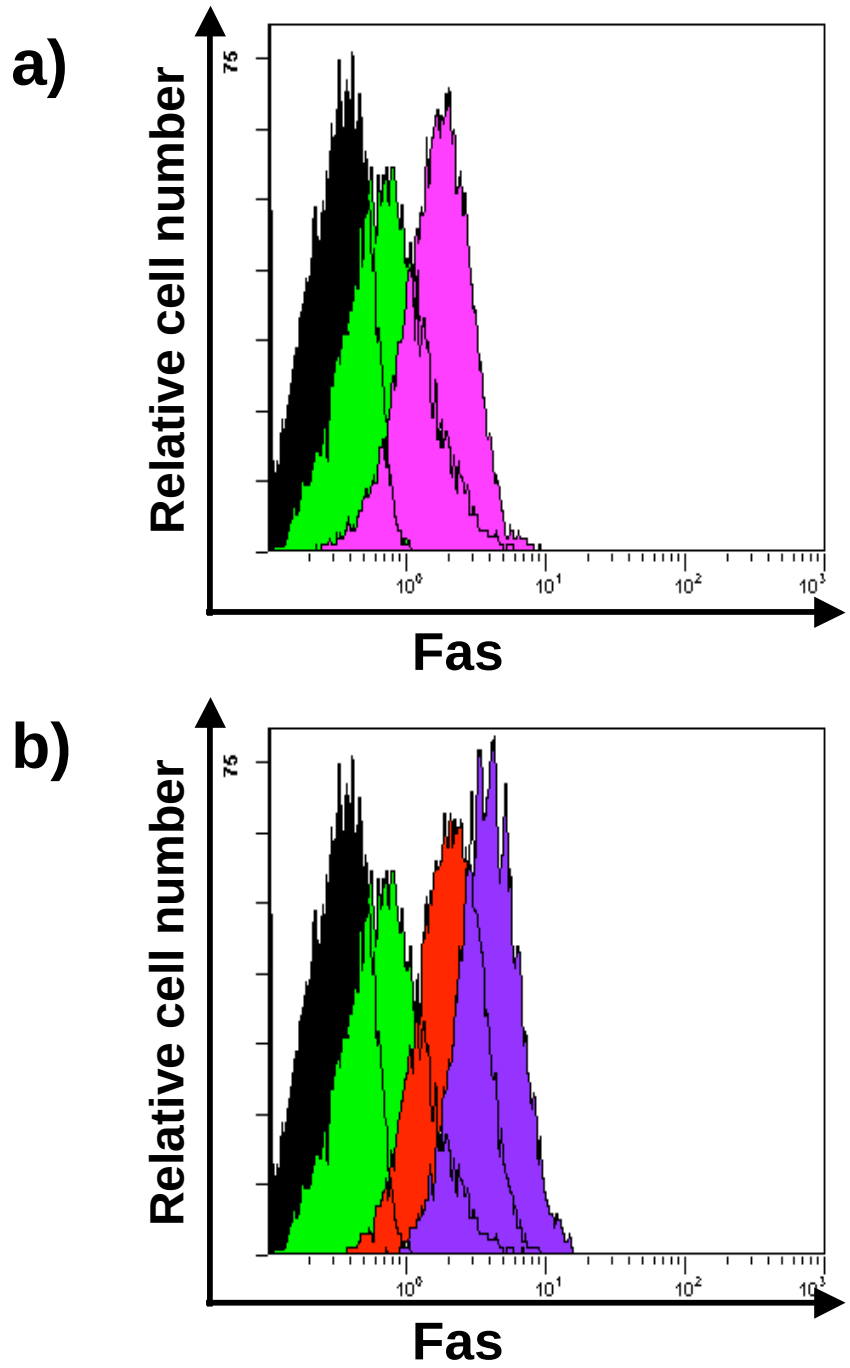

Figure 4.10 IFNγ potentiates Jurkat induced HaCaT Fas. Fas expression by HaCaTs was analysed using flow cytometry. (a) Histogram represents expression of Fas by HaCaT controls (green histogram) and HaCaTs incubated with 100ng IFNγ for 48hr (pink histogram). (b) HaCaT controls (green histogram), Jurkat co-culture induced Fas expression (red histogram) and HaCaT-Jurkat co-culture with 100ng IFNγ (purple histogram). The black histogram represents staining of an isotype-matched control Ab. Histograms are a representation of 3 separate experiments.

Figure 4.11

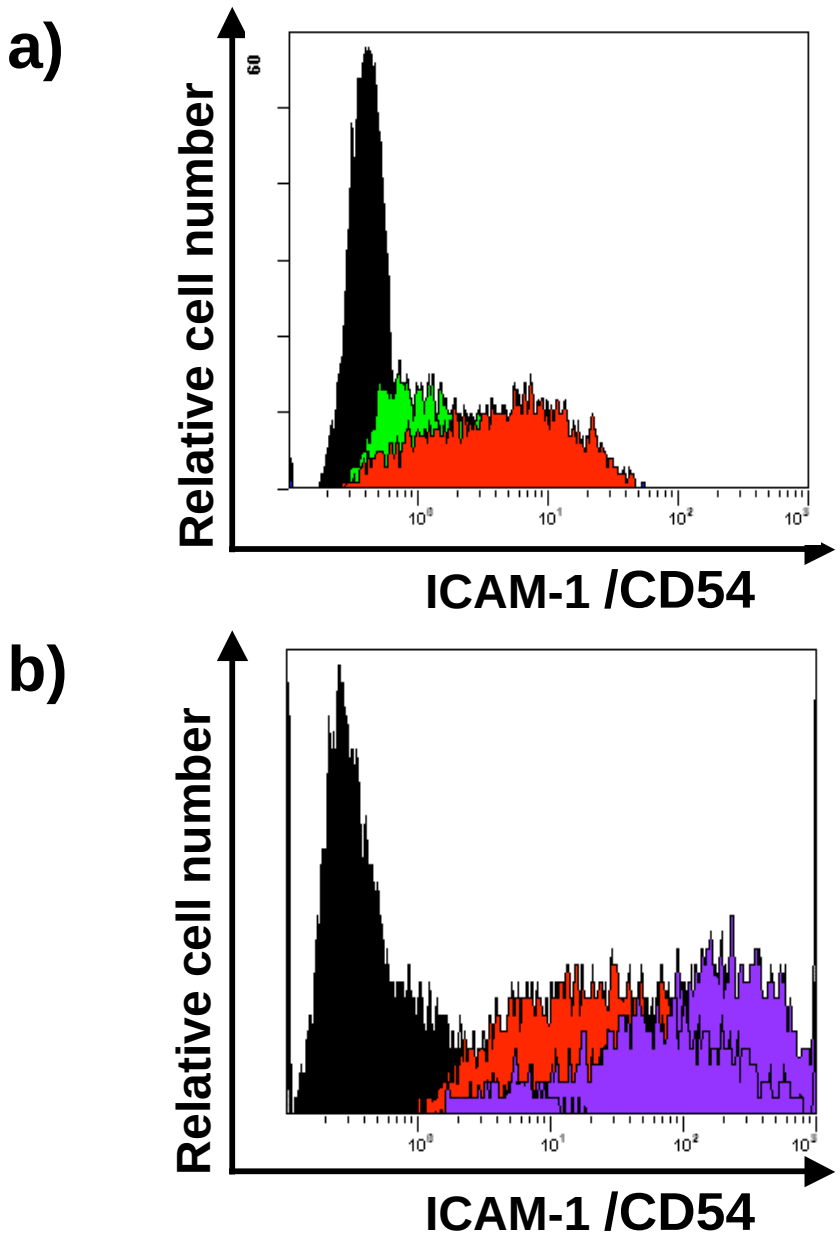

Figure 4.11 IFNγ potentiates Jurkat induced ICAM-1 expression by HaCaTs. ICAM-1 expression of HaCaTs was analysed using flow cytometry. (a) Histogram represents expression of ICAM-1 by HaCaT controls (green histogram) and of HaCaT-Jurkat co-culture (red histogram). (b) ICAM-1 staining of HaCaT-Jurkat co-culture (red histogram) and ICAM-1 staining of Jurkat co-culture with IFNγ (100ng; purple histogram). Black histogram represents staining of an isotype-matched control Ab. Histogram is a representation of 2 separate experiments.

4.4 Summary

The studies in this chapter were undertaken to establish a cell culture system capable of mimicking the induction of keratinocyte apoptosis by T-lymphocytes, evident in AE. From the results discussed in this chapter the following points can be made:

- Jurkat activation and their direct interaction with HaCaTs in co-culture is required to induce HaCaT apoptosis.
- Jurkat induced HaCaT apoptosis was Fas mediated.
- IFNγ may modulate apoptosis by upregulating keratinocyte Fas. This may sensitise HaCaTs to the death signal delivered by Jurkat T-lymphocytes.

The results presented in this Chapter demonstrate that activation of Jurkat T-lymphocytes with PMA induced surface FasL expression. Together with upregulated HaCaT Fas expression in co-culture, Jurkat T-lymphocytes were capable of inducing HaCaT apoptosis via activation of caspase 3. By blocking Fas, it was observed that Jurkat induced HaCaT apoptosis was inhibited, supporting a Fas dependent mechanism. The results presented in this chapter also demonstrated that IFNγ potentiated Jurkat induced HaCaT apoptosis which may be attributed to IFNγ induced Fas expression. The increased ICAM-1 expression by HaCaTs may facilitate Fas/FasL interactions by enhancing cell to cell contact in co-culture.

Figure 4.12 describes a proposed working model for explaining the events involved in Jurkat T-lymphocyte induced HaCaT apoptosis. Jurkat activation with PMA (10ng/ml)

results in increased FasL expression and secretion of sFasL (Figure 4.12 a). The Jurkat T-lymphocytes as well as IFNγ upregulate HaCaT Fas expression (Figure 4.12 b). The interaction between T-lymphocyte and HaCaTs is potentially facilitated by the increased cell to cell adhesions via upregulation of ICAM-1 by HaCaTs (Figure 4.12 c). Binding of T-lymphocyte associated FasL to upregulated keratinocyte Fas, leads to activation of effector caspase 3 (Figure 4.12 d). Caspase activation has been associated with key events in apoptosis such as loss of cell membrane symmetry, that results in phosphotidylserine being exposed on the cell surface and nuclear condensation and fragmentation (Fadok *et al.* 1998) (Figure 4.12 e). Finally, keratinocytes lose their inter-cellular connections and detach from the culture plate as they begin to disintegrate and form apoptotic bodies.

Figure 4.12

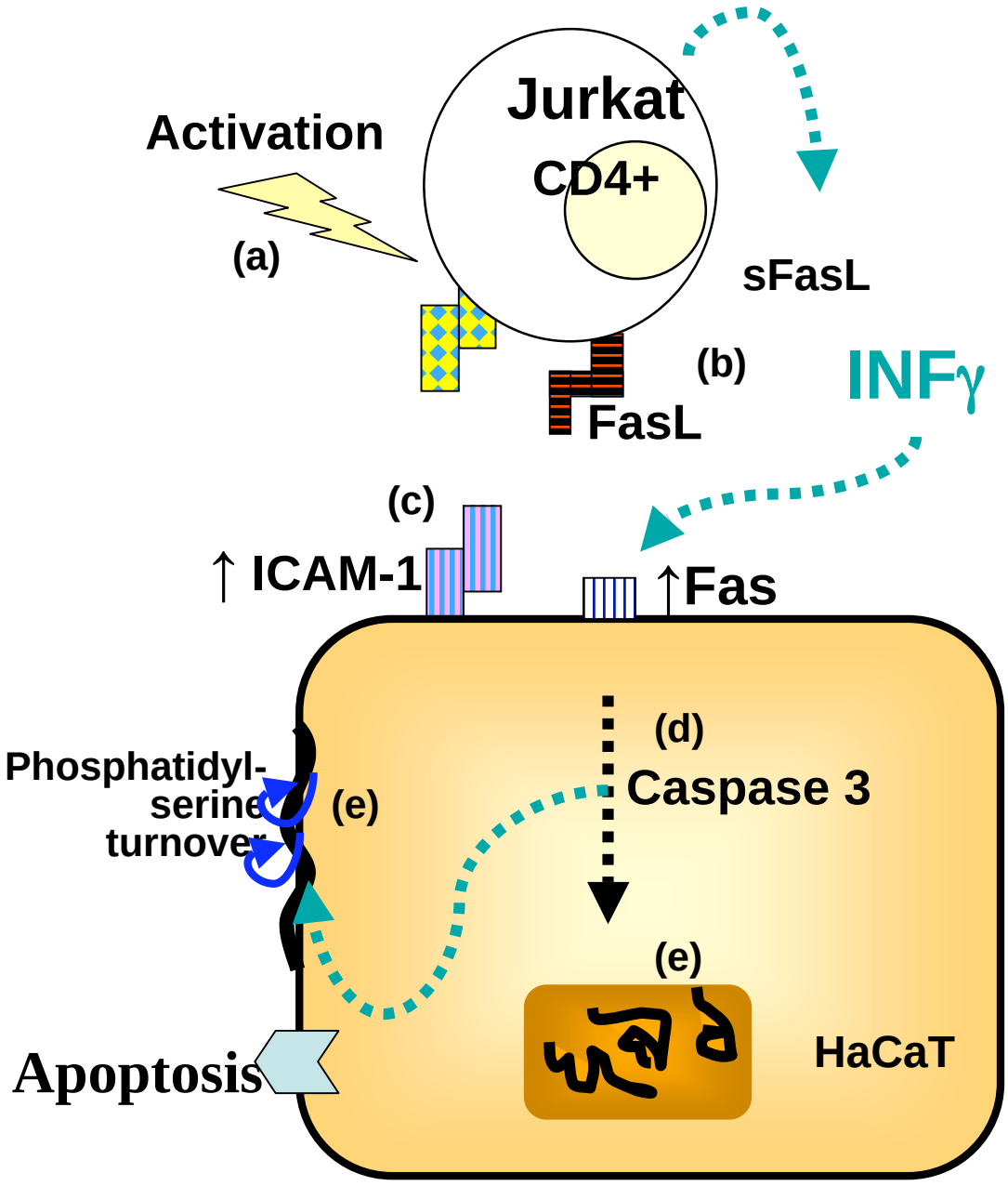

Figure 4.12. IFNγ in Jurkat T-lymphocyte co-culture induced Fas mediated HaCaT apoptosis.

CHAPTER 5

5 PRIMARY T-LYMPHOCYTE INDUCED KERATINOCYTE APOPTOSIS

5.1 Introduction

The primary aims of this thesis were to establish a cell system suitable for investigating the induction of epidermal cell death by T-lymphocytes, and to use this model to examine how growth factors may ameliorate this process. A co-culture system was established using Jurkat T-lymphocytes and HaCaTs in Chapter 4, with studies showing that Jurkat T-lymphocytes induced Fas mediated apoptosis of HaCaTs. The studies in this Chapter aimed to extend this work and establish a primary cell co-culture system using peripheral blood derived CD4+ T-lymphocytes together with HaCaTs and skin derived normal human epidermal keratinocytes (NHEK). The mechanisms mediating T-lymphocyte induced keratinocyte apoptosis were further characterised using the primary cell culture system.

The studies in this Chapter were divided into the following specific aims;

1. Establish the effects of primary CD4+ T-lymphocytes on HaCaT and NHEK apoptosis.

Studies were performed to identify conditions necessary for non-autologous CD4+ T-lymphocytes to induce HaCaT and NHEK apoptosis. These studies were based on the results obtained using Jurkat T-lymphocytes and HaCaTs in Chapter 4 as well as previous reports using autologous T-lymphocytes (Trautmann *et al.* 2000a).

2. Confirm the involvement of the Fas pathway in T-lymphocyte induced keratinocyte apoptosis

The results in Chapter 4 implicated the Fas pathway in Jurkat induced HaCaT apoptosis. To verify these findings, similar studies were performed using CD4+ T-lymphocytes, HaCaTs and NHEKs. Moreover, as IFNγ and TNFα have been shown to be released by T-lymphocytes in AE and play an important role in maintaining chronic inflammation of the skin (Spergel *et al.* 1999, Sumimoto *et al.* 1992, Takahashi *et al.* 1992). Their capacity to influence the development of lesions in AE may be due to their ability to induce Fas expression by keratinocytes in skin from people with AE (Trautmann *et al.* 2000a). The importance of cytokines in keratinocyte apoptosis, was indicated in Chapter 4 as Jurkat induced HaCaT apoptosis was potentiated by the presence of IFNγ. This response appeared to be mediated by the synergistic upregulation of HaCaT Fas by IFNγ (Chapter 4, section 4.3.5). To extend these results, the studies in this Chapter investigated IFNγ and TNFα release by T-lymphocytes following activation and during co-culture, to associate it with the effects of IFNγ on T-lymphocyte induced keratinocyte apoptosis and Fas expression.

Increased adhesion molecule expression appears to assist in the development of AE lesions by retaining T-lymphocytes in the skin (Nickoloff *et al.* 1993). In Chapter 4 Section 4.3.2, it was shown that direct cell-cell interaction between the Jurkat T-lymphocytes and HaCaTs was important for inducing HaCaT apoptosis with ICAM-1 expression by HaCaTs implicated to support the cell-cell interaction (Section 4.3.6). For this reason, ICAM-1 expression by keratinocytes and the expression of its integrin LFA-1, by T- lymphocyte was investigated.

3. To examine the differentiation status of keratinocytes induced to undergo apoptosis.

The primary function of keratinocytes is to maintain the skin barrier function primarily via undergoing terminal differentiation. To begin the differentiation process, keratinocytes initially detach from the basement membrane as a result of decreased integrin expression. Throughout the course of differentiation, the keratinocytes produce different intermediate filament proteins such as keratins (Polakowska *et al.* 1994, Webb *et al.* 2004). The effect of T-lymphocytes on keratinocyte differentiation is unknown, so the studies in the final section of this Chapter aimed to examine the differentiation status of keratinocytes induced to undergo apoptosis by T-lymphocytes. Basal and epidermal stem cells express high levels of alpha-6 (α6) integrin (α6-bright), but as they begin to differentiate, α6 expression is decreased (α6-dim) (Webb *et al.* 2004). The studies in this chapter examined the effect of T-lymphocytes on keratinocyte α6 expression as a marker of early keratinocyte differentiation. Experiments were also performed assessing the

expression of later stage differentiation markers; Keratin 10 (committed cells) and involucrin (fully differentiated cells) by keratinocytes.

5.2 Methods

5.2.1 Primary CD4+ T-lymphocyte and HaCaT co-culture

Peripheral blood mononuclear cells (PBMCs) containing CD4+ T-lymphocytes were obtained from fresh blood as described in Methods section 2.3.4 a (PBMC resting profile - Appendix 5). The CD4+ T-lymphocytes were separated from other mononuclear cells, by positive selection using CD4+ Micro Beads (Method section 2.3.4 b). Immediately after isolation, the primary CD4+ T-lymphocytes (5×10^5/ml) were stimulated with PMA (10ng/ml) and ionomycin (500ng/ml) and co-cultured with HaCaTs in DMEM containing 1% FBS for 48 hrs. HaCaT controls were incubated with PMA and ionomycin without T-lymphocytes for 48 hrs. The CD4+ depleted preparation was also collected and the effect of activated cells on HaCaT apoptosis was assessed (results described in Appendix 6 and 7).

Keratinocyte apoptosis was measured by Annexin V staining (Methods Section 2.5.1) and cell morphology was imaged by phase contrast microscopy. Wells stained with HOECHST 33342 were first washed twice with PBS to remove T-lymphocytes (Methods Section 2.6.1). The cell-free conditioned media from these experiments was collected and stored at -20°C for IFNγ or TNFα measurements as described in Methods Chapter 2 (Section 2.11).

5.2.2 Primary CD4+ T-lymphocyte and primary keratinocyte co-culture

In preliminary studies, PMA was found to induce NHEK apoptosis, making it necessary to pre-activate T-lymphocytes before adding them to the NHEKs. Isolated primary CD4+ T-lymphocytes were pre-stimulated with PMA (10ng/ml) and ionomycin (500ng/ml) in KBM for 48 hrs and washed twice with PBS before co-culture. Co-culture was established by adding pre-activated T-lymphocytes (5×10^5/ml) to second passage NHEKs grown to sub-confluence in keratinocyte basal medium (KBM). NHEK controls were left untreated in KBM and in some experiments, 100ng/ml recombinant IFNγ was added to the co-cultures for 48 hr.

After 48 hr co-culture, adherent NHEKs were collected as described in Methods section 2.3.2 and pooled with the conditioned media containing T-lymphocytes and non-adherent cells. Apoptosis of NHEKs was measured by flow cytometry (Annexin V/PI staining) as described in Methods section 2.5.1 using a gate to exclude based on cell size the T-lymphocytes. Nuclear staining experiments, were performed using HOECHST 33342 (Methods section 2.6.1).

5.2.3 Cytokine measurement

Primary CD4+ T-lymphocytes were stimulated with PMA (10ng/ml) and ionomycin (0.5μg/ml) and incubated for 48 hrs in basal media, controls were left unstimulated. Conditioned media from co-culture experiments was also collected. Cell-free supernatant/conditioned media were stored at -20°C. IFNγ or TNFα levels were

measured in conditioned media by ELISA as described in Methods Chapter 2 (section 2.11).

5.2.4 Keratinocyte differentiation

Adherent HaCaTs or NHEKs were released by incubating with trypsin (0.25%)-EDTA and pooled with conditioned media containing non-adherent cells and T-lymphocytes. HaCaTs or NHEK differentiation marker expression was measured by intracellular staining for keratin 10 and involucrin and assessment by flow cytometry as described in Methods section 2.5.3. α6-integrin expression was determined by cell surface staining on HaCaTs and NHEKs as described in Methods section 2.5.2.

In some experiments HaCaTs were dual stained for α6-integrin and Annexin V. This was performed by staining cells in binding buffer for 15 mins at RT in the dark. Samples were resuspended in 200µl binding buffer and analysed by flow cytometry within 1 hour of staining.

5.3 Results

5.3.1 Primary CD4+ T-lymphocytes induced HaCaT apoptosis

The studies in this Chapter aim to investigate the effects of primary CD4+ T-lymphocytes derived from peripheral blood on HaCaT and NHEK apoptosis. To determine the conditions required to achieve reproducible HaCaT apoptosis, co-cultures were established using the mitogen activated and non-activated of the T-lymphocytes. These studies showed that activation of 1 x 10^6 CD4+ T-lymphocytes with PMA (10ng/ml) and a combination of PMA and ionomycin (0.5ug/ml) both induced significant HaCaT apoptosis. PMA and ionomycin however induced an overall higher level of HaCaT apoptosis than PMA alone (Figure 5.1).

The effect of varying T-lymphocyte numbers on HaCaT apoptosis was also investigated. HaCaTs (5 x 10^5) were incubated with 104, 5 x 10^4, 10^5, 5 x 10^5 and 10^6 CD4+ T-lymphocytes/ml giving T-lymphocyte and HaCaT ratios of 1:10, 1:2, 1:1, 2:1 respectively. The T-lymphocytes were activated with PMA 10ng and ionomycin 0.5ug and the HaCaT cell morphology and nuclear fragmentation was assessed after 48 hr along with quantification of apoptosis by Annexin V staining. As shown by the representative images, untreated HaCaTs and control HaCaTs treated with 10ng/ml PMA and 0.5µg/ml ionomycin demonstrated normal cell morphology (Figure 5.2 a and b). HaCaTs co-cultured with 5 x 10^4 T-lymphocytes also displayed normal cell morphology (Figure 5.2 c). Increasing the numbers of T-lymphocytes to 1 x 10^5, 5 x 10^5

and 1 x 10^6 T-lymphocytes per ml, resulted in a progressive increase in HaCaT cell shrinkage, membrane blebbing and cell separation indicative of loss of inter-cellular connections, the number of cell detached from culture plate (Figure 5.2 c-f) and increase in apoptotic body formation. The arrows in Figure 5.2 d and e point to HaCaTs cell detachment from other cells and the culture plate by lose of inter-cellular connections and the arrow in Figure 5.2 f points to apoptotic bodies. Nuclear fragmentation in these cells was visualized using the HOESCHT 33342 stain and demonstrated that compared to HaCaT controls, which had minimal nuclear staining (Figure 5.2 g), HaCaTs co-cultured with 1 x 105 activated CD4+ T-lymphocytes had increased nuclear condensation and fragmentation (arrows; Figure 5.2 h).

The effect of increasing CD4+ T-lymphocyte numbers from 10^4-10^6 on HaCaT apoptosis was shown in the representative dot plots in Figure 5.3. Most control HaCaTs (containing 10ng/ml PMA and 0.5µg/ml ionomycin) were negative for Annexin or PI staining (Figure 5.3 a). Co-culture caused a T-lymphocyte dependent increase in the number of HaCaTs induced to undergo apoptosis, as shown by the cells present in the EA and LA quadrants (Figure 5.3 b-e). Despite the effect of T-lymphocytes on HaCaT apoptosis, there was no change in the number of necrotic cells (PI positive/Annexin negative; Figure 5.3 a-e). Figure 5.3 f shows the combined results from three independent experiments and demonstrates that HaCaT apoptosis reached a statistically significant level of 28% when HaCaTs were incubated with 5 x 10^5 T-lymphocytes per ml. Maximal apoptosis (43%) was observed when HaCaTs were incubated with 1 x 106 T-lymphocytes per ml ($p<0.05$; Figure 5.3 f). Based on these results, the sub-maximal T-

Figure 5.1

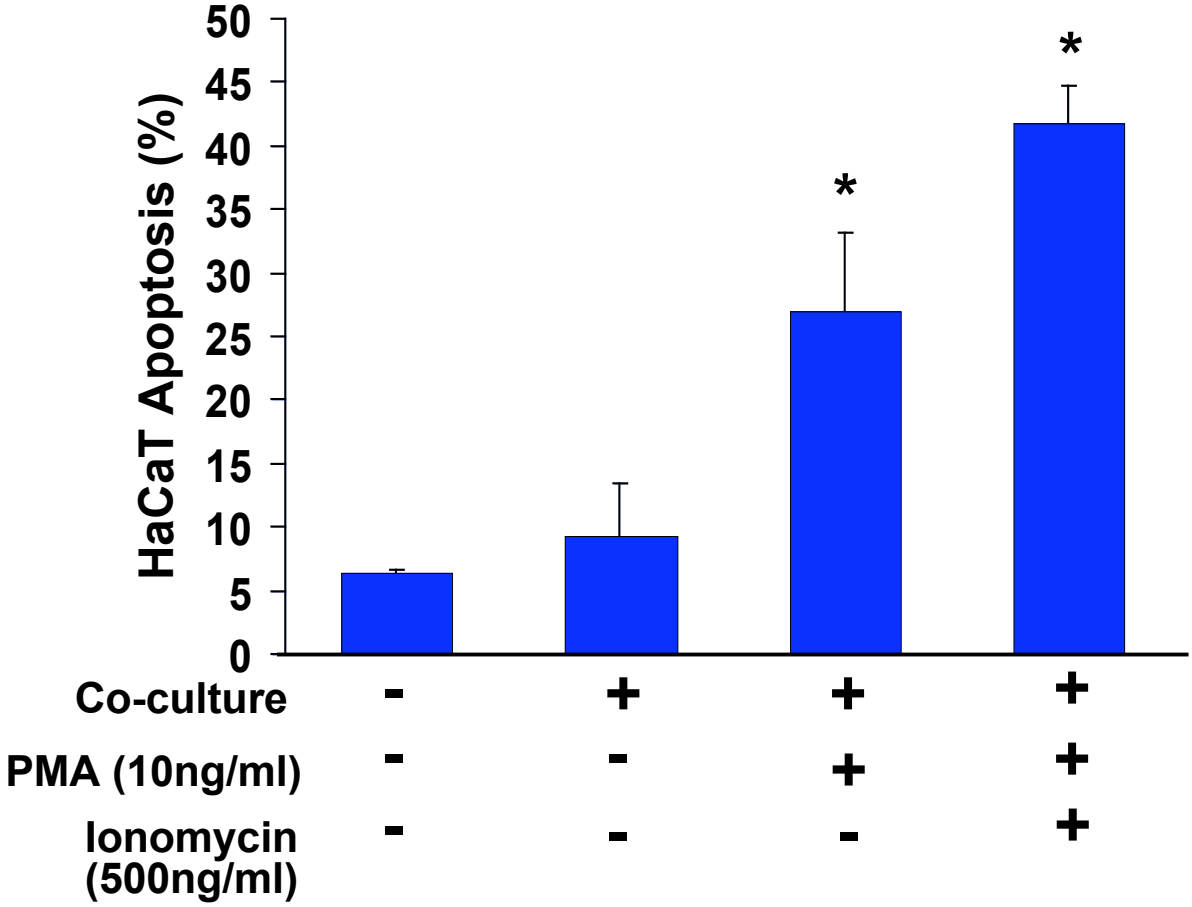

Figure 5.1 Effect of T-lymphocyte activation on HaCaT apoptosis in co-culture. HaCaT were co-cultured with T-lymphocytes and different mitogen combinations for 48hr. HaCaTs were stained with Annexin V and PI and analysed by flow cytometry. Values represent the percentage of apoptotic cells mean ± SEM of 3 independent experiments. The data was analysed using one-way analysis of variance (ANOVA) with significance compared to control shown (*$p<0.05$).

Figure 5.2

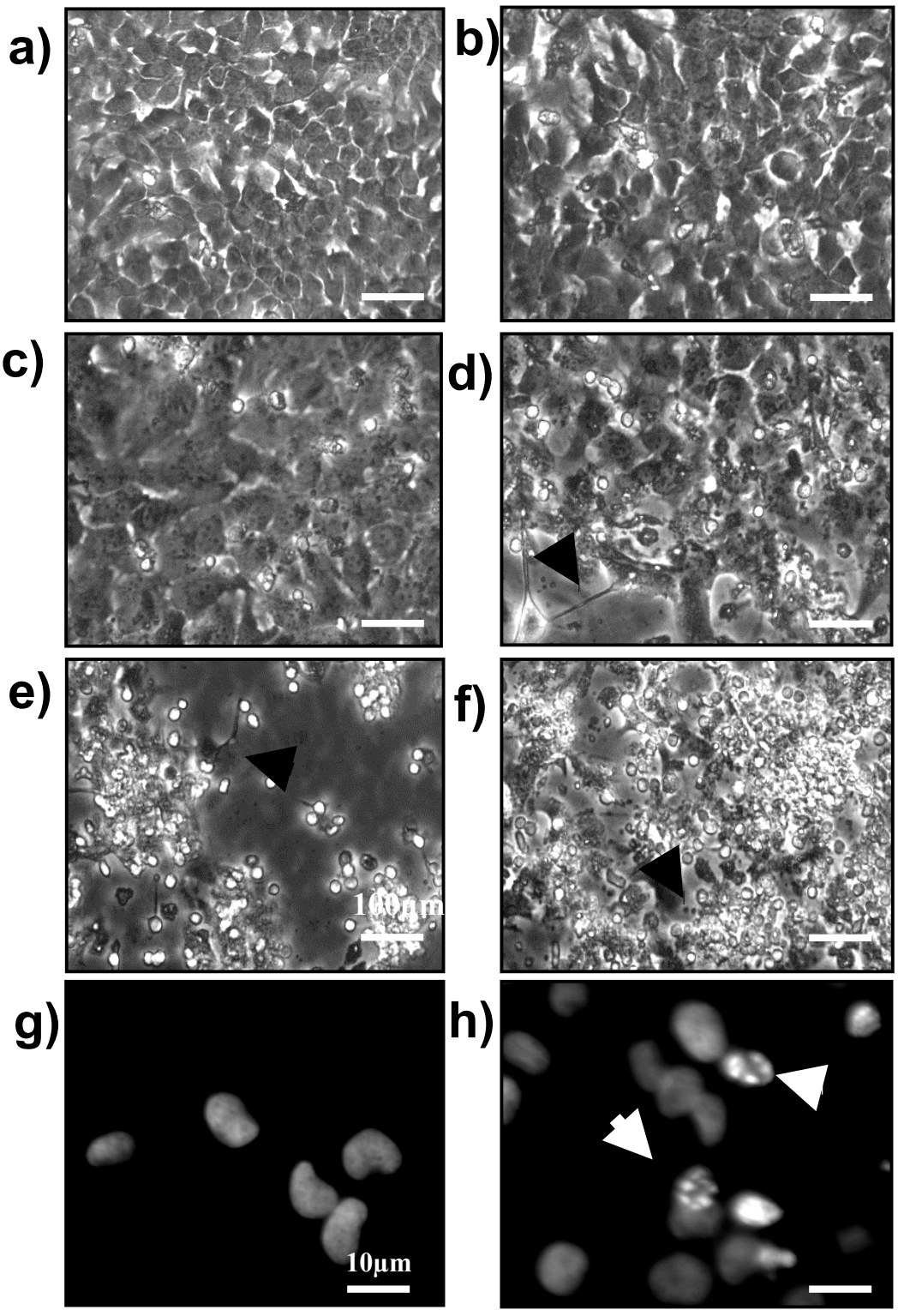

Figure 5.2 Effect of T-lymphocyte co-culture on HaCaT cell morphology and nuclear fragmentation. (a) Phase contrast microscopy of untreated HaCaTs, (b) HaCaT controls incubated with PMA and ionomycin, (c-f) HaCaTs co-cultured with $5x10^4$, $1x10^5$, $5x10^5$ and $1x10^6$ activated T-lymphocytes for 48hrs respectively. Arrows in (d) and (e) point to HaCaT detachment and arrows in (f) point to an apoptotic body (g) HOESCHT 33342 fluorescent staining of control HaCaTs and (h) HaCaTs incubated with $5x10^5$ activated T-lymphocytes for 48hrs, arrows point to fragmented nuclei. Scale bar represents 100µm for the phase contrast images and 10µm for the HOESCHT 33342 images.

Figure 5.3

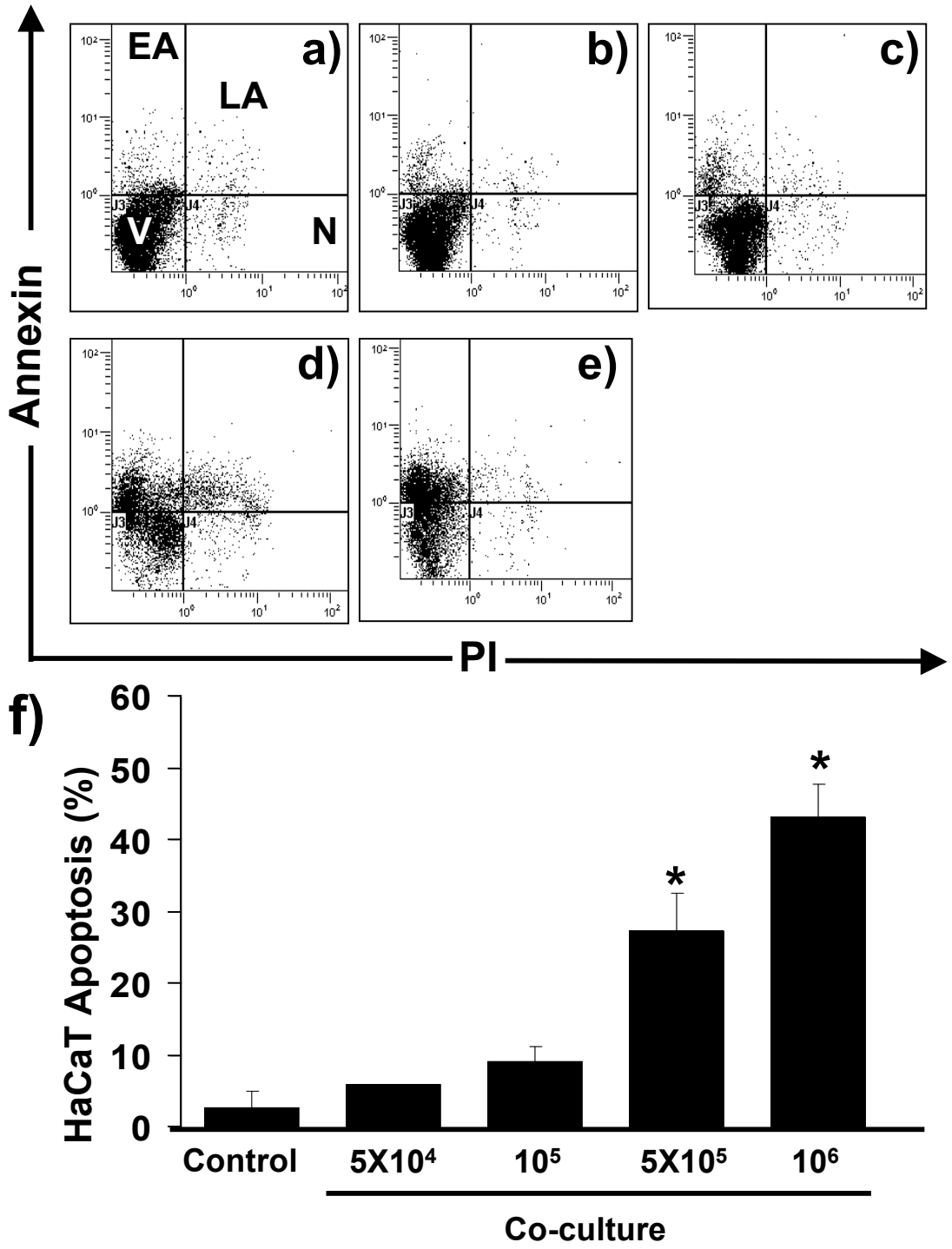

Figure 5.3 Effect of T-lymphocyte co-culture on HaCaT apoptosis. (a) Representative dot plots of Annexin V and propidium iodide (PI) stained HaCaT controls incubated with PMA and ionomycin and (b-e) HaCaTs co-cultured with $5X10^4$, $1X10^5$, $5X10^5$ and $1X10^6$ activated T-lymphocytes for 48hrs respectively. Annexin V and PI negative HaCaTs were viable (V), the Annexin V positive/PI negative HaCaTs were early apoptotic (EA), Annexin V and PI positive cells were late apoptotic (LA) and Annexin V negative /PI positive HaCaTs were necrotic (N). (f) Apoptotic HaCaTs [EA + LA] of samples described in (a-e). Bar graphs represent the percentage of apoptotic cells mean ± SEM of 3 independent experiments. The data was analysed using one-way analysis of variance (ANOVA) with significance compared to control shown (*$p<0.05$).

lymphocyte concentration of 5 x 10^5 giving a HaCaT:T-lymphocyte ratio of 1:1 was used in subsequent experiments.

5.3.2 FasL expression by CD4+ T-lymphocytes increases with activation

Mitogen activation of Jurkat T-lymphocytes resulted in upregulation of membrane bound FasL and induction of HaCaT apoptosis (Chapter 4 section 4.3.1 and 4.3.2). The expression of FasL by unactivated or PMA and ionomycin activated CD4+ T-lymphocytes was assessed by flow cytometry after 48 hr incubation. Figure 5.4 a demonstrates that incubation with PMA and ionomycin resulted in an increase in the number of T-lymphocytes expressing FasL compared to unactivated controls (from 17% to 68%; Figure 5.4 a). CD4+ T-lymphocytes incubated with PMA and ionomycin also had increased CD25 expression, consistent with an activation response and previous data presented in Chapter 4 (Figure 5.4 b).

5.3.3 T-lymphocyte induced HaCaT apoptosis was mediated by Fas

Increased Fas expression by HaCaTs was shown to be important for mediating apoptosis induced by Jurkat T-lymphocytes (Chapter 4 section 4.3.5). The studies in this chapter examined the effect of CD4+ T-lymphocytes on HaCaT Fas expression, after 48 hr co-culture. Figure 5.5 a demonstrates that compared to Fas expression by control HaCaTs (green histogram), CD4+ T-lymphocytes caused a marked increased in HaCaT Fas expression (yellow histogram- from MFI 0.5 to MFI 1.07).

To determine if T-lymphocyte induced apoptosis of HaCaTs was mediated by a Fas dependent mechanism, HaCaTs were pre-treated for 1hr with a Fas blocking antibody (anti-Fas 10ug/ml) before co-culture. Figure 5.5 b demonstrates that blocking Fas resulted in significant inhibition of T-lymphocyte induced HaCaT apoptosis assessed by Annexin V ($p<0.05$). The effect of the Fas blocking antibody on HaCaT apoptosis by was further investigated by assessment cell morphology and nuclear fragmentation. Compared to untreated T-lymphocyte co-cultures, pre-incubation with the anti-Fas antibody reduced HaCaT cell shrinkage and membrane blebbing, with a decrease in cell separation and a reduction in the number of detached cells from the culture plate (Figure 5.6 b and c). The anti-Fas antibody appeared to have prevented T-lymphocyte induced apoptosis of HaCaTs as they looked similar in appearance to the control cells shown in Figure 5.6 a. Furthermore, the anti-Fas antibody reduced the HOESCHT 33342 positive staining showing condensed nuclei and fragmentation induced by T-lymphocytes (Figure 5.6 e and f).

5.3.4 Co-culture induced adhesion molecule expression

To help define a role for the adhesion molecule ICAM-1 and its integrin LFA-1 in mediating HaCaT/T-lymphocyte interactions, the effect of co-culture on their expression was examined (Methods section 2.5.2). The yellow histogram in Figure 5.7 a demonstrates a marked increased in ICAM-I expression by HaCaTs after 48 hr co-culture compared to the green histogram showing HaCaT controls (MFI: from 0.3 to 1.15). Concomitantly, there was an increase in T-lymphocyte LFA-1 expression by T-

Figure 5.4

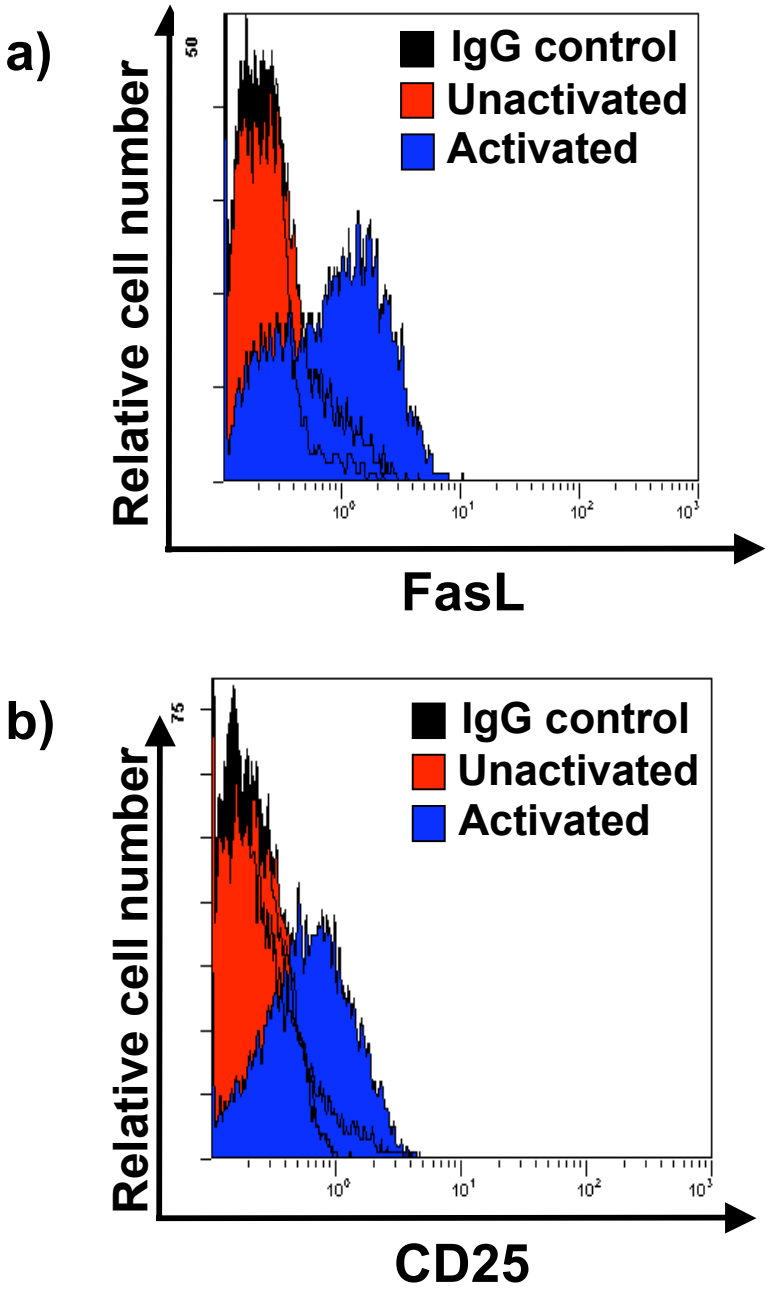

Figure 5.4 Effect of T-lymphocyte activation. (a) FasL expression by unactivated CD4+ T-lymphocytes (red histogram) and FasL expression of activated T-lymphocytes (10ng PMA and 0.5ug ionomycin; blue histogram). (b) CD25 expression of unactivated T-lymphocytes (red histogram) or activated T-lymphocytes (10ng PMA and 0.5ug ionomycin; blue histogram). The black histogram represents staining of an isotype-matched control Ab. Histograms are a representation of 3 separate experiments.

Figure 5.5

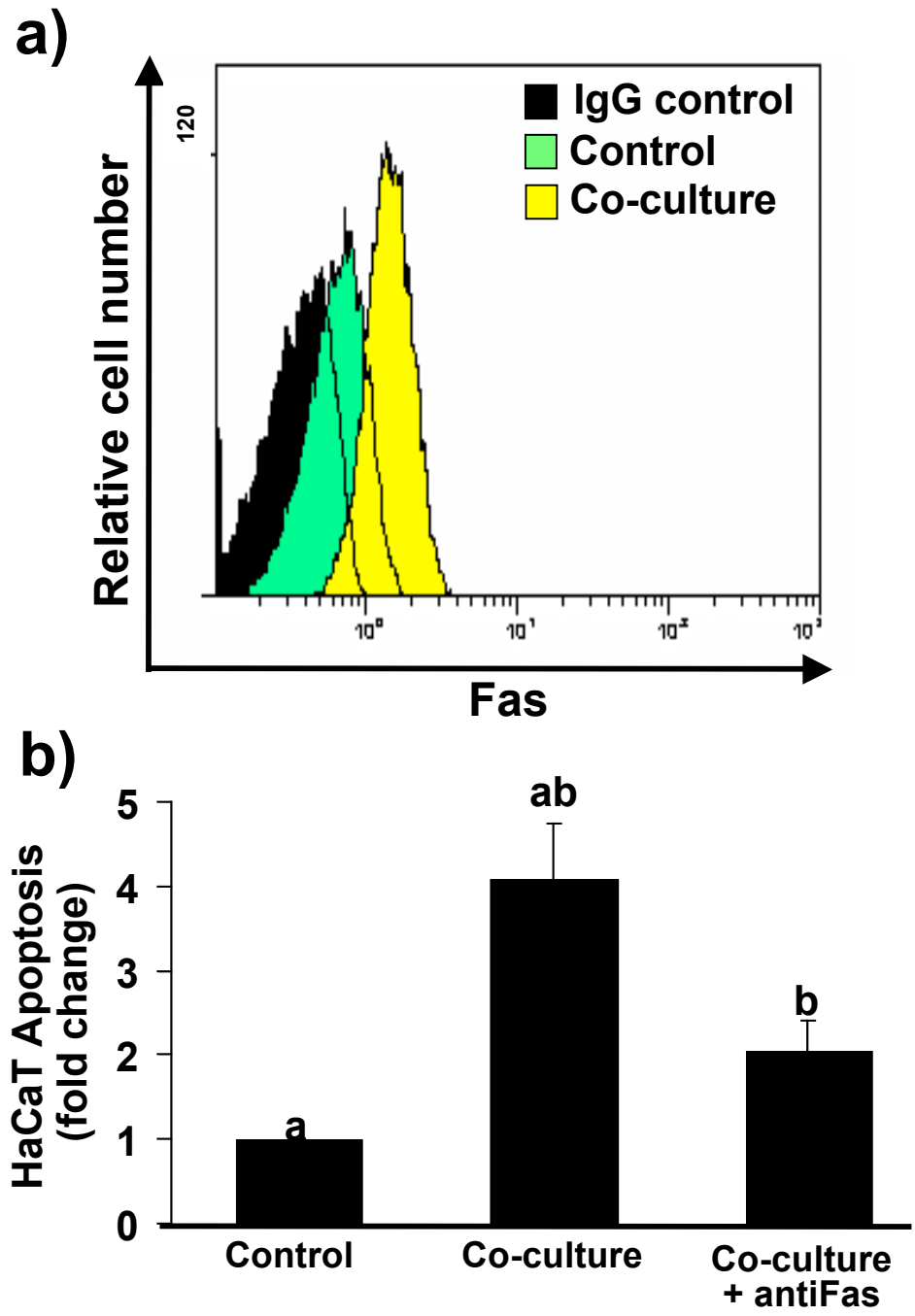

Figure 5.5 Effect of T-lymphocyte co-culture on HaCaT Fas expression. (a) Fas expression by HaCaTs after 48hr co-culture with CD4+ T-lymphocytes was analysed using flow cytometry. Histogram represents Fas expression by control HaCaTs (green histogram) and HaCaTs co-cultured with activated T-lymphocytes (yellow histogram). The black histogram represents staining of an isotype-matched control Ab. Histograms are a representation of 3 separate experiments. (b) HaCaTs were pretreated with 10ug/ml antiFas antibody for 1hr before 48hr co-culture with activated T-lymphocytes, HaCaTs were stained with Annexin V and PI and analysed by flow cytometry. Values represent the mean percentage of apoptotic cells ± SEM of 3 independent experiments the data was analysed using one-way analysis of variance (ANOVA) and post-hoc t-test with significance ($p<0.05$) between treatments shown by the matching symbols (a, b).

Figure 5.6

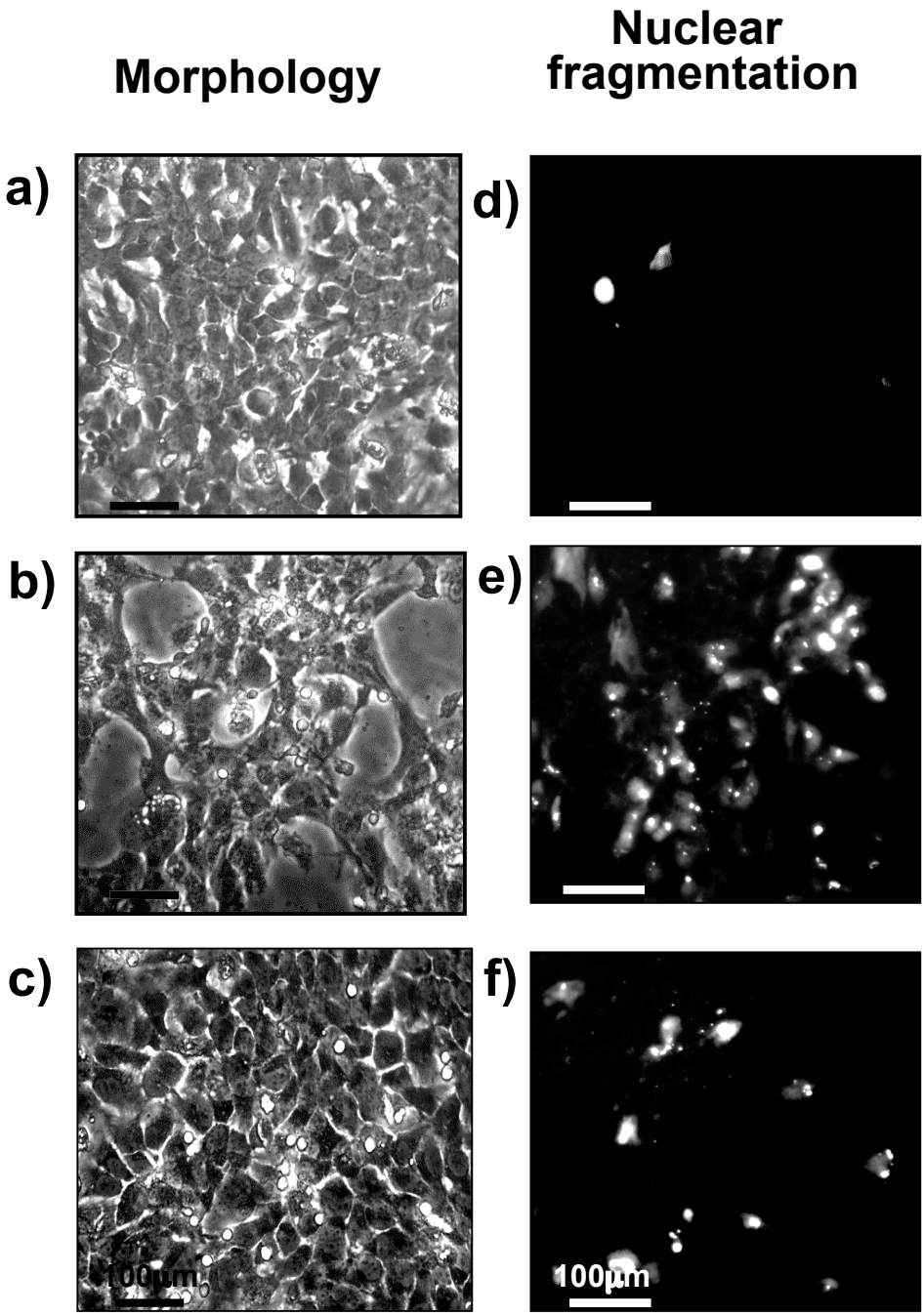

Figure 5.6 Effect of anti-Fas on HaCaT morphology and nuclear fragmentation. (a) Phase contrast microscopy of control HaCaT controls (b) incubated with $5x10^5$ PMA and ionomycin activated T-lymphocytes and (c) HaCaTs pretreated for 1hr with 10ug antiFas antibody before co-culture with T-lymphocytes for 48hr. Nuclear fragmentation identified by HOESCHT 33342 fluorescent staining is shown in (d) control HaCaT cells, (e) HaCaTs co-culture with activated T-lymphocytes for 48hr and (f) HaCaTs pretreated for 1hr with 10ug antiFas antibody before co-culture with T-lymphocytes. Scale bar represents 100µm for the phase contrast images and 100µm for the HOESCHT 33342 images.

Figure 5.7

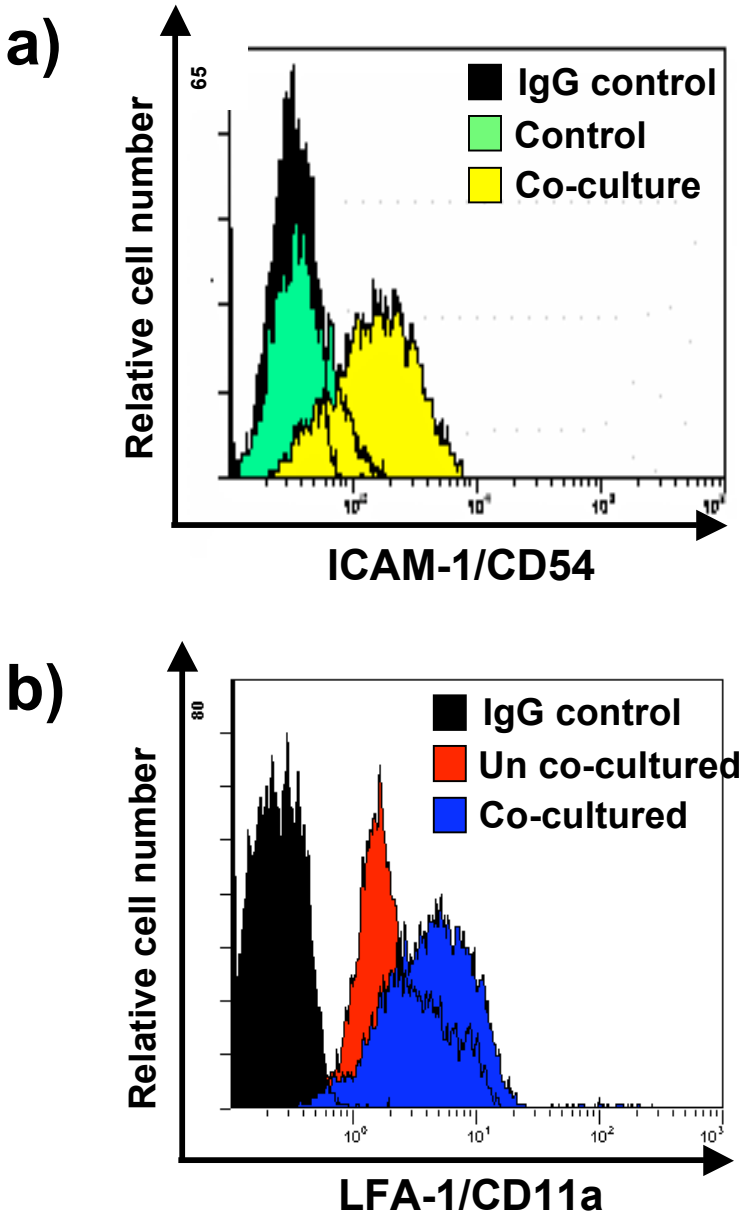

Figure 5.7 Effect of co-culture on adhesion molecule expression by HaCaTs and T-lymphocytes. ICAM-1 expression by HaCaTs and LFA-1 expression by T-lymphocytes was analysed by flow cytometry (a) green histogram represents ICAM-1 staining by HaCaT controls the red histogram represents ICAM-1 staining by HaCaT-T-lymphocyte co-culture. (b) Red histogram represents LFA-1 expression by un-co-cultured activated T-lymphocyte and blue histogram represents LFA-1 expression after 48hr co-culture. Histogram is a representation of 3-4 separate experiments. Black histogram represents staining of an isotype-matched control Ab. Histograms are a representation of 3 separate experiments.

lymphocytes co-cultured with HaCaTs compared to T-lymphocyte only controls (MFI: from 1.15 to 1.6, Figure 5.7 b).

5.3.5 T-lymphocytes induced Fas mediated apoptosis of normal human epidermal keratinocytes

Given the HaCaT results, subsequent studies were performed to determine the effect of pre-activated CD4+ T-lymphocytes on NHEK apoptosis as described in section 5.2.2. The combined results from three independent experiments showed that when NHEKs were co-cultured with CD4+ T-lymphocytes the total number of apoptotic cells increased significantly to 76% from 26.7% in control conditions ($p<0.05$ Figure 5.8 a). Compared to controls (Figure 5.8 b), the T-lymphocytes also induced apoptosis related changes in NHEK morphology such as membrane blebbing and loss of inter-cellular connections (Figure 5.8 c). T-lymphocyte co-culture resulted in a marked increase in the number of HOESCHT 33352 positive NHEKs, showing condensed and fragmented nuclei (Figure 5.8 e) compared to untreated NHEKs (Figure 5.8 d).

As Fas was shown to be upregulated by HaCaTs after co-culture with both Jurkat and Primary T-lymphocytes and it appeared to mediate HaCaT apoptosis (section 4.3.5 and 5.3.3), the effect of co-culture on Fas expression by NHEKs was investigated. Figure 5.9 a demonstrated that compared to control NHEKs (orange histogram), T-lymphocytes increased NHEK Fas expression (aqua histogram; MFI from 0.9 to MFI 1.15). ICAM-1 expression by NHEKs was also found to be markedly increased by co-culture with

Figure 5.8

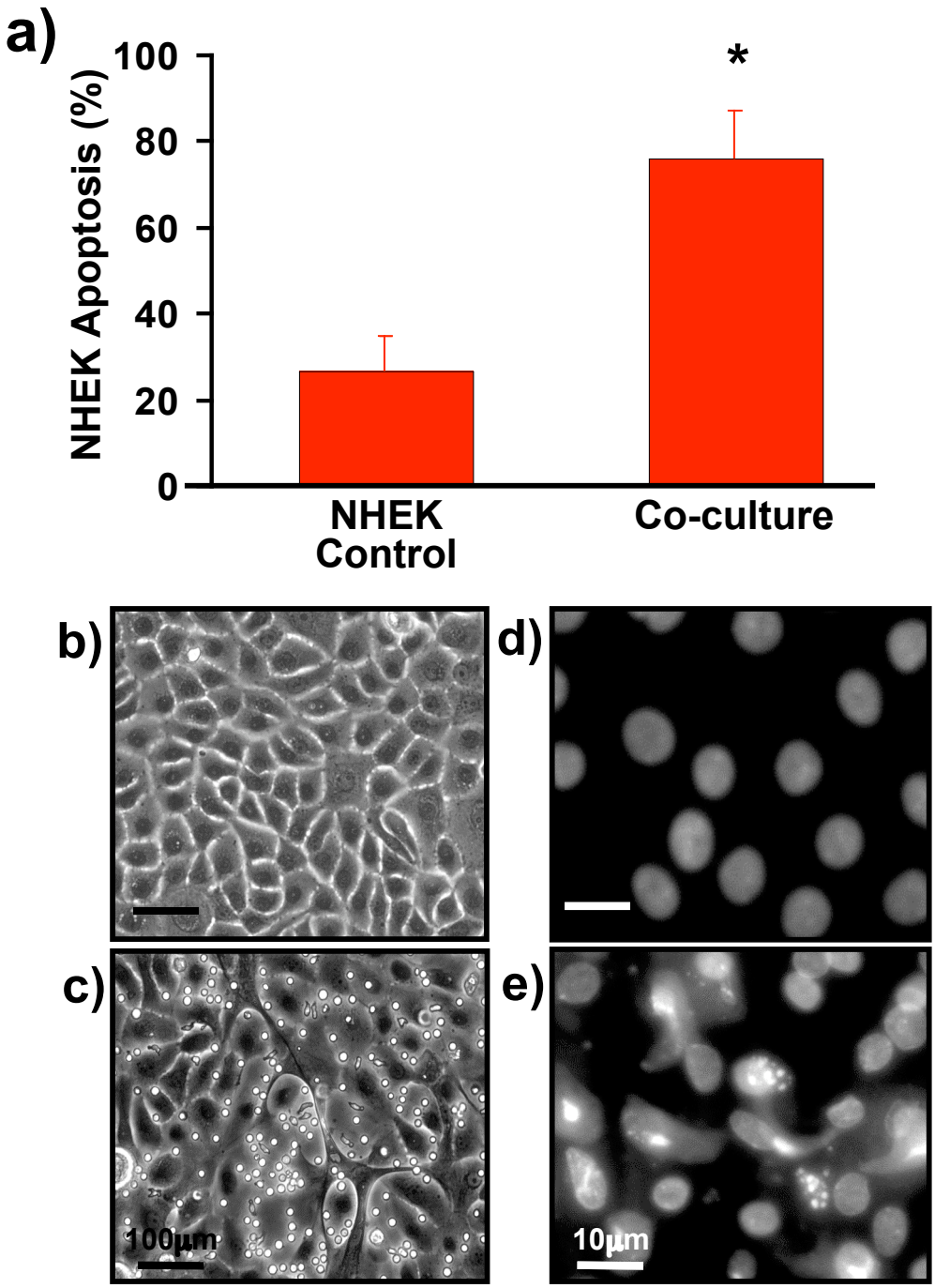

Figure 5.8 Effect of T-lymphocyte co-culture on NHEK apoptosis. (a) Apoptosis was quantified by Annexin V and PI staining of control NHEKs and NHEKs co-cultured with $5x10^5$ pre-activated T-lymphocytes for 48hr. Bar graphs represent the mean ± SEM percentage of cells in 3 separate experiments, the data was analysed using one-way analysis of variance (ANOVA) and significance compared to control shown *$p<0.05$. (b) Phase contrast microscopy of NHEK controls in KBM and (d) NHEKs incubated with pre-activated T-lymphocytes. (c) Nuclear fragmentation visualised by HOESCHT 33342 fluorescent staining is shown in control NHEK cells and (e) NHEKs co-culture with pre-activated T-lymphocytes for 48hr. Scale bar represents 100µm for the phase contrast images and 10µm for the HOESCHT 33342 images.

Figure 5.9

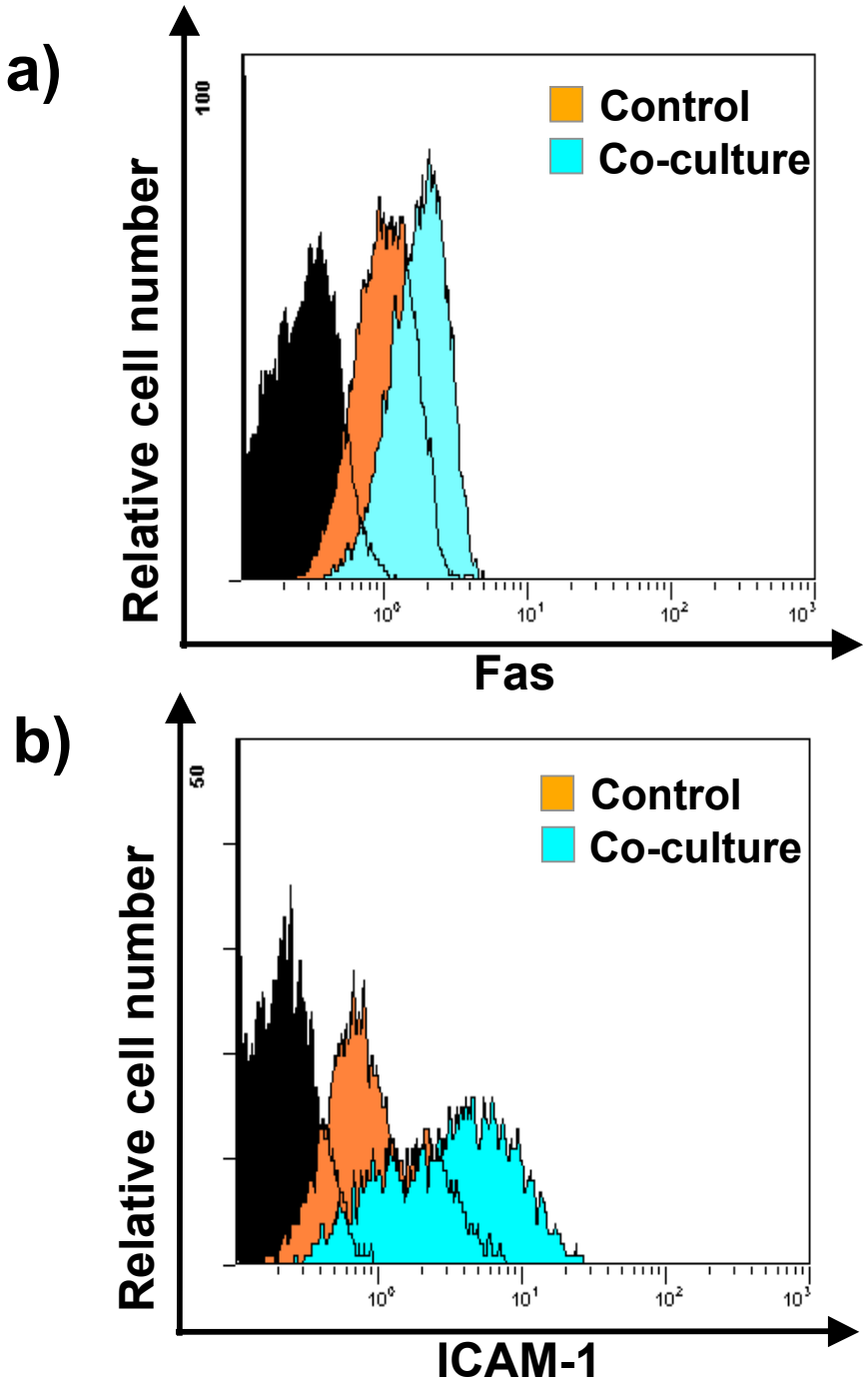

Figure 5.9 Effect of T-lymphocyte co-culture on NHEK Fas expression. (a) Histograms represent Fas expression by NHEK controls (orange histogram) and NHEK co-cultured with pre-activated T-lymphocytes for 48hr (aqua histogram). (b) ICAM-1 expression by control NHEKs (orange histogram) and NHEKs co-cultured with pre-activated T-lymphocytes (aqua histogram). The black histogram represents staining of an isotype-matched control Ab. Histograms are a representation of 3 separate experiments.

Figure 5.10

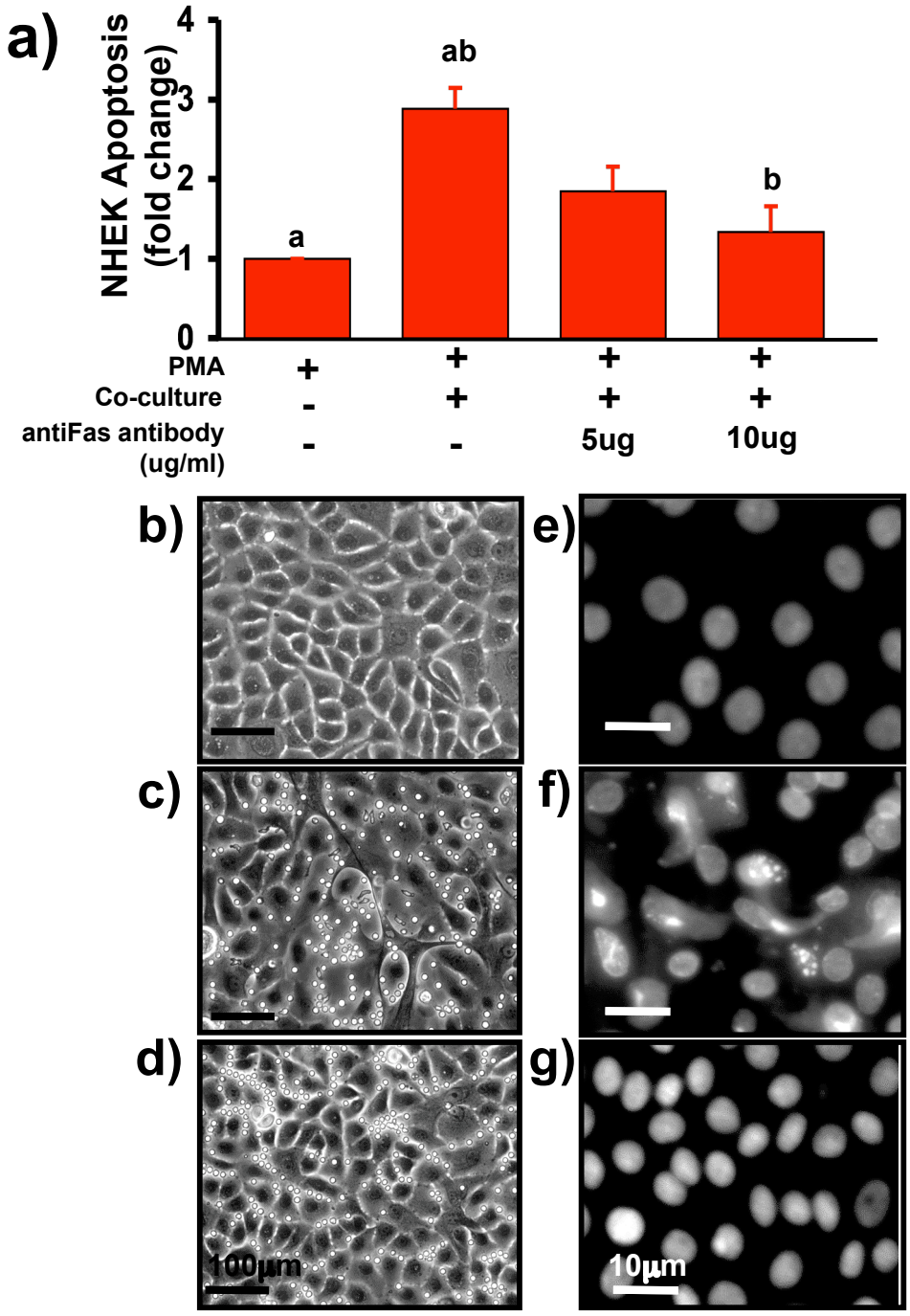

Figure 5.10 Effect of antiFas antibody on T-lymphocyte co-culture induced HaCaT apoptosis. (a) Annexin V and PI staining of NHEKs pretreated with 5 and 10ug/ml antiFas antibody for 1hr before co-culture with pre-activated T-lymphocytes. Values represent the mean percentage of apoptotic cells ± SEM of 3 independent experiments the data was analysed using one-way analysis of variance (ANOVA) and post-hoc t-test with significance ($p<0.05$) between treatments shown by the matching symbols ($^{a, b}$). (b) Phase contrast microscopy of control NHEKs, (c) NHEK-T-lymphocyte co-culture and (d) NHEKs pretreated for 1hr with 10ug antiFas antibody before co-culture with T-lymphocytes. (e) HOESCHT 33342 fluorescent staining of control NHEKs, (f) NHEKs co-cultured with activated T-lymphocytes and (g) NHEKs pretreated with 10µg antiFas antibody before co-culture. Scale bar represents 100µm for the phase contrast images, 10µm for the HOESCHT 33342 images.

CD4+ T-lymphocyte compared to NHEK control (aqua and orange histogram respectively- Figure 5.9 b; MFI from 0.8 to MFI 1.4).

To determine if blocking Fas could prevent T-lymphocyte induced NHEK apoptosis, as previously shown for HaCaTs, NHEKs were pre-incubated with two doses of anti-Fas antibody before co-culture with the primary T-lymphocytes. Figure 5.10 a demonstrates that the anti-Fas antibody prevented T-lymphocyte induced NHEK apoptosis in a dose dependent manner, with a significant effect observed when a concentration of 10ug/ml was used ($p<0.05$ Figure 5.10 a). The anti-Fas antibody (10ug/ml) treated NHEKs displayed reduced cell shrinkage and membrane blebbing, there was not as much cell separation and the number of NHEKs detached from the culture plate was reduced, compared to untreated T-lymphocyte co-cultures (Figure 5.10 d and c respectively). Although there are T-lymphocytes in the culture, NHEK morphology looked similar in appearance to control cells (Figure 5.10 b). Consistent with the morphological observations and Annexin V data, the degree of NHEK nuclear condensation and incidence of fragmentation induced by T-lymphocytes shown in Figure 5.10 f was decreased by the anti-Fas antibody (Figure 5.10 g).

5.3.6 IFNγ is release during co-culture

To assess the levels of inflammatory cytokines release by T-lymphocytes, the conditioned media from unactivated or PMA and ionomycin activated CD4+ T-lymphocytes was collected and the levels of IFNγ and TNFα released by T-lymphocytes were measured by ELISA after 48 hr incubation. Figure 5.11 a demonstrates that

unactivated T-lymphocytes released low levels of IFNγ (0.16ng/ml) and TNFα (0.14ng/ml). Following activation however, IFNγ levels increased significantly to 2.1ng/ml ($p<0.05$). There were also variable levels of TNFα released into the conditioned media although the mean increase to 1.2ng/ml was not significant. IFNγ and TNFα were also measured in the conditioned media from HaCaT controls and T-lymphocyte co-cultures after 48 hr. The levels of IFNγ were significantly higher in HaCaT co-cultures (1.7ng/ml) compared to control HaCaTs (0.2ng/ml; $p<0.05$; Figure 5.11 b). TNFα levels however, were not different in co-culture supernatants (0.06ng/ml) compared to HaCaT control supernatants (0.04ng/ml; $p<0.05$; Figure 5.11 b).

5.3.7 IFNγ increased T-lymphocyte induced keratinocyte apoptosis

IFNγ is a key mediator of apoptosis in skin (Spergel *et al.* 1999). Given that the level of IFNγ levels were shown to be increased in co-cultures and the addition of IFNγ to co-cultures was found to potentiate Jurkat mediated HaCaT apoptosis (Chapter 4 Section 4.3.5). Figure 5.12 a demonstrates that there was a small but non significant increase in HaCaT apoptosis in co-cultures supplemented with IFNγ (100ng/ml) compared to T-lymphocyte co-cultures alone. Similar results were obtained with NHEKs, where IFNγ increased T-lymphocyte induced apoptosis from 77.8% to 89.3%, however this increase was also not statistically significant ($p<0.05$; Figure 5.11 b). In spite of that, apoptosis was still significantly higher in IFNγ treated co-cultures, compared to controls in both cell types.

Figure 5.11

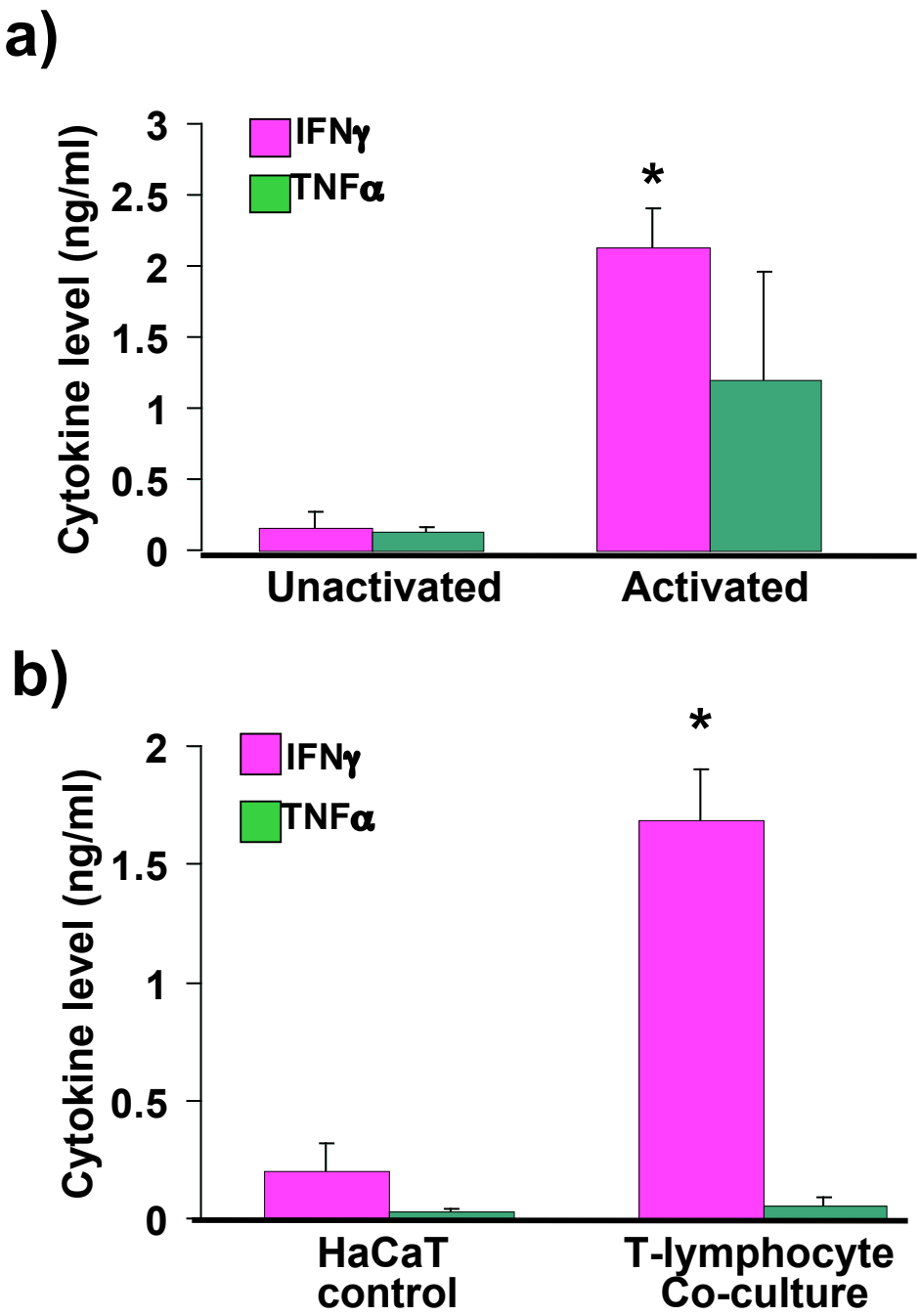

Figure 5.11 IFNγ and TNFα levels release by T-lymphocytes and released during co-culture. (a) Levels of inflammatory cytokine IFNγ (pink) and TNFα (green) in conditioned media from unactivated and PMA + ionomycin activated CD4 T-lymphocytes. (b) Levels of IFNγ (pink) and TNFα (green) in conditioned media from HaCaT controls and HaCaTs co-cultured with activated CD4+ T-lymphocytes. Values represent the mean release of cytokine ± SEM of 4 independent experiments. The data was analysed using one-way analysis of variance (ANOVA) with significance compared to controls shown (*$p<0.05$).

Figure 5.12

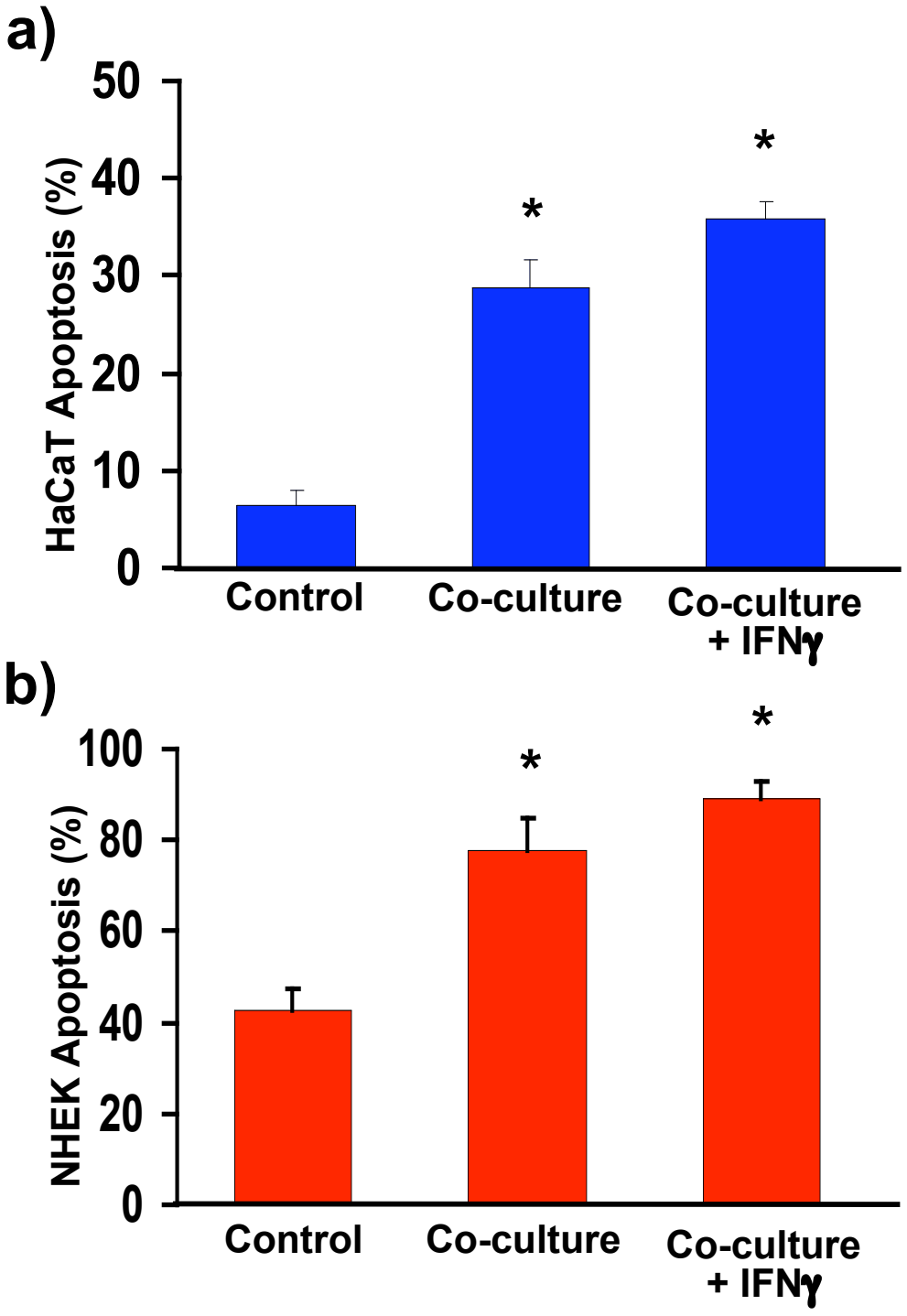

Figure 5.12 Effect of IFNγ on T-lymphocyte induced HaCaT and NHEK apoptosis. (a) Apoptosis by Annexin V and PI staining of HaCaT controls, HaCaT-T-lymphocyte co-culture and HaCaT co-culture + 100ng/ml IFNγ. (b) Apoptosis of NHEK controls, NHEK-T-lymphocyte co-culture and NHEK co-culture + 100ng IFNγ. Values represent the mean release of cytokine ± SEM of 3-4 independent experiments. The data was analysed using one-way analysis of variance (ANOVA) with significance compared to controls shown (*$p<0.001$).

The effect of IFNγ on co-culture induced HaCaT apoptosis was also assessed by morphology and nuclear fragmentation. Compared to HaCaT controls and T-lymphocyte co-cultures (Figure 5.13 a and b), the addition of IFNγ to co-cultures resulted in more profound apoptosis associated morphological changes and a higher number of cells found to be detached from the culture plate (Figure 5.13 c). HOESCHT 33352 staining demonstrated that even though most T-lymphocytes had detached from the culture plate in IFNγ treated co-cultures, there was a higher number of cells with HOESCHT 33352 positive staining and showing nuclear fragmentation (Figure 5.13 f).

5.3.8 IFNγ potentiated T-lymphocyte induced Fas expression of keratinocytes

Studies in Chapter 4 found that IFNγ increased Jurkat induced HaCaT apoptosis potentially by synergistically upregulating HaCaT Fas expression (Chapter 4 Section 4.3.6); therefore the effect of IFNγ on HaCaT and NHEK Fas expression was investigated. Results shown in Figure 5.14 demonstrate that compared to HaCaT controls (green histogram), 100ng/ml IFNγ increased HaCaT Fas expression (pink histogram; Figure 5.14 a). In Figure 5.14 b, T-lymphocyte induced Fas expression by HaCaTs (yellow histogram) was shown to be further increased by treating the cells with 100ng/ml IFNγ, with a greater number of HaCaTs expressing upregulated Fas (purple histogram; MFI: from 1.05 to 1.15). Similarly in NHEKs, T-lymphocyte induced Fas expression (aqua histogram) was also shown to be further increased by IFNγ (purple histogram; MFI: from 1 to 1.1; Figure 5.14 c).

Figure 5.13

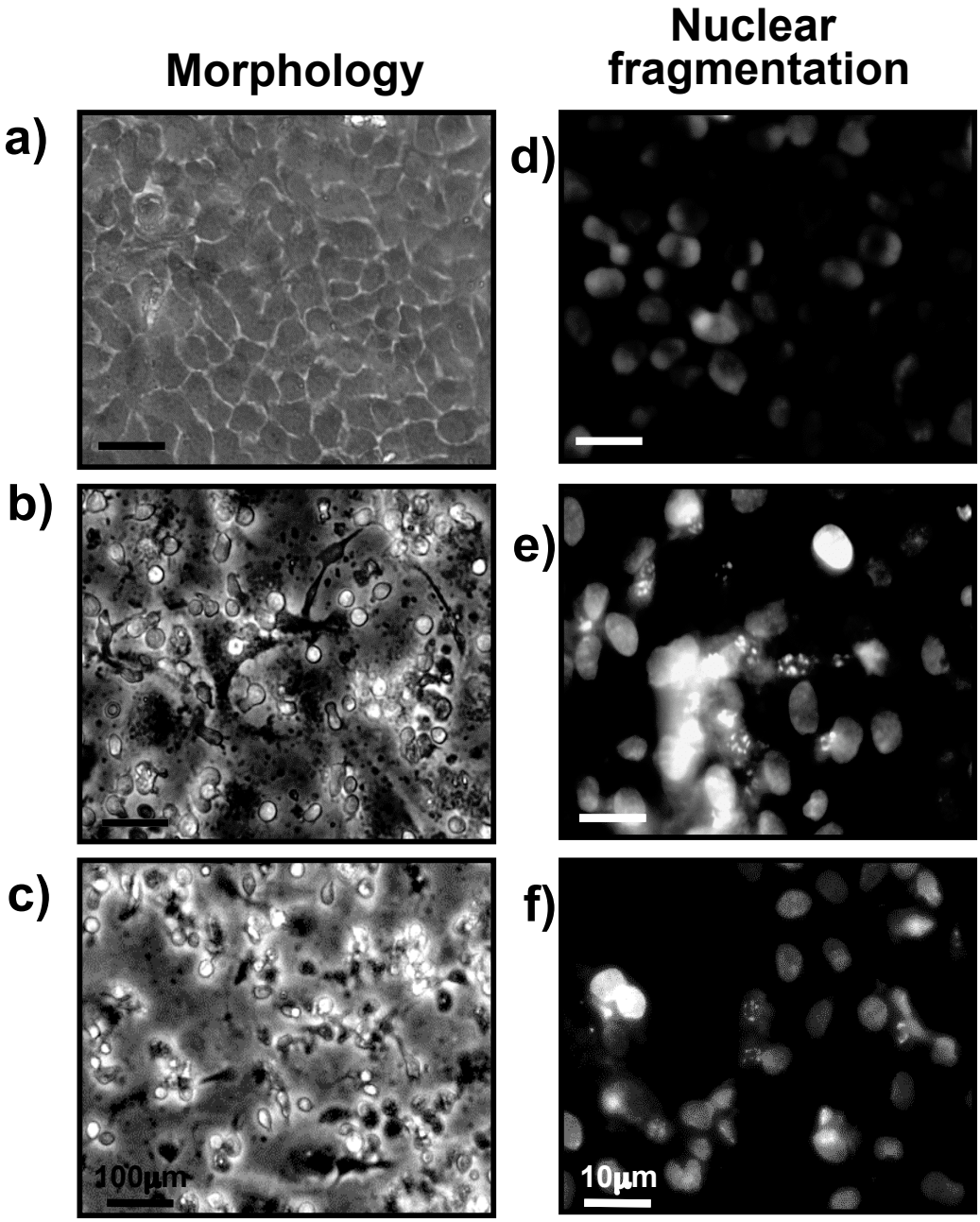

Figure 5.13. Effect of IFNγ on T-lymphocyte induced HaCaT morphology and nuclear fragmentation. Phase contrast microscopy of (a) control HaCaT cells, (b) HaCaT- T-lymphocyte co-culture and (c) HaCaT co-culture + (100ng) IFNγ. HOESCHT 33342 fluorescent is shown in (d) control HaCaTs, (e) HaCaT-T-lymphocyte co-culture and (f) HaCaT co-culture + IFNγ (100ng). Pictures are a representation of 4 separate experiments. Scale bar represents 100µm for the phase contrast images and 10µm for the HOESCHT 33342 images.

Figure 5.14

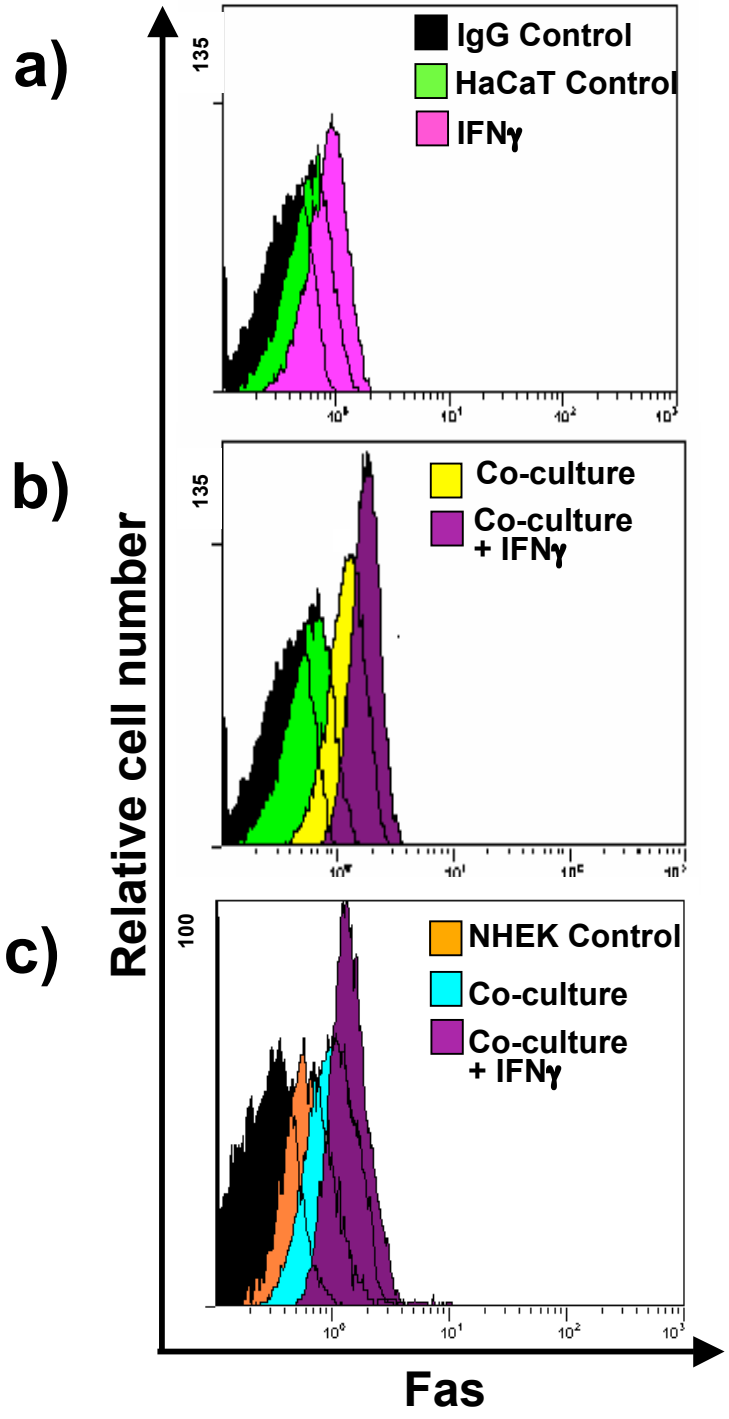

Figure 5.14. Effect of IFNγ on T-lymphocyte induced HaCaT and NKEK Fas expression. Fas expression by HaCaTs and NHEKs was analysed by flow cytometry. (a) Green histogram demonstrates HaCaT control Fas staining , pink histogram represents 100ng IFNγ induced Fas staining. (b) Yellow histogram demonstrate Fas staining by T-lymphocytes and purple histogram demonstrates Fas staining by HaCaT-T-lymphocyte co-culture with IFNγ. (c) Orange histogram demonstrates NHEK control Fas staining, aqua demonstrates Fas staining by T-lymphocyte co-culture and purple histogram demonstrates Fas staining by NHEK-T-lymphocyte co-culture with IFNγ. Black histogram represents staining of an isotype-matched control Ab. Histograms are a representation of 2-3 separate experiments.

5.3.9 T-lymphocyte co-culture induced HaCaT early differentiation

To investigate whether T- lymphocyte co-culture altered the differentiation status of the keratinocytes as well as inducing apoptosis, the intracellular expression of the terminal differentiation marker, involucrin (expressed in the stratum corneum) and the suprabasal cell marker, keratin-10 (K-10; expressed by cells committed to differentiate) was examined. The surface expression of the basal cell marker α6-integrin (expressed by undifferentiated and early differentiating keratinocytes) by HaCaTs and NHEKs was also examined after co-culture (Methods section 2.5.2 and 5.3.3). Involucrin and K-10 expression by HaCaT controls, HaCaT in co-cultures with T-lymphocytes and HaCaTs in co-cultures supplemented with IFNγ (100ng/ml) was shown in histograms in Figure 5.15. Figure 5.15 b shows that compared to controls (Figure 5.15 a), T-lymphocyte co-cultures did not change involucrin expression. However, the addition of IFNγ to the co-cultures caused an increased in the number of involucrin expressing HaCaTs (Figure 5.15 c). T-lymphocyte co-cultures did not alter the pattern of HaCaT K-10 expression compared to controls (Figure 5.15 d and e). No change in K-10 expression was observed in HaCaT co-cultures in the presence of IFNγ as these cells demonstrated a similar expression pattern as control HaCaTs (Figure 5.15 f).

Although it appeared that T-lymphocytes had little effect on the expression of the committed and terminal differentiation markers, more profound effects were observed when α6-integrin expression was assessed. Figure 5.16 a shows that HaCaTs are high expressors of α6 under control conditions (α6-bright; -bri). Results shown in Figure 5.16

b demonstrate that although the over all number of stained cells did not change when HaCaTs were co-cultured with T-lymphocytes, a population emerged that were low expressors of α6 integrin (α6-dim), indicating that cells shifted from α6-bright to α6-dim. The decrease in HaCaT α6 expression induced by T-lymphocytes was augmented by the presence of IFNγ in co-cultures (Figure 5.16 c). Consistent with HaCaTs, NHEKs were also found to be high expressors of α6 under control conditions (Figure 5.16 d) and when co-cultured with T-lymphocytes, α6 expression was also decreased (Figure 5.16 e). Unlike HaCaTs, T-lymphocyte co-culture shifted almost the entire NHEK cell population from α6-bright to α6-dim expressing cells (Figure 5.16 e; MFI: from 15 to 10.5). Moreover, when IFNγ was added to NHEK and T-lymphocyte co-cultures, a further decrease in α6 expression, resulting in a greater (almost complete) shift to the α6-dim region (Figure 5.16 f; MFI: from 10.5 to 10).

Figure 5.17 a shows the total number of α6-dim HaCaTs from 3 independent experiments replicating these described in Figures 5.16. It was demonstrated that T-lymphocytes in co-culture significantly increased the percentage of α6-dim HaCaTs from 14.2% to 39.6% and this was further increased to 52.2% with IFNγ (* $p<0.05$). Furthermore, T-lymphocytes in co-culture did not express α6 (Figure 5.17 b).

Figure 5.15

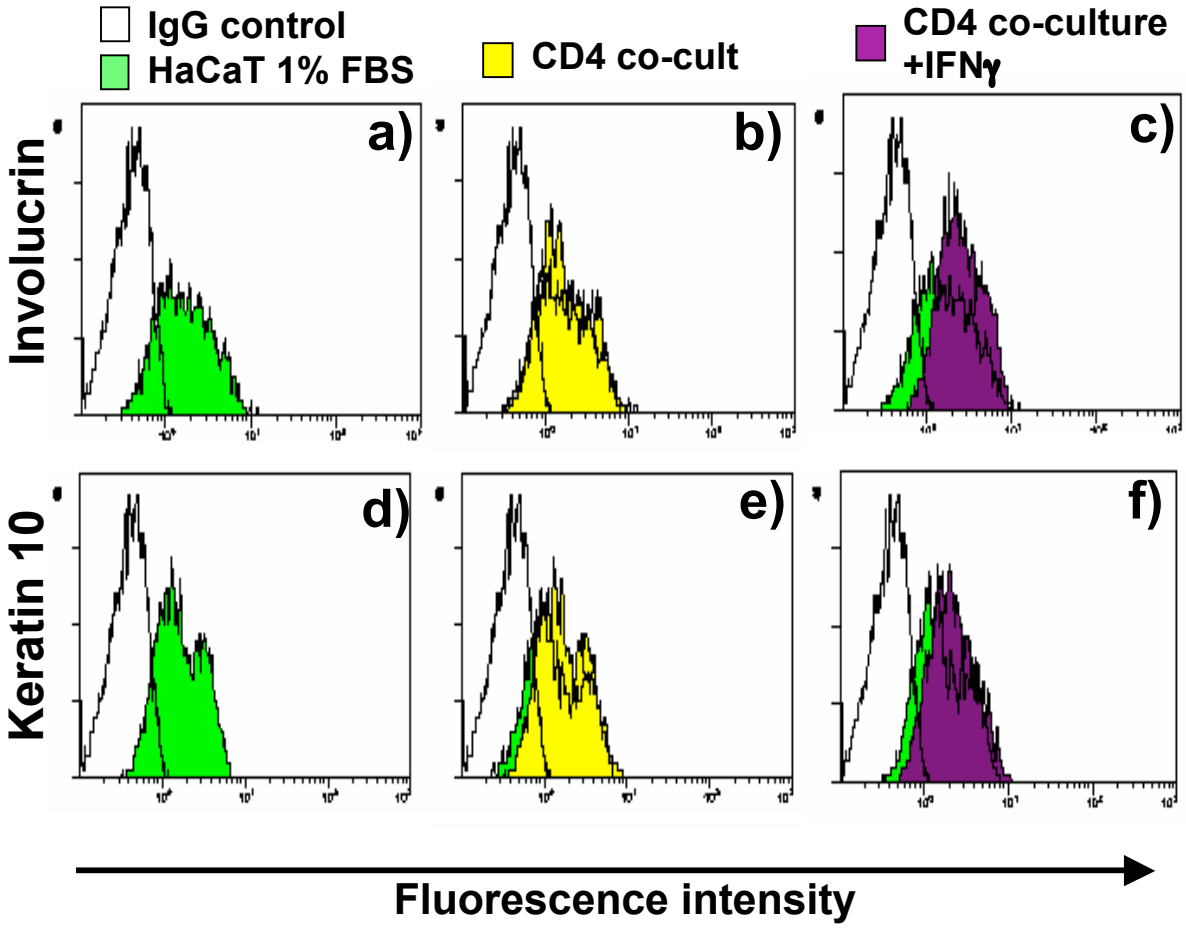

Figure 5.15. Effect of T-lymphocytes and IFNγ on HaCaT terminal differentiation.
Intracellular expression of (a-c) Involucrin and (d-f) keratin-10 (K-10) by HaCaT controls (green histograms), HaCaT-T-lymphocyte co-cultures (yellow histograms) and HaCaT-T-lymphocyte co-culture + IFNγ (purple histograms) was assessed using flow cytometry. The unfilled histogram represents staining of an isotype-matched control Ab. Histograms are a representation of 2 separate experiments.

Figure 5.16

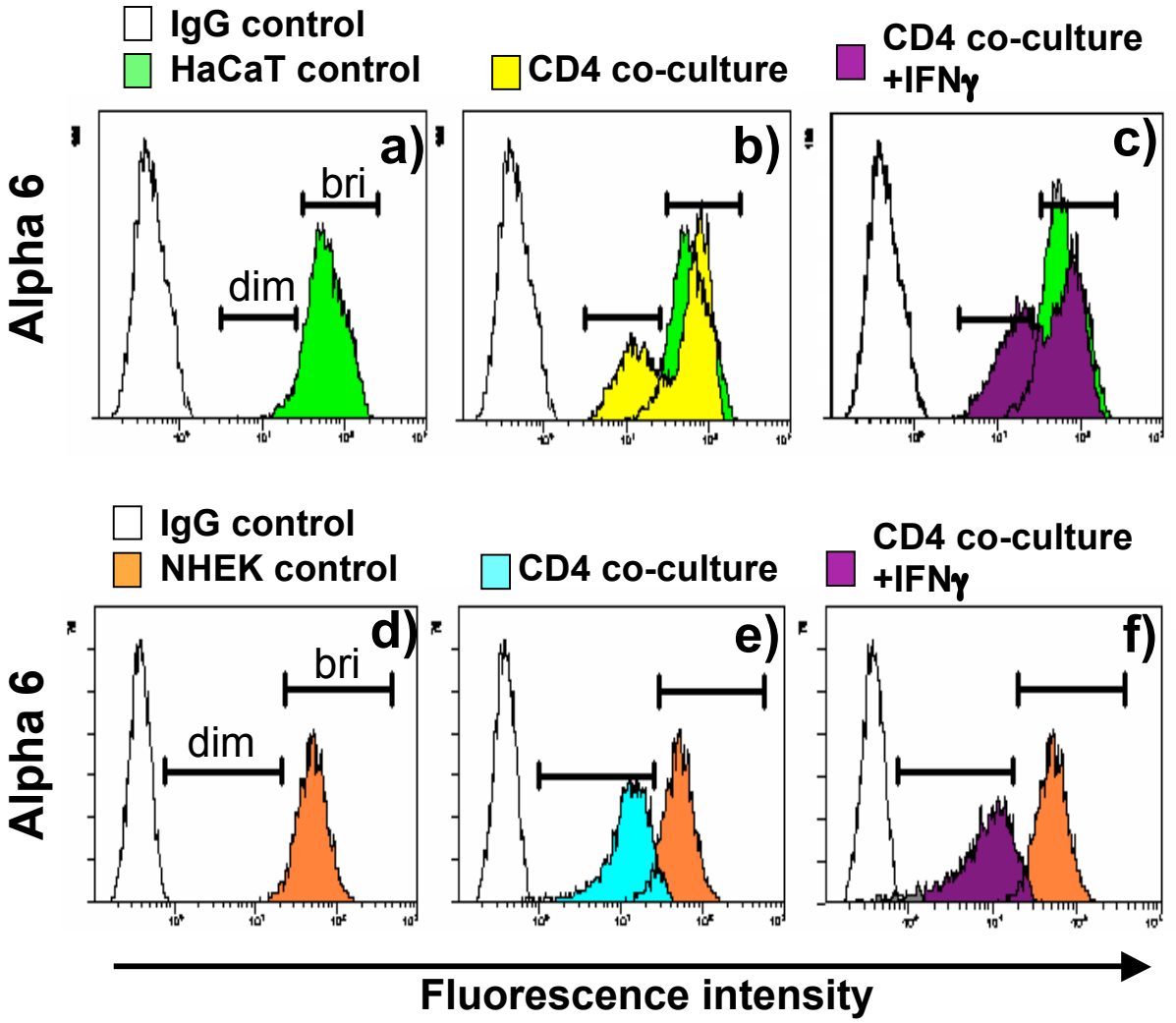

Figure 5.16. Effect of T-lymphocytes and IFNγ on HaCaT and NHEK α6 expression. (a) Surface expression of α6 integrin by HaCaT controls (green histogram), (b) CD4 T-lymphocyte co-cultures (yellow histograms) and (c) HaCaT-T-lymphocyte co-culture + IFNγ (purple histograms) was assessed by flow cytometry. (d) α6 integrin expression by NHEK controls (orange histogram), (e) CD4 T-lymphocyte co-cultures (aqua histograms) and (f) HaCaT-T-lymphocyte co-culture + IFNγ (purple histograms). The unfilled histogram represents staining of an isotype-matched control Ab. The upper gated region indicates the α6 expressing cells "bri", the lower gated region indicates the lower α6 expressing cells "dim". Histograms are a representation of 3-4 separate experiments.

Figure 5.17

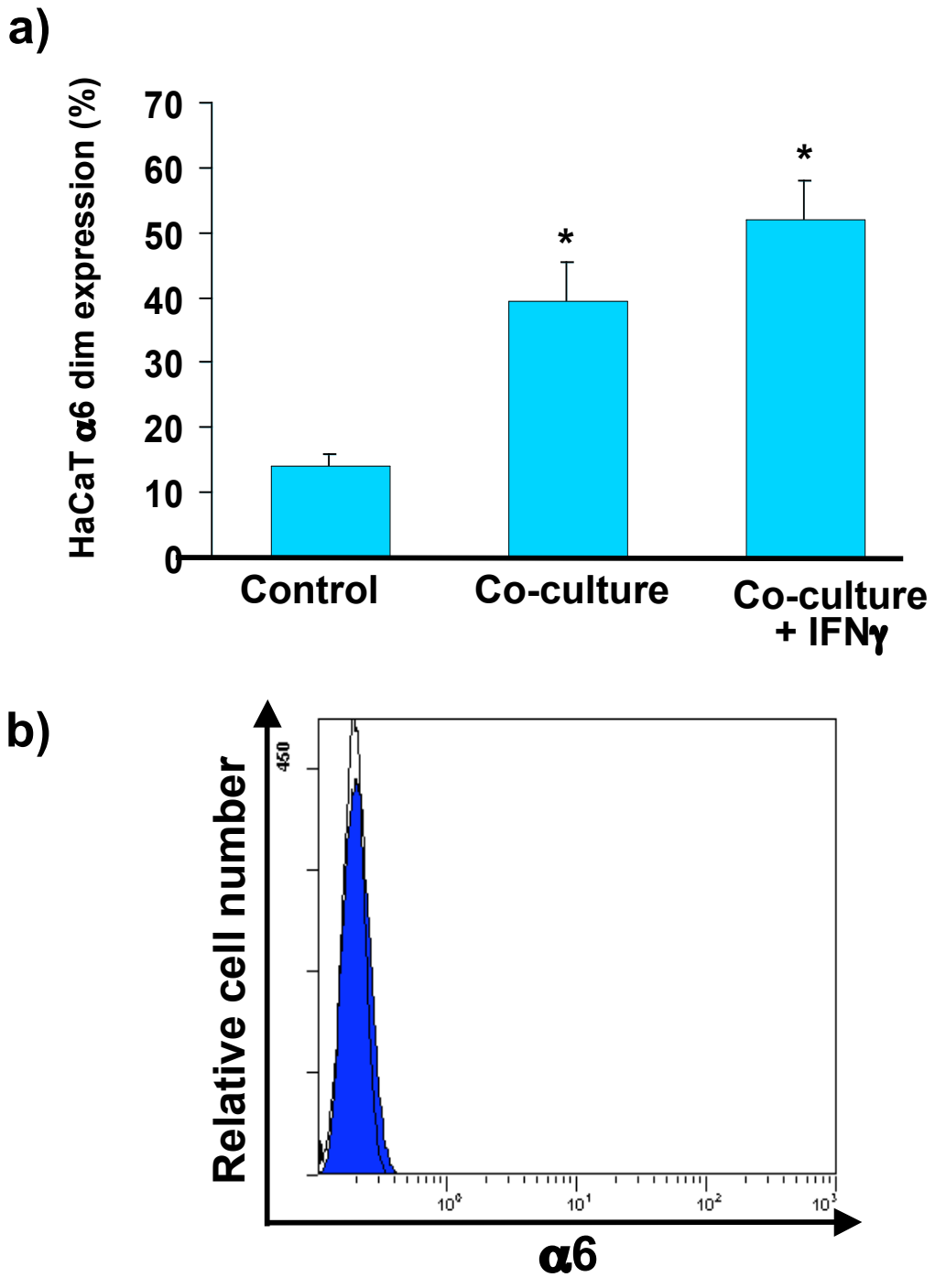

Figure 5.17. Effect of T-lymphocytes and IFNγ on HaCaT α6 dim expression. Percentage α6 dim expression of HaCaT controls, HaCaT-T-lymphocyte co-cultures and HaCaT co-cultures + IFNγ (100ng/ml). Bar graphs represent the mean ± SEM percentage of cells in 3 separate experiments. (ANOVA) considered significant at *p<0.05. (b) Surface expression of α6 integrin by T-lymphocyte controls (blue histogram) was assessed by flow cytometry. The unfilled histogram represents staining of an isotype-matched control Ab. Histogram is a representation of 4 separate experiments.

5.3.10 T-lymphocyte induced keratinocyte apoptosis was associated with α6-dim expression

To associate the differentiation status of keratinocytes with apoptosis, double staining of HaCaTs with Annexin V and α6 was performed and a gate was set to identify both the apoptotic and the early differentiating cells. Representative dot-plots from 2 independent experiments shown in Figure 5.18 demonstrate the changes in α6 expression relative to Annexin V staining of HaCaTs in co-culture (+/-IFNγ). Under control conditions, HaCaTs stained brightly for α6 and were mainly negative for Annexin V with only 7% of cells in the α6-dim and Annexin V positive region (Figure 5.18 a). However, T-lymphocyte co-culture induced Annexin V staining was associated with a marked decrease in α6 expression by HaCaTs. Overall co-culture resulted in a 34.6% of HaCaTs shifting from Annexin V negative and α6-bright to Annexin V positive and α6-dim (Figures 5.16 b). The addition of IFNγ to co-cultures resulted in 46% of HaCaTs being Annexin V and α6-dim.

Figure 5.18

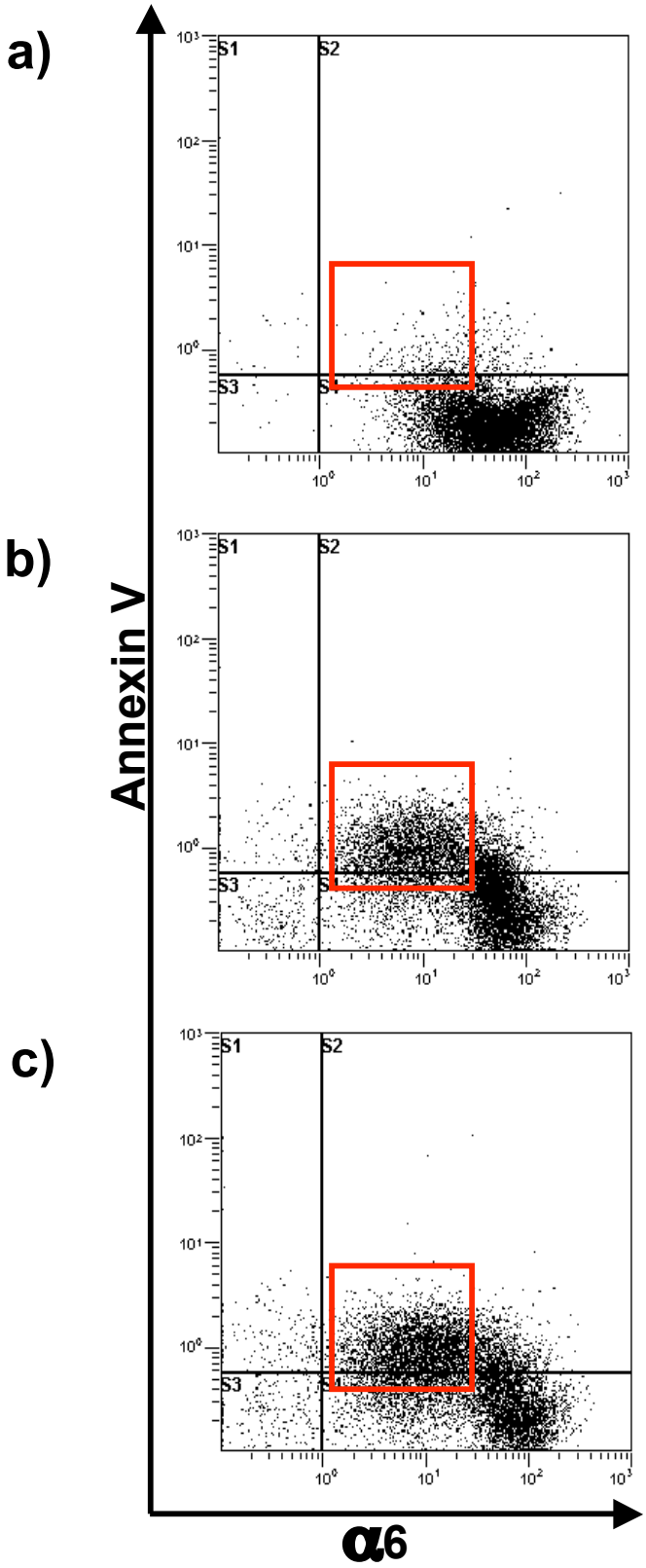

Figure 5.18. Effect of T-lymphocyte co-culture and IFNγ on HaCaT Apoptosis and differentiation. Co-staining with Annexin V and α6 of (a) HaCaTs controls, (b) HaCaT-T-lymphocyte co-culture and (c) HaCaT-T-lymphocyte co-culture + IFN γ was assessed by flow cytometry. Dot-plots are a representation of 2 separate experiments.

5.4 Summary

The following conclusions may be drawn from the results presented in this Chapter:

- Primary CD4+ T-lymphocytes induced Fas mediated apoptosis of keratinocytes in co-culture.
- IFNγ may play a role in mediating apoptosis by upregulating keratinocyte Fas and potentially making them more susceptible to T-lymphocyte's FasL.
- T-lymphocyte induced keratinocyte apoptosis was associated with the induction of the initial stages of keratinocyte differentiation.

The results presented in this Chapter show that Primary T-lymphocytes were capable of inducing keratinocyte apoptosis via a Fas dependent pathway, consistent with the Jurkat T-lymphocyte studies reported in Chapter 4.

Studies in this Chapter also investigated the effect of T-lymphocytes on keratinocyte differentiation. T-lymphocytes were shown to induce keratinocyte early differentiation which was detected by a decrease in α6-integrin expression (Figure 5.14 and 5.15). Unlike other markers for basal keratinocytes such as Keratin 14 (K-14), α6 appears to distinguish undifferentiated basal keratinocytes from keratinocytes entering the early stages of the differentiation pathway (Webb *et al.* 2004). Co-staining with Annexin V confirmed that the apoptotic keratinocytes were indeed the α6-dim cells. It can be speculated that the keratinocytes die at this stage and T-lymphocytes do not modulate the progression of keratinocytes through the later phases of differentiation, which was

demonstrated by no change in the relative expression of keratinocyte intermediate or late differentiation markers.

Figure 5.19 illustrates a proposed working model for explaining the events involved in T-lymphocyte induced keratinocyte apoptosis. T-lymphocyte activation results in increased FasL expression and release of IFNγ (Figure 5.19 a and b). The IFNγ released by T-lymphocytes upregulates keratinocyte Fas expression and therefore makes the keratinocytes more susceptible to the apoptotic signal (Figure 5.19 c). The apoptotic signal is provided by binding of T-lymphocyte associated FasL to keratinocyte Fas, leading to activation of the Fas death pathway and subsequent effector caspase 3 (Figure 5.19 d). Caspase activation results in changes in cell morphology such as loss of membrane asymmetry resulting phosphotidylserine been exposed on the cell surface (Fadok *et al.* 1998), cell shrinkage and nuclear condensation and fragmentation (Figure 5.19 e). The interaction between T-lymphocyte and keratinocytes is potentially facilitated by increased cell to cell adhesions via upregulation of ICAM-1 on keratinocytes and increased LFA-1 expression by the T- lymphocytes (Figure 5.19 f). In addition, given the results in this Chapter, it is proposed that T-lymphocytes initiate the onset of keratinocyte terminal differentiation by decrease in α6 integrin expression (Figure 5.19 g). Finally, keratinocytes lose their inter-cellular connections and detach from the culture plate as they begin to disintegrate and form apoptotic bodies.

In subsequent chapters the T-lymphocyte and keratinocyte co-culture model characterised here was used to address the second main objective of this thesis, which

was to examine the ability of insulin-like growth factor-1 (IGF-1) and transforming growth factor β (TGFβ) in protecting keratinocytes from T-lymphocyte induced apoptosis.

Figure 5.19

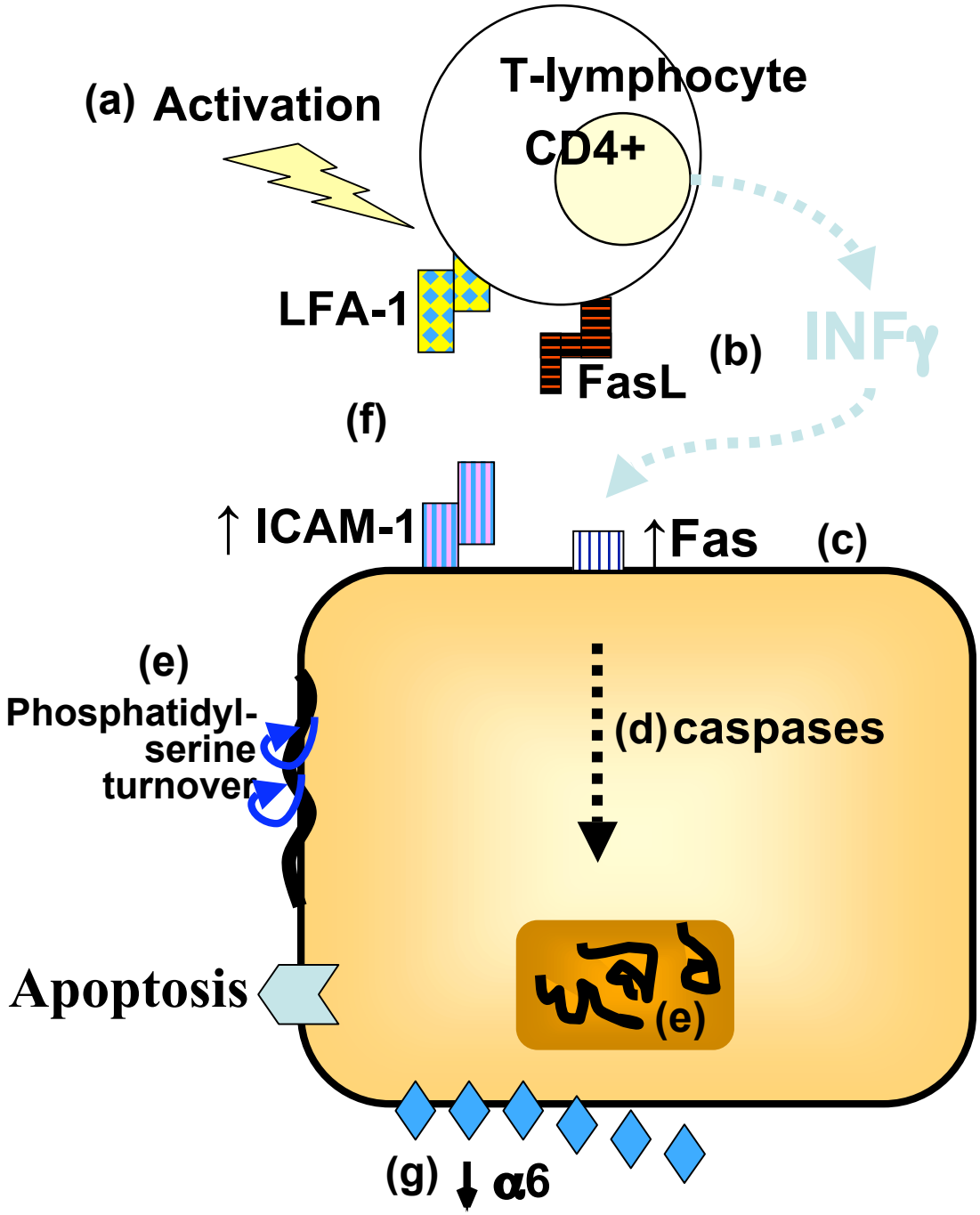

Figure 5.19. T-lymphocyte co-culture induced early differentiation and Fas mediated keratinocyte apoptosis model.